

**Analyzing Uncertainty in Probable
Maximum Precipitation Estimation using
the Moisture Maximization Method**

YOUNGKYU KIM

2021

**Analyzing Uncertainty in Probable
Maximum Precipitation Estimation using
the Moisture Maximization Method**

by

YOUNGKYU KIM

Kyoto University

Graduate School of Engineering

Dept. of Civil and Earth Resources Engineering

2021

ACKNOWLEDGMENT

This thesis was completed in the Hydrology and Water Resources Research Laboratory, Department of Civil and Earth Resources Engineering, Kyoto University.

I would like to deeply thank my supervisor, Professor Sunmin KIM for his encouragement and guidance during the past three years. I benefited so much from his passion and insight into research. I have enjoyed the years studying with him. Thanks to his advice, I could successfully finish my Ph.D. course. I would have never been able to accomplish my thesis without his kind supervision. I would like to really thank Professor Yasuto TACHIKAWA for accepting me as a laboratory member and giving me professional suggestions and creative ideas. I also would like to give my gratitude to Professor Eiichi NAKAKITA. He gave me advice and many comments about this study.

I am also thankful to Professor Ichikawa, Professor Yorozu., and Professor Tanaka who gave me constructive comments during my laboratory life. They also gave me much meaningful advice from his sophisticated expertise and outstanding knowledge. I am deeply grateful to all of my laboratory members who met in the Hydrology and Water Resources Research Laboratory during the Ph.D. course. They helped me kindly during living in Japan.

I am deeply grateful to Professor Kwansue JUNG from Chungnam National University, Daejeon, South Korea. I was enrolled in his laboratory as a bachelor course student, and he has motivated me to continue research work and warmly encouraged me to go abroad to do further studies. Also, I would like to thank Professor Giha LEE, Professor Minwoo SON, Dr. Joocheol KIM, Dr. Minseok KIM, Dr. Yeonsu KIM, Dr. Wansik YU, Dr. Mikyoung CHOI, Dr. Anchul JEONG, Dr. Seongwon KIM, Dr. Taeun KANG, Dr. Daeop LEE, Dr. Jisun BYUN, and all my colleagues for giving me the confidence to conduct the study.

I also extend my special thanks to my parents Myungsuk LEE, Eunsoo KIM, my sister Suna KIM, and my wife Juhee LEE for tremendously supporting me. They always gave me unconditional love and assistance.

Lastly, I want to thank all the taxpayers in Japan, Honjo International Scholarship Foundation, because of whom all the funding for this thesis work and also, my fellowship was possible.

March 2021

Youngkyu KIM

Analyzing Uncertainty in Probable Maximum Precipitation Estimation using the Moisture Maximization Method

Abstract

by YOUNGKYU KIM

Large-scale hydraulic structures, such as dams, levees, and nuclear plants, are designed based on the probable maximum precipitation (PMP) to safely prevent failure due to inundation and overtopping in extreme flooding events. PMP is one of the most important key indices in hydrological design, and it should be estimated without the risk of overestimation or underestimation. However, observed extreme rainfall is insufficient to evaluate the estimated PMP in most regions, and there are no conclusive criteria to evaluate the possibility of PMP over- or underestimation.

This study aims to analyze the uncertainty of the PMP estimation approach using a moisture-maximization method. This method enables the estimation of precipitable water (PW) based on a surface dew point (SDP) under a pseudo-adiabatic assumption. However, the deviation of the PW estimated using the SDP from the actual observed PW in upper-air data (UAD) mostly leads to an inaccurate PMP estimation. This is because it is difficult to estimate the actual atmospheric moisture content in an air column using the SDP alone.

In this study, PMP variables estimated using the SDP (SDP-based estimation approach) are compared with those estimated using the actual PW obtained in UAD (UAD-based estimation approach), at 30 points across Japan. Here, PMP variables are event PW, maximum PW, and moisture maximizing ratio (MMR). The study employed and verified the reanalysis data from “Japanese 55-year Reanalysis” (JRA-55) to consider sufficient atmospheric data, spanning a long-

term period. In the verification of the JRA-55 data, it showed good reliability for the observed SDPs and actual PW values at 10 points across Japan.

The deviation between the SDP- and UAD-based PMP variables was subsequently analyzed using the JRA-55 data. To quantify the deviation, the errors of the PMP variables estimated using the SDP approach to those of the UAD approach were determined. The event PWs estimated using the SDP approach were overestimated than those obtained using the UAD approach in the northern areas of Japan. MMRs of the SDP approach were also underestimated than those of the UAD approach, particularly in the area of Japan with a relatively low SDP. Further, the deviation of MMRs between the two approaches was related to that of event PWs. Consequently, the event PW was considered as the largest source of error in the PMP estimation, and the error magnitude was highly correlated with the SDP as the area with low SDPs showed a high deviation between the two approaches.

To identify the cause of the deviation between PMP variables estimated using the two approaches, the vertical profiles of the atmospheric variables (dew point, mixing ratio, and PW) observed through a radiosonde in the air column were analyzed against those estimated through the SDP and the pseudo-adiabatic assumption. In the southern areas of Japan with high SDPs, the dew points, mixing ratios, and PW profiles estimated using the pseudo-adiabatic assumption showed the low deviations compared to actually observed profiles in the air column.

In contrast, in the northern areas of Japan with low relatively SDPs, the dew points, mixing ratios, and PW profiles estimated through the assumption showed the high deviations compared to the profiles observed through the radiosonde in the air column. This implies that the SDP approach under the pseudo-adiabatic assumption may not reflect the actual atmospheric conditions in the upper-air at a location with low SDPs. In addition, the high deviation between the observed and estimated profiles was related to low SDPs. Hence, the SDP approach using the pseudo-adiabatic assumption can make it difficult to estimate a reasonable amount of PW for heavy rainfalls with low SDPs. To reduce the deviation when using the pseudo-adiabatic assumption, a PMP estimation based on the moisture-maximization method should be carefully considered in regions and events with relatively low SDPs (e.g., lower than 18 °C).

Furthermore, the estimated PMPs were evaluated with extreme-scale reference precipitation determined using the large ensemble climate-simulation data (d4PDF) to check the

possibility of the over- and underestimation of PMP. This reference value corresponds to a 3,000-year return period. The d4PDF allowed the evaluation of the PMP under sufficient extreme events. By using the d4PDF database, the reference precipitation can be estimated empirically without statistical models or methods.

The UAD-based estimation showed a reasonable PMP with a low deviation from the reference precipitation in most target areas, whereas the SDP-based estimation showed overestimated PMP with the reference precipitation in areas with low SDPs. This implies that the UAD approach can reasonably estimate PMP, unlike the SDP approach. However, it is difficult to use the UAD approach in practice because it is difficult to construct the actual observed PW from the UAD such as the radiosonde. Meanwhile, the SDP approach is relatively easy to use in practice because the SDP data is well established even in areas where the radiosonde is not installed. Therefore, there is a need for an alternative approach that can help estimate the PMP using the SDP approach reasonably, even in northern areas with relatively low SDPs.

To control the PMP overestimation in the SDP-based approach, the upper bound of the MMR in the SDP-based approach was limited to 2.0 in this study. Consequently, by limiting the upper bound of MMR, the SDP approach could reduce the deviation between the PMPs and reference values in areas with low SDPs and the possibility of PMP overestimation. This study indicates that it would be possible to estimate a reasonable PMP using the SDP approach by limiting the upper bound of MMR for each area instead of using the UAD approach, which is difficult to utilize in practice.

For a deeper understanding of the topic, this study evaluated the PW used to estimate PMP as a key meteorological factor in the moisture-maximization method and determined the most dominant meteorological factors for extreme precipitation events. This analysis allows the re-evaluation of the use of SDP and PW in the moisture-maximization method. This study analyzed historical heavy rainfall events and their corresponding meteorological factors. The factors considered in this study are PW, SDP, temperature, relative humidity (RH), convective available potential energy (CAPE), and vertical wind velocity (VVEL) in eight regions in Japan.

To collect sufficient data, the JRA-55 was utilized, and the relationship between historical rainfall events and selected factors was analyzed via the cumulative density function (CDF) exceeding 0.95. In southern Japan, VVEL and PW were highly correlated factors for historical

events. In northern Japan, PW was the most strongly correlated factor to historical rainfall events. As the magnitude of rainfall increased, the extreme ratio of VVEL was highly estimated. Consequently, VVEL showed a high correlation with the stronger magnitude of rainfall events. This study also established that PW is a key factor in estimating reasonable extreme precipitation in the moisture-maximization method and the dominant factor in the historical rainfall events to support the physical basis of the numerical approach.

In this study, the uncertainty in PMP estimation using the moisture-maximization method was evaluated through various analyses. The main findings of this study are as follows. (1) The PMP estimated using the SDP approach shows a high deviation compared to that estimated using the UAD approach, especially in the northern area of Japan with a relatively low SDP. (2) The SDP and pseudo-adiabatic assumption may not reflect the actual atmospheric conditions in the upper air at a location with low SDPs, and the deviation between the observed and estimated profiles is highly related to the magnitude of the SDP. (3) In Japan, a high deviation occurs at the SDP below 18 °C. Furthermore, if the pseudo-adiabatic process is applied within the range of SDPs from 18 to 23 °C, a PMP with a significantly low deviation can be estimated. (4) The UAD approach can reasonably estimate the PMP compared to the reference value in most Japanese areas, and the SDP approach overestimates the PMP compared to the reference value in the areas with low SDPs. (5) However, if the upper bound of the MMR is limited to a specific value, the SDP approach may be able to estimate the PMP reasonably even in the northern area of Japan with low SDPs. The SDP approach with limiting the MMR can be utilized in the PMP estimation instead of the UAD approach. (6) The PW was highly correlated with historical rainfall events.

Contents

1. Introduction	1
1.1 Background	2
1.2 Objectives of the Study	5
1.3 Outline of Thesis	6
2. Methodologies in PMP Estimation Theories	11
2.1 PMP Estimation Methods	11
2.1.1 PMP Estimation using the Statistical Method	11
2.1.2 PMP Estimation using the Numerical Method	12
2.1.3 PMP Estimation using the Moisture-maximization Method	13
2.2 PW Estimation using the Surface Dew Point	16
2.2.1 Pseudo-adiabatic Assumption	16
2.2.2 Problems of the Pseudo-adiabatic Assumption	17
3. Uncertainty in the Moisture Maximization Method	21
3.1 Data and Target Area	22
3.2 JRA-55 Verification	25
3.3 Deviation Estimation of PMP Variables	27
3.3.1 Event PW	28
3.3.2 Maximum PW	31
3.3.3 Moisture Maximizing Ratio	33
3.4 Relationship of PMP Variables	35
3.5 Conclusion	37
4. Evaluation on the Pseudo-adiabatic Process using Atmospheric Profiles	39
4.1 Data and Target Area	40
4.2 Relation between Event PW and Surface Dew Point	42
4.3 Atmospheric Profiles and Pseudo-adiabatic Profiles	44

4.3.1 Dew Point Profile from Surface to Upper-air	44
4.3.2 Mixing Ratio Profile from Surface to Upper-air.....	49
4.3.3 Total PW Profile from Surface to Upper-air.....	51
4.4 Discussion	53
4.5 Conclusion	53
5. Evaluation on the Moisture Maximization Method using Large Ensemble	
Climate Simulation Outputs	56
5.1 Data and Target Area	58
5.1.1 d4PDF	58
5.1.2 Comparison of the d4PDF Data and Observed Atmospheric Variables	60
5.2 PMP Estimation and Comparison	65
5.2.1 Deviation of Event PW	65
5.2.2 Deviation of MMR.....	68
5.2.3 Deviation of PMP	70
5.3 Evaluation of the PMP Estimation with a Reference Precipitation	74
5.3.1 Estimation of the Largest Precipitation using d4PDF.....	74
5.3.2 Evaluation of the PMPs Estimated using the SDP and UAD	75
5.4 Limiting MMR in SDP-based Estimation.....	78
5.5 Conclusion	81
6. Analyzing Dominant Meteorological Factors in Extreme Rainfall Events ...	84
6.1 Data and Target Area	85
6.2 Analysis Design	88
6.3 Correlation Analysis between Storm Events and Meteorological Factors	91
6.3.1 Results for the Top 50 Rainfall Events	92
6.4 Discussion	94
6.5 Conclusion	95
7. Concluding Remarks	98
References.....	101

List of Figures

Figure 1-1. Roadmap of this thesis.	9
Figure 2-1. The pseudo-adiabatic process in the moisture-maximization method.	17
Figure 3-1. Target points in Japan. (a) The 30 selected points in Japan. (b) The points used to verify the JRA-55 data based on the installed radiosondes in Japan.	23
Figure 3-2. Comparison of observed SDP with SDP of JRA-55 for approximately 50 rainfalls at Fukuoka, Wajima, Wakkanai points, Kagoshima, Tateno, and Kushiro points.	26
Figure 3-3. Comparison of observed PW with PW of JRA-55 for approximately 50 rainfalls at Fukuoka, Wajima, Wakkanai, Kagoshima, Tateno, and Kushiro points.	26
Figure 3-4. Actual event PW versus event PW estimated using the SDP under the pseudo-adiabatic assumption.	30
Figure 3-5. Resulting map of the average errors between the actual event PW values and estimated event PW values for the top three rainfalls at 30 points in Japan.	30
Figure 3-6. Actual maximum PW values using the actual PWs of the UAD versus maximum PW values estimated using the SDPs under the pseudo-adiabatic assumption.	32
Figure 3-7. Resulting map of the average errors between the actual maximum PW values and estimated maximum PW values for the top three rainfalls at 30 points in Japan.	32
Figure 3-8. Actual moisture-maximizing ratio (MMR) using actual PWs of the UAD versus MMR estimated using the SDPs under the pseudo-adiabatic assumption.	34
Figure 3-9. Resulting map of the average error between the actual MMR and estimated MMR for the top three rainfalls at 30 points in Japan.	34
Figure 3-10. Relationship between the probable maximum precipitation (PMP) variable errors.	36
Figure 4-1. Target areas based on station installed the radiosonde.	41
Figure 4-2. Actual PW values and SDPs for all of the top three rainfalls at 30 points. The dashed line refers to the ideal curve when the PW is pseudo-adiabatically estimated according to each SDP.	43

Figure 4-3. The dew point profiles observed from the radiosonde stations and those estimated using the pseudo-adiabatic lapse rate.	47
Figure 4-4. The dew point profiles observed from the radiosonde stations and those estimated by the pseudo-adiabatic lapse rate.	47
Figure 4-5. The dew point profiles observed from the radiosonde stations and those estimated by the pseudo-adiabatic lapse rate with the actually observed temperature profiles (Northern areas of Japan).	47
Figure 4-6. All of the dew point profiles from the surface to 300 hPa at the Kagoshima, Fukuoka, Shionomisaki, Kushiro, Wakkanai, and Sapporo points.	48
Figure 4-7. The mixing ratio profiles observed from the radiosonde stations and those estimated using the pseudo-adiabatic lapse rate.	50
Figure 4-8. The mixing ratio profiles observed from the radiosonde stations and those estimated by the pseudo-adiabatic lapse rate.	50
Figure 4-9. Accumulative PW profiles according to the atmospheric vertical pressure at Sapporo, Kushiro, and Wakkanai points.	52
Figure 4-10. Accumulative PW profiles according to the atmospheric vertical pressure at Kagoshima, Fukuoka, and Shionomisaki points.	52
Figure 5-1. Target areas. Kagoshima, Fukuoka, Kochi, and Matsue are located in the southern part of Japan; Sapporo, Obihiro, Asahikawa, and Kushiro are located in the northern part of Japan.	59
Figure 5-2. Histograms of daily rainfall extracted from d4PDF and from observed data.	62
Figure 5-3. Histograms of daily surface dew point (SDP) extracted from d4PDF and from observed data.	63
Figure 5-4. Histograms of daily precipitable water (PW) extracted from d4PDF and from observed data.	64
Figure 5-5. The SDP-based event PWs versus the UAD-based event PWs in Kagoshima, Fukuoka, Kochi, Matsue, Sapporo, Obihiro, Asahikawa, and Kushiro.	67
Figure 5-6. Box plots of event PWs estimated using SDP and UAD in eight areas.	67
Figure 5-7. The SDP-based MMRs versus the UAD-based MMRs in Kagoshima, Fukuoka, Kochi, Matsue, Sapporo, Obihiro, Asahikawa, and Kushiro.	69
Figure 5-8. Box plots of MMRs estimated using the SDP and UAD in eight areas.	69
Figure 5-9. The SDP-based PMPs versus the UAD-based PMPs in Kagoshima, Fukuoka, Kochi, Matsue, Sapporo, Obihiro, Asahikawa, and Kushiro.	72

Figure 5-10. Box plots of PMPs estimated using the SDP and UAD in eight areas. (a) Areas located in the southern part of Japan with a relatively high SDP.....	72
Figure 5-11. Average errors between PMP variables estimated using the SDP and UAD approach in eight areas. Red bars refer to the average error of event PW, and blue bars refer to the average error of PMP.	73
Figure 5-12. Cumulative density function estimated from the d4PDF database (60 years \times 50 ensembles) and the largest value has a 3,000-years return period in term of the probable frequency of rainfall.	75
Figure 5-13. Comparison between the PMPs estimated using the SDP and UAD approaches and the largest precipitation obtained from the d4PDF.	77
Figure 5-14. Average errors of the PMPs using the SDP and UAD for the largest precipitation in the eight areas.	77
Figure 5-15. Comparison between the PMPs estimated using the SDP approach with limiting the upper bound of MMR and the largest precipitation obtained from the d4PDF.	80
Figure 5-16. Average errors of the PMPs using the SDP when limiting the upper bound of MMR with Figure 12. Green bars show the average error between the reference value and PMPs estimated using the limited upper bound of MMR to 2.0.	80
Figure 6-1. The eight target areas in Japan.	86
Figure 6-2. The procedure to find the dominant meteorological factors with historical rainfall event.	90
Figure 6-3. CDF curves for 8 meteorological factors at Kagoshima. The red points show the CDF of the factors at top 50 rainfall events.	91
Figure 6-4. The result of counting the events exceeding the CDF of 0.95 out of 50 events.	93

List of Tables

Table 3-1. Description of data sources used in this study.....	24
Table 3-2. Validation of reanalysis data by using CC and RMSE.	27
Table 3-3. SDPs for the top three rainfalls (°C) RMSE.	28
Table 5-1. Average precipitation and 12-hr persisting surface dew point (SDP) for the top rainfall events for each ensemble of 50 ensembles.	59
Table 5-2. Average rainfall, SDP, and PW of the top 50 events for the d4PDF and observed data.	61
Table 5-3. Average errors of the SDP-based event PWs to the UAD-based event PWs.....	66
Table 5-4. Average errors of the SDP-based MMRs to the UAD-based MMRs.	70
Table 5-5. Average errors of the SDP-based PMPs to the UAD-based PMPs.	73
Table 6-1. The selected meteorological factors and description.....	87
Table 6-2. The result of the extreme ratio of each meteorological factor for the top 50 rainfall events in all areas.	93

Chapter 1

Introduction

Numerous water-related infrastructures have been constructed to facilitate irrigation, hydropower generation, transportation, and municipal-water usage. Owing to impact on the climate change, extreme precipitation events are projected to be more frequent and intense, exceeding known historical records (Allan and Soden, 2008; Kunkel et al., 2013a; Trenberth et al., 2003). These extreme events can be devastating, for instance, by triggering natural hazards, such as floods, landslides, and debris flows, and causing significant human and economic losses (Easterling et al., 2000).

Large-scale hydraulic structures, such as dams, levees, and nuclear plants, are designed based on the probable maximum precipitation (PMP) to safely prevent their failure from inundation and overtopping in the case of extreme flooding events. The PMP can also be used to assess the risk of flooding to critical infrastructure (Huffman et al., 2014). PMP is defined as the greatest theoretical depth of precipitation for a given duration in a particular geographical location at a specific time of the year (World Meteorological Organization [WMO], 1986, 2009). PMP is also a variable that should neither be underestimated, to ensure the security of people living near large-scale hydraulic structures, nor be overestimated, which could result in overdesign and a waste of economic resources (Rousseau et al., 2014).

1.1 Background

WMO proposed several methods for PMP estimation: statistical, transposition, and moisture-maximization methods (Hershfield, 1965; Rakhecha and Kennedy, 1985; Rakhecha and Singh, 2009; WMO, 1986; WMO, 2009). The moisture-maximization method is the most popular PMP estimation method and has been adopted by various government agencies for practical purposes (Rouhani and Leconte, 2016). The moisture-maximization method focuses on specific observed extreme storm events and maximizes the atmospheric moisture conditions of the observed event to extreme historical climatic conditions. In this method, severe rainfall events are adjusted to represent the most extreme atmospheric moisture conditions, which are expressed using atmospheric variables to estimate the PMP. Here, precipitable water (PW) is used to express atmospheric moisture availability; however, it is difficult to collect actual PW values obtained from upper-air data (UAD) over a long period. Surface dew point (SDP) information is used as a proxy to estimate the PW via the pseudo-adiabatic process and assumption. In this process, water vapor in the atmosphere is removed as precipitation as soon as it condenses. Each PW value for each SDP is indirectly estimated and available in various tables and graphs expressed by WMO (2009).

The use of SDP under the pseudo-adiabatic assumption for estimating PMP was proposed in the 1940s (U.S. Weather Bureau [USWB], 1941) and later evaluated using the surface and upper-air observations of 21 storms that occurred between 1939 and 1952 in California (USWB, 1954, 1960). The pseudo-adiabatic assumption was also evaluated using actual PW observations of the Hawaiian Islands (USWB, 1963). In these studies, PW was slightly overestimated by the SDP based on the research parameters; however, an insignificant difference was observed between the actual and estimated PW values. The results of this deviation were relatively practical for the high SDP and heavy rainfall cases. Therefore, researchers concluded that the use of the pseudo-adiabatic assumption would be practical in heavy rainfall situations and areas with high surface and atmospheric moisture (USWB, 1954, 1960, 1963). This history indicates that the PW could be satisfactorily estimated using SDPs (USWB, 1954, 1960, 1963).

However, despite the benefits of using the SDP for PMP estimation, USWB (1947) noted that it would be difficult to estimate the PW value using SDP, owing to the fluctuations of atmospheric variables that depend on the geographical regions and seasons (Reber and Swope

1972; Robinson 2000; Viswanadham 1981). In addition, Fletcher (1951) pointed out that deviations might even occur during heavy rainfall events, especially in cases where the atmosphere is in a convectively unstable condition. Chen and Bradley (2006) closely re-evaluated the assumption for PMP estimation according to the radiosonde data obtained in the central U.S. region. They collected information on 57 storm events that occurred in the central U.S. and evaluated the assumption by unifying the extensive study areas. The results indicated that the assumption systematically overestimated the PW for heavy rainfall events and climatological maximum moisture conditions.

The issues regarding the deviation between the actual and SDP-estimated PW values are still noteworthy. Many studies have reported that the SDP-based approach overestimates the PMP more than the UAD-based approach, and it is less accurate than the UAD-based approach (Chen & Bradley, 2006; Kim et al., 2019; Micovic et al., 2015; Rouhani & Leconte, 2020). According to Micovic et al. (2015), although SDPs can be used to estimate the PMP, they are less accurate than the actual PW owing to the pseudo-adiabatic assumption. Their study showed that the SDP approach overestimated the PMP variables compared to the UAD approach using the actual PWs. Recently, Rouhani and Leconte (2020) analyzed these deviations using the PW and SDP data obtained from climate simulation model outputs. They concluded that the actual PW is more physically-based than the SDP-estimated PW in the estimation of PMP.

In addition, Kim et al. (2020) noticed that the SDP approach is highly likely to overestimate PMP in regions with low SDPs. They showed clear deviations between the SDP and UAD-based estimations by comparing the vertical profiles of atmospheric variables (dew point, mixing ratio, and PW) observed from the radiosonde. In an attempt to obtain a more accurate PW value, researchers have proposed an empirical method, for instance, the use of regression equations to determine the relationship between the PW and surface humidity (e.g., Choudhury, 1996; Reber and Swope, 1972; Reitan, 1963; Sinha and Sinha, 1981; Wahab and Sharif, 1995; Chen and Bradley, 2006). However, it is difficult to represent the PW using only surface humidity and to provide an adequate physical explanation for the empirical method (Tuller, 1977). Consequently, despite the benefits of using SDP for PMP estimation, the use of an SDP-based PWs may lead to uncertainty in the PMP estimation using the moisture-maximization method.

The SDP-based PMP estimations may require an ‘evaluation’ to provide a reasonable design rainfall value for large-scale hydraulic structures. However, it is difficult to accurately

evaluate the reasonability of the estimated PMP. The reason is that first, there is an insufficient number of extreme rain events for analyzing the reasonability of the SDP-based approach in PMP estimation. The U.S. Weather Bureau (1954, 1960, 1963) recommends applying the SDP approach under conditions of extreme rain events and high moisture cases; extreme rain events should be sufficient to analyze the reasonability of PW and PMP estimated using the SDP approach because the approach shows a different tendency compared to the UAD approach in PW and PMP estimations based on the number of extreme events (Micovic et al., 2015). Further, Papalexiou and Koutsoyiannis (2006) reported that the SDP-based PMP estimation is sensitive to available data because missing one or two events can change PMPs by at least 20% in the moisture-maximization method. Further, with sufficient rainfall events, PWs estimated using the SDP should be compared with a sufficient number of actual PWs obtained in the UAD. This is to sufficiently evaluate the deviation of the SDP-based approach from the UAD-based approach; however, historically observed PW in the UAD continues to remain scarce, and the time series are too short to compare in many regions.

Further, conclusive criteria to assess the over- and underestimation possibilities of PMPs estimated using the SDP and UAD approaches are lacking. Moreover, it is difficult to present the reference precipitation that can be used to evaluate the PMP that corresponds to the range from 10^{-3} to 10^{-10} in terms of the frequency of probable rainfall which is a very long return period (Schaefer, 1994; Schaefer & Barker, 2005; Rousseau et al., 2014). Although the precipitation value with a relatively long return period can be presented using historical observed data and frequency analysis, it is unsuitable and highly uncertain because of the very short observed data period compared to the long return period of the PMP (Alaya et al., 2018; Klemes 1986, 1987, 2000). Therefore, to evaluate the reasonability of PMPs estimated using the moisture-maximization method accurately, the evaluation should be conducted under sufficient extreme rainfall events, actual PWs in the UAD, and SDPs. In addition, a reasonable extreme-scale reference value is required to evaluate the possibility of PMP over- and underestimation. The uncertainty evaluation of the moisture-maximization method and the pseudo-adiabatic assumption for the PMP estimation is the main subject to be discussed in this study.

1.2 Objectives of the Study

This study aimed to analyze the uncertainty in PMP estimation using the moisture-maximization method. The SDP-based PMP estimation approach is evaluated by analyzing the deviation of each PMP variable estimated using the SDP approach (PMP estimation using PW derived from the SDP approach and pseudo-adiabatic assumption) and UAD approach (PMP estimation using actual PWs obtained from the UAD), as well as atmospheric moisture profiles in the air column. Further, this study evaluates the possibility of PMP over- and underestimation for the two approaches with extreme-scale reference precipitation by using large ensemble climate simulation outputs. In addition, the dominant meteorological factor for the historical extreme rainfall events is identified in this study.

Most previous studies have been focused on the U.S., and evaluations of the deviation between the two approaches have rarely been conducted elsewhere. This study was conducted in Japan, considering its variable climatic and atmospheric conditions. The PMP is a very important value that has been utilized as a design variable in the construction of dams in Japan and Korea. Japan can be used to analyze various local climatic characteristics, as it is surrounded by sea and has widely established topographic characteristics from northern to south latitudes; additionally, storm events are frequent in most areas. Specifically, the detailed objectives of this study are as follows:

To compare the SDP-based PMP variables estimated using the pseudo-adiabatic assumption with the UAD-based PMP variables estimated using the actual PWs by utilizing the reanalysis data.

To analyze the deviation between the atmospheric variables using the SDP and UAD approaches by using the actual atmospheric profiles observed from the radiosonde in the air column.

To evaluate the possibility of the PMP over- and underestimation for the SDP and UAD approaches with extreme-scale reference precipitation obtained using the d4PDF data.

To determine the most dominant factors for estimating reasonable PMP by analyzing the relationship between the historical events and meteorological factors used in PMP estimation.

1.3 Outline of Thesis

Figure 1-1 shows the roadmap of this thesis. The rectangles represent the title and objective of each chapter and the arrow represent the relation between the chapters.

This thesis mainly consists of three parts that discuss PMP estimation using the moisture-maximization method. The first part focuses on analyzing the deviation of each PMP variable between the SDP and UAD approaches (Chapters 3 and 4). The second part focuses on evaluating the PMP estimated using the moisture-maximization method with reference precipitation (Chapter 5). The third part focuses on determining the dominant meteorological factor to reasonably estimate PMP (Chapter 6).

In Chapter 2, the representative PMP estimation methods and the pseudo-adiabatic process are explained. Methods that have been widely used in the past are mainly explained, and the advantages and disadvantages of each method are discussed. A literature review was also conducted on previous studies related to each method. In addition, the most important pseudo-adiabatic process in the moisture-maximization method is elucidated in detail. An explanation of the PW estimation in the air column by using the SDP is provided, along with the uncertainty implication of the PWs calculated using the SDP in the PMP estimation. Several uncertainties for the use of the SDP and pseudo-adiabatic processes in the PMP estimation are also elucidated in detail.

The deviation in the PMP estimation using SDP under the pseudo-adiabatic process with the PMP estimation using the actual PW is analyzed in Chapter 3. Here, the deviation estimation is conducted for the PMP variables (event PW, maximum PW, and MMR) at 30 points in Japan. This chapter employs and verifies the reanalysis data obtained from “Japanese 55-year Reanalysis” (JRA-55) to consider abundant atmospheric data spanning a long-term period. After identifying the availability of JRA-55, to quantify the deviation, the errors between the PMP variables determined using the SDP and actual PW extracted from the JRA-55 were estimated according to each area. All of these results were divided by the values from their respective regional points to analyze the relationship between the deviation and regional characteristics. This analysis allows the analysis of the characteristics of deviation in each area of Japan.

In Chapter 4, the cause of the deviation between the PMP variables estimated using the two approaches, identified in Chapter 3, is analyzed in depth by using the actual observed atmospheric conditions. Further, the relationship between the SDP and actual PW values is analyzed to identify the cause of the deviation. The previous chapter focused on the effect of the deviation on the result of the PMP estimation, whereas Chapter 4 is systematically organized to determine the effect of the pseudo-adiabatic assumption on the deviation of the actual profiles in the air column and upper air. This chapter analyzes and compares the profiles of the atmospheric variables observed from radiosondes with those estimated through the pseudo-adiabatic process according to the atmospheric pressure layers from the surface to 300 hPa, where the saturated air parcel is very thin. Here, the actual atmospheric profiles observed from the radiosonde were used. The results of the analysis allow us to more clearly analyze the deviations resulting from fluctuations of the atmospheric variables, by analyzing deviations of the actual atmospheric conditions with the assumed atmospheric conditions.

Chapter 5 presents the analysis of the deviation between the SDP- and UAD-based PMP estimations under the sufficient extreme rainfall events and the evaluation of the possibility of the PMP over- and underestimation for the SDP- and UAD-based approaches with extreme-scale reference precipitation values. In this study, the d4PDF data based on a large ensemble climate simulation database were utilized. The deviations of the event PWs, MMRs, and PMPs between the SDP and UAD-based estimations were estimated, and the deviation patterns were checked in the context of regional climatic characteristics in target areas. Further, extreme-scale reference precipitation values were proposed by collecting annual maximum precipitation values obtained from the d4PDF database for each area. With the reference value, the over- and underestimation possibilities of PMPs estimated using the SDP and UAD approaches were evaluated. For the SDP-based estimation, an alternative limiting the upper bound of MMR was applied to reduce the possibility of overestimation. Consequently, this study not only evaluated the tendency of deviation between the PMPs estimated by the two approaches in each region with different climatic characteristics, under sufficient extreme rainfall events, but it also presented the reasonability of the two approaches by comparing them using a reference extreme precipitation.

Chapter 6 presents the evaluation of the PW used to estimate PMP as a key meteorological factor in the moisture-maximization method and determines the most dominant meteorological factors for extreme precipitation events. In this study, the cumulative density function (CDF) was

applied to determine the dominant meteorological factors for extreme precipitation. In this chapter, the location of the 50 values of each factor is identified on the CDF curve; if a majority of the top 50 event values are located near 1 on the CDF, the correlation with the magnitude of extreme precipitation is higher. To quantify the number of the top 50 rainfall events that are correlated with the selected factors, the number of rainfall events exceeding 0.95 on the CDF is counted. An analysis is then conducted on the assumption that if more values exceed 0.95 on the CDF curve, the correlation between the factors and rainfall events is higher. Accordingly, the factor with the highest correlation is determined as the dominant factor for extreme precipitation. This analysis allows the re-evaluation of the use of SDP or PW in the moisture-maximization method.

Finally, Chapter 7 summarizes the study with concluding remarks.

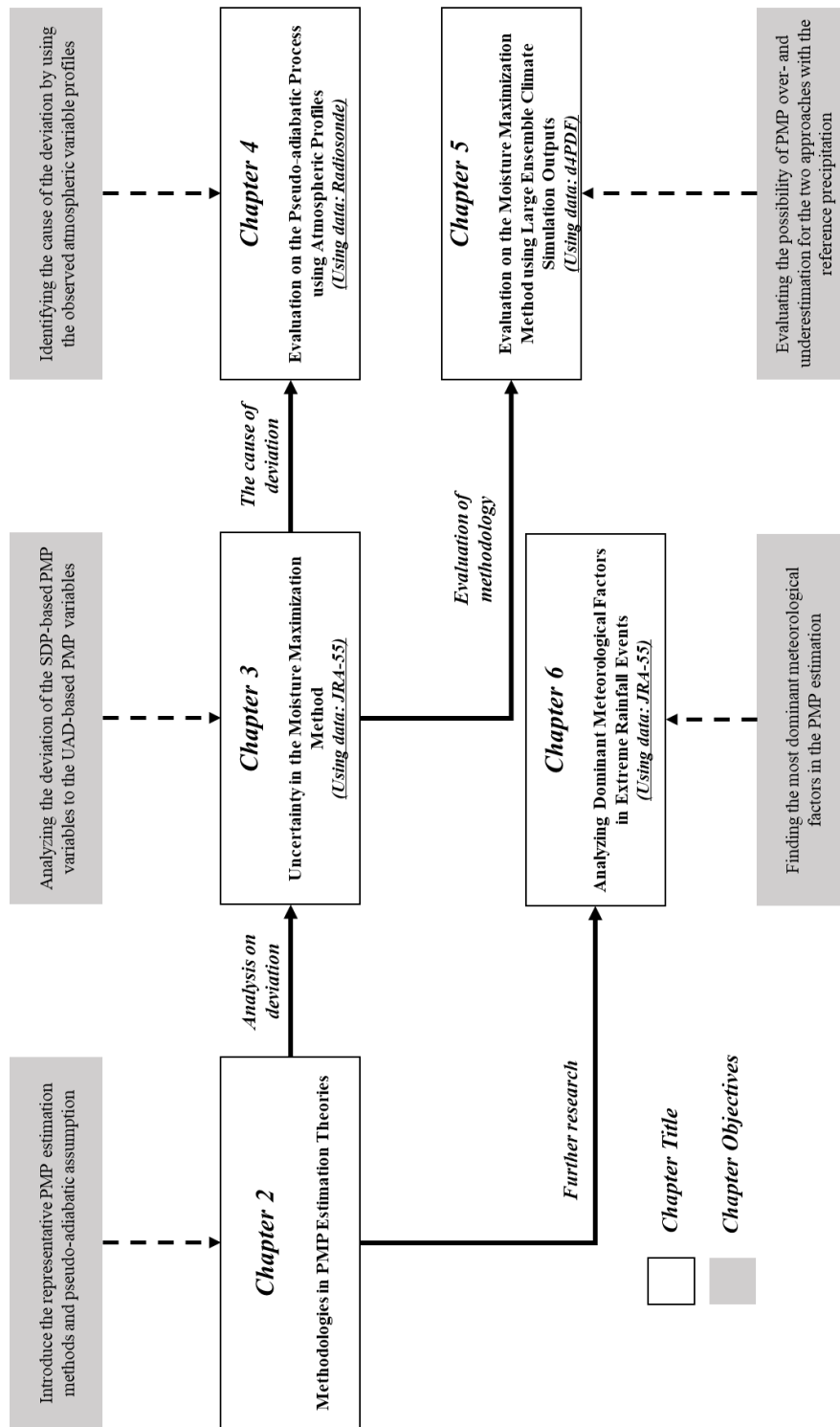


Figure 1-1. Roadmap of this thesis.

Chapter 2

Methodologies in PMP Estimation Theories

2.1 PMP Estimation Methods

Extreme storm events have physical upper limits, which are referred to as PMP. It should be noted that due to the physical complexity of the phenomena and limitations in data and the meteorological and hydrological sciences, only approximations using the meteorological factors are currently available for the upper limits of storms. Hence, PMP estimation is based on maximizing precipitation events. There are three representative methods to estimate the PMP: Statistical method, numerical method, and moisture-maximization method.

2.1.1 PMP Estimation using Statistical Method

Hershfield (1965) suggested a statistical method in the 1960's adapting the following frequency equation for PMP estimation, which was originally proposed by Chow for analyzing flood events (Chow, 1951). PMP is derived using rainfall data obtained from numerous rainfall gauge stations.

In equation (2-1), X is the magnitude of a rainfall event of a given duration at a particular probability level, \bar{X} is the mean of the time series of annual maxima, K is a frequency factor and S_X is the standard deviation of the series (Hershfield, 1981). To estimate PMP from equation (2-1), Hershfield adjusted the K factor to produce a precipitation event for which the return period is theoretically infinite. WMO recommends this PMP estimation approach for small size watersheds.

$$X = \bar{X} + S_X K \quad (2-1)$$

The main advantage of statistical approaches such as Hershfield's method is their ease and quick to obtain PMP estimates (Casas et al., 2011). However, a disadvantage of such approaches is that the K value of equation (2-1) is sensitive to the historical record length and rainfall data quality (Koutsoyiannis, 1999). In addition, this method has a high probability of under- or overestimation. Therefore, PMPs are subject to change as historical records become more complete. Another drawback of statistical approaches is that they are not physically based; in other words, they do not consider the physics behind extreme rainfall generation. A physically based approach should be more amenable to generate realistic extreme rainfall events.

2.1.2 PMP Estimation using the Numerical Method

A numerical approach has been introduced to evaluate some of the assumptions adopted in the PMP estimation using the moisture-maximization method (Abbs, 1999). The advantage of this method lies in its capacity to simulate complex atmospheric processes upon rainfall (Abbs, 1999). Recently, a PMP estimation approach has been developed based on utilizing numerical weather prediction models (Ohara et al., 2011). Studies using numerical models have been carried out to estimate PMP in a variety of ways by using some meteorological factors (Ishida et al., 2015a; Ishida et al., 2015b; Ishida et al., 2018; Ohara et al., 2011; Tan, 2010; Yajima et al., 1996; Yigzaw et al., 2013).

To estimate PMP in the numerical method, similar to the moisture-maximization method, large events are selected in the maximization process. Then, hydro-meteorological conditions precluding these storms are used as input to a numerical weather prediction model. The PMP is obtained by modifying the initial condition to the most favorable boundary conditions which bring the largest depths of rainfall. For instance, moisture availability (usually by setting relative

humidity RH to 100%) increase, air temperature increase, initial and boundary conditions are shifted, and convergent wind fields artificially generate.

The main advantage of this approach is its independence from the usual assumptions in the PMP estimation, such as linearity between precipitation and PW. Moreover, since the atmospheric model directly simulates an extreme precipitation event, results are deemed more reliable than scaling a large rainfall with a factor. Meanwhile, a numerical model approach requires careful verification, as the physical basis has not been thoroughly established (Chen et al., 2017). However, up to now, the numerical method has not been widely validated. Further, there has been no comprehensive study investigating the key meteorological factors in the numerical model to estimate PMP (Chen and Hossain, 2018). This is because there is no consensus on how to physically “maximize” the historical storms for PMP estimation (Chen and Hossain, 2018). In addition, studies related to the numerical model have focused on storm maximization to estimate the “upper bound” of the precipitation.

2.1.3 PMP Estimation using the Moisture-maximization Method

The most widely used PMP estimation method is the moisture-maximization method (WMO, 1986, 2009), and various government agencies have adopted it for practical purposes (Rouhani and Leconte, 2016). The moisture-maximization method is based on the physical phenomena which take place upon extreme precipitation. The idea of this method is to select historical large storm events and maximize them using the atmospheric moisture ratio. The logic behind the method is in estimating the potential upper bound of the precipitation amount by maximizing the atmospheric moisture, which is related to storm formation and development (Rakhecha and Singh, 2009).

In the moisture-maximization method, the observed heavy rainfall is maximized to more extreme atmospheric conditions, using Equations (2-2a) and (2-2b). In these equations, $P_{observed}$ is the observed precipitation for the large storm event, PW_{max} is the climatological maximum precipitable water (PW) at the same particular time of year in the same location, PW_{event} is the representative PW for the event. In the PW_{max} , the maximum PW with a 100-year return period

estimated by statistical analysis, using the PW values for a rainy day and non-rainy day, has been used. This is because for PMP estimations with a short data-period less than 50 years (WMO, 1986), the maximum PW may not be representative of the “true” maximum value. Consequently, a maximum PW of a specified return period, e.g. 100-year, should be used instead (WMO, 2009). The moisture maximizing ratio (MMR) is a ratio of the maximum PW and event PW and is used to reflect extreme precipitation conditions.

$$PMP = P_{observed} \times (PW_{max}/PW_{event}) \quad (2-2a)$$

$$= P_{observed} \times MMR, \quad (2-2b)$$

In the process of moisture-maximization, the moisture for an individual storm can be maximized only up to a specific limit without altering the dynamic structure of the storm (Hansen et al., 1988). Adding excessive moisture to a rainfall event can alter its dynamics; if the moisture-maximizing ratio is too high, the basic assumption will become weak, and the original dynamic structure of the storm will change. Therefore, the MMR should be limited to maintain the original dynamic structure of the storm (Hansen et al., 1988). Thus, a confining upper bound needs to be determined for the MMR.

Initially, Schreiner and Riedel (1978) stated that if the MMR is greater than 1.5, it should be compared to PMP estimates in other nearby watersheds to ensure consistency. Later, it was suggested that for southeast Australia, the MMR should not exceed 1.8 (Minty et al., 1996). Further, in another study, the proposed limit was set to 2 for tropical storms in Australia, which was the second-largest (i.e., omitting the largest one) MMR (Walland et al., 2003). This limit was adopted in many other studies. To obtain reliable PMPs and to not produce exaggerated maximized PMP, the maximum value for MMR was set to 2.0 for events in summer/fall (CEHQ and SNC-Lavalin, 2003). Rousseau et al. (2014) applied the MMR of 2.0 because it was more recent and the limit is rather conservative.

In this method, precipitable water (PW) is one of the most essential meteorological factors to represent atmospheric moisture availability. The PW is defined as the depth of water in a column

of the atmosphere if all of the water in that column was to precipitate as rain. It can be measured directly through an upper air sounding of the atmospheric moisture profile, e.g., with a radiosonde. PW can be estimated from equation (3).

$$PW = \frac{1}{\rho_w g} \int_{p_1}^{p_2} q \times dp \quad (2-3)$$

Where ρ_w =density of water (g/m^3); g = gravitational acceleration (m/s^2); q = specific humidity or mixing ratio (kg/kg); p = pressure (Pa); and indices 1 and 2 = different atmospheric levels, usually 300 and 1,000 hPa (Chen and Bradley 2006).

However, because atmospheric moisture in the air column is difficult to observe directly, the PW is generally estimated using surface dew point (SDP) data, under the pseudo-adiabatic assumption. To characterize the available moisture feeding a storm under this assumption, a persisting dew point is usually employed as an index for representing the mean atmospheric moisture availability. A 1000-mbar, 12-hour persisting dew point is generally chosen for the estimation of the PW. The WMO (1986, 2009) tabulated the relationship between the PW and dew point under the pseudo-adiabatic assumption.

Studies based on the moisture-maximization method are widely conducted not only with historic observation data but also with outputs obtained from climate models and reanalysis data. The outputs from climate models have been used to derive PMP values based on the moisture-maximization method (Beauchamp et al., 2013; Chen et al., 2017; Kunkel et al., 2013; Rouhani and Leconte, 2016). Then, based on the moisture-maximization method, the PMP estimated using the climate model was evaluated to address the uncertainty of the PMP (Alaya et al., 2018; Rousseau et al. 2014). The outputs from reanalysis data were used to evaluate the climate models in the PMP estimation (Alaya et al., 2019; Chen et al., 2017; Rouhani and Leconte, 2016; Sheffield et al., 2013). Alaya et al. (2019) compared the PMP estimated using climate models to the PMP derived from reanalysis data. They mentioned that the reanalysis data and climate model outputs are useful to estimate the PMP.

2.2 PW Estimation using the Surface Dew Point

2.2.1 Pseudo-adiabatic Assumption

The pseudo-adiabatic process models the ascent of a saturated air parcel within a convective cell; the process is utilized to approximate the saturated water vapor in the air column. In the moisture-maximization method, it is assumed that air parcels follow the pseudo-adiabatic process from the surface of the atmosphere, and air parcels are condensed as soon as the air parcel ascends from the surface (Figure 2-1). This is called a pseudo-adiabatic assumption. In this assumption, the air parcel starts to ascend from the SDP. The water that condenses during the air parcel ascent is discarded as precipitation.

In the pseudo-adiabatic assumption, to create the atmospheric conditions for the immediate condensation of the atmospheric moisture (which is related to the PMP estimation), the SDP is a key factor, as it represents the temperature to which a given air parcel mass must be cooled to become saturated with water vapor (Schreiner and Riedel, 1978). Based on the SDP and pseudo-adiabatic assumption, a moisture adiabatic process (pseudo-adiabatic process) starts without a dry adiabatic process from the surface to the upper air (Figure 2-1). Thus, it is possible to achieve the immediate condensation condition on the atmospheric surface using only the SDP and pseudo-adiabatic assumption.

Accordingly, to approximate the total amount of water condensed under the pseudo-adiabatic assumption during an air parcel ascent, the SDPs should be utilized. If the SDPs can be obtained, it is possible to estimate the dew points; these decrease pseudo-adiabatically from the surface based on the pseudo-adiabatic lapse rate, in each atmospheric vertical layer. Subsequently, it is possible to estimate the amount of water vapor, by converting the dew points in the air column into the water vapor at each atmospheric vertical pressure. The dew point temperature is proportional to the amount of saturated water vapor in a given parcel of air. As a result, the total PW can be estimated by integrating the saturated water vapor into the air column.

If the actual observed atmospheric PW could be obtained, we could estimate the PMP without the estimated PW, based on the SDP under the pseudo-adiabatic assumption. However, it is difficult to collect the actual observed atmospheric PW. The atmospheric PW is mostly observed via radiosondes, but radiosonde data contains many missing and/or outlier values, and the observation period is generally very short. Radiosondes are also installed in relatively few areas. Hence, the pseudo-adiabatic process is one of the most important components for estimating the PMP. The moisture-maximization method for estimating the PMP was developed using the SDP under this assumption.

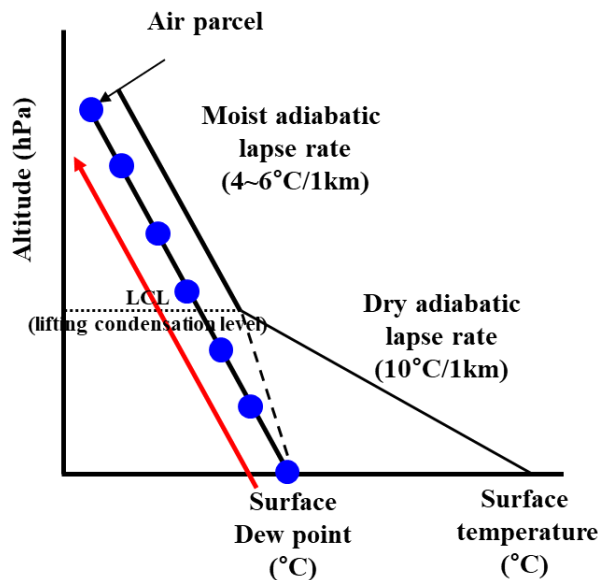


Figure 2-1. The pseudo-adiabatic process in the moisture-maximization method.

2.2.2 Problems of the Pseudo-adiabatic Assumption

Several problems related to the use of the pseudo-adiabatic assumption to estimate the PW have been identified.

First, it is difficult to represent the actual atmospheric moisture conditions using only the SDP. As the SDP is the temperature at which condensation begins on the surface, it might not represent the total moisture content of the air column. Generally, in the process of observing the atmosphere from the surface to the upper air using a radiosonde, actual atmospheric variables such as the dew point may fluctuate according to the altitude, without a constant pattern. However, if the pseudo-adiabatic process is assumed in the air column, dew points with a constant tendency are estimated by using a pseudo-adiabatic lapse rate for each atmospheric vertical pressure. Thus,

it is difficult to represent the fluctuations of the actual atmospheric conditions using estimated values with a constant tendency.

In addition, it is rare for all of the actual air parcels in an air column to be saturated during the parcels' ascent, unlike the estimated air parcels under the pseudo-adiabatic assumption. If the SDPs are relatively high and the air column is assumed that the pseudo-adiabatic process occurs from the surface to the upper air, the estimated PW under the pseudo-adiabatic assumption may be overestimated as compared to the actual PW, as it is difficult for an actual air column to be completely saturated from the surface to the upper air. Overestimation may also occur because a high SDP and low pseudo-adiabatic lapse rate effectively maintain the estimated dew points in an air column with rising altitudes; this is the result of a moist air mass on the surface (high SDP) having a dry mass above it (low actual dew points in the air column) (USWB, 1960). To reduce this variation, previous studies have suggested that the pseudo-adiabatic assumption should only be applied to heavy rainfall events or high-moisture cases (USWB, 1960, 1963). In such scenarios, the actual atmosphere would be relatively highly saturated, and the deviation of the assumed atmospheric conditions from the actual conditions would decrease. Hence, if the PW were to be estimated under the assumption of a non-rainy day, the estimated PW might not represent the observed PW in the actual atmosphere.

However, to estimate the maximum PW in PMP methodology, the PW values for a rainy day and non-rainy day (from a survey of long records) are generally combined. Therefore, although the pseudo-adiabatic assumption should be applied to heavy rainfall events or high-moisture cases, the maximum PW is estimated by combining all of the dew points for both non-rainy and rainy days. In general, the actual observed PW in an unsaturated atmosphere for non-rainy days might be lower than the estimated PW using the SDP under the assumption. Frequency analysis is also utilized to statistically determine the climatological maximum PW. Therefore, the maximum PW will be overestimated, owing to the dew points of the non-rainy days and the frequency analysis.

In some cases, the PW may be underestimated under the assumption. Chen and Bradley (2006) proposed that the estimated PW is higher in a warm season (high SDP temperature) and smaller in a cold season (low SDP temperature) than the observed PW. The reason for the underestimation is that the SDPs are generally low for the heavy rainfalls occurring in the cold season. The low dew points in an air column are estimated by a low SDP and high pseudo-adiabatic lapse rate, and the low dew points are converted into the low amount of PW. It indicates that a low

SDP leads to a low PW estimation under the assumption. This also means that the PW estimated under the assumption is highly related to the SDP temperature, but the actual observed PW has a relatively low correlation with the SDP. E.g. the actual observed dew points near the surface are sometimes higher than the SDP. Thus, the PW under the assumption is underestimated than the observed PW when dry air masses on the surface (low SDP) have moist air masses above (high actual dew points above the surface) (USWB, 1960). This phenomenon is frequently observed when the SDP is lower than the specific value of SDP.

As stated above, the pseudo-adiabatic assumption may not precisely reflect the actual upper atmospheric conditions. The accuracy of using this assumption may be highly related to the SDP temperature. Existing studies related to the moisture-maximization method have focused on identifying the deviation of the PW as estimated using the SDP from the actual observed PW, and there remains a lack of research on PMP estimation based directly on actual deviations in the air column occurring from actual atmospheric fluctuations (e.g., using profiles of the upper air). This study analyzes not only the deviation of the estimated PW (SDP approach) from the actual PW (UAD approach) but also the deviations in the air columns of atmospheric profiles assumed under the pseudo-adiabatic process from actual atmospheric profiles observed by a radiosonde.

Chapter 3

Uncertainty in the Moisture Maximization Method

First of all, to identify the uncertainty on the use of the pseudo-adiabatic assumption in PMP estimation, it is necessary to analyze the deviation between PWs estimated using the SDP and UAD approaches. Here, the SDP-based approach refers to the approach using the SDP under the pseudo-adiabatic assumption to estimate the PW. The UAD-based approach refers to the approach using the actual PW obtained from the upper-air data (UAD). The deviation analysis focused on the PMP variables, related to the moisture-maximization method proposed by the WMO (1986, 2009). Here, PMP variables mean the event PW, maximum PW, and MMR as shown in Equation 2-2. In this chapter, this study estimated the deviation between the SDP and UAD approaches for the PMP variables.

In this chapter, to obtain abundant atmospheric data spanning a long-term period, the actual PW and SDPs of JRA-55 are utilized, focusing on Japan. However, as the reanalysis data is simulation data obtained through data assimilation and not direct observations from a meteorological station, it is necessary to verify the JRA-55 data. Before utilizing such data, this study verifies it using atmospheric PW data obtained via radiosondes and using SDPs from data of the Automated Meteorological Data Acquisition System (AMeDAS) for the top 50 rainfalls in 10 areas with radiosondes. Through this process, this study estimates the correlation coefficient (CC) and root mean square error (RMSE) between the observed data and JRA-55 data for further analysis.

After being verified the reasonability of JRA-55, the PMP variables using the UAD approach are directly estimated using the total PW values, as obtained from the total column analysis fields of JRA-55 for the top 50 rainfalls at 30 points in Japan. The PMP variables using the SDP approach are indirectly estimated under the pseudo-adiabatic assumption by using the

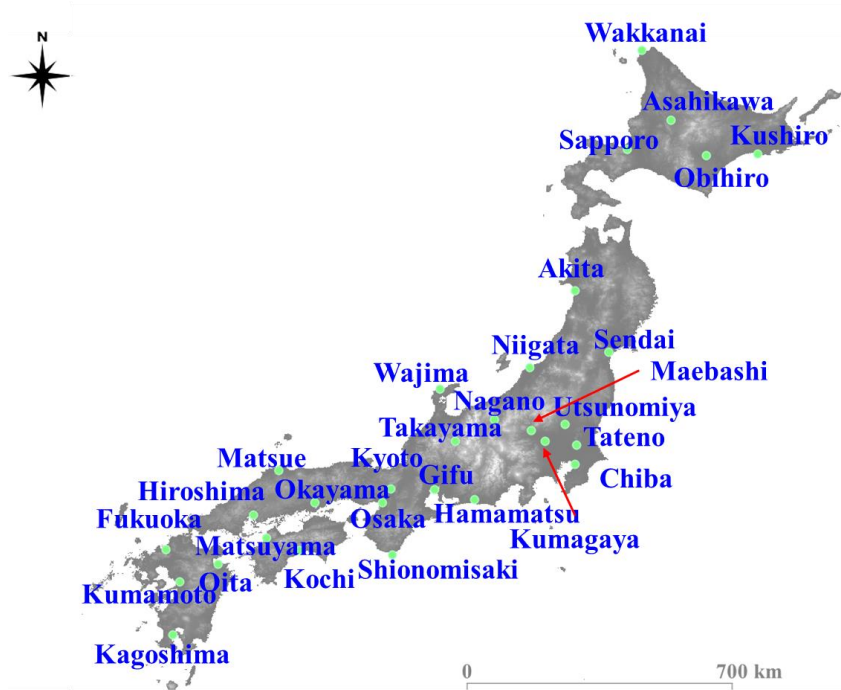
SDPs of JRA-55 for the same rainfall events. The variables using the UAD are compared with the variables using the SDP at each point. To quantify the deviation of the estimated variables from the actual ones, the average errors for the top three rainfalls at the 30 points in Japan are estimated, checking for positive or negative errors. All of these results are divided by the values from their respective regional points to analyze the correlations between the deviation and regional characteristics.

3.1 Data and Target Area

AMeDAS is a high-resolution surface observation network developed by the Japan Meteorological Agency (JMA) and is used for gathering regional weather data and verifying forecast performances. The observations at manned stations cover weather, wind direction and speed, types and amounts of precipitation, types and base heights of cloud visibility, air temperature, humidity, sunshine duration, and atmospheric pressure. All of these are observed automatically. In this chapter, this study utilized precipitation data and SDP data obtained from AMeDAS. To perform this study, 50 rainy days were selected, based on the heaviest 50 daily rainfalls (0–24 hours) for each selected point from 1960 to 2017. To verify the JRA-55 data, 12-hour persisting SDP data are extracted from data of AMeDAS from 1984 to 2017. Here, the 12-hour persisting SDP is the maximum value on one day from among the minimum values from the 12-hour moving window (Table 3-1).

A weather or sounding balloon is a balloon that carries instruments aloft. These instruments send back information regarding the atmospheric pressure, temperature, humidity, and wind speed, using a small, expendable measuring device called a radiosonde. Upper-air observations using radiosondes are carried out daily at regular intervals worldwide. In Japan, radiosonde observations are conducted at 16 local meteorological office stations nationwide, and at the Showa Station in Antarctica. In this study, to verify the PW data of JRA-55, 10 radiosonde stations were selected as shown in Figure 3-1 (b), and the daily maximum atmospheric PW data from 1984 to 2017 were extracted (Table 3-1). Radiosonde data provided by the University of Wyoming were also utilized.

(a) Target area in Japan



(b) The installed radiosonde in Japan

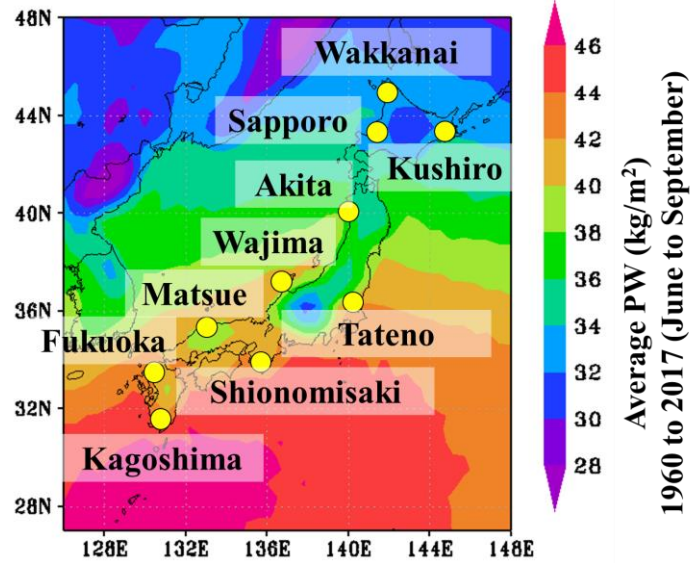


Figure 3-1. Target points in Japan. (a) The 30 selected points in Japan. (b) The points used to verify the JRA-55 data based on the installed radiosondes in Japan.

Table 3-1. Description of data sources used in this study.

Variable	Data source	Data period utilized (year)
Precipitation	Automated Meteorological Data Acquisition System (AMeDAS)	1960 to 2017
SDP	AMeDAS	1978 to 2017
	"Japanese 55-year Reanalysis" (JRA-55)	1960 to 2017
Precipitable water	Radiosonde	1978 to 2017
	JRA-55	1960 to 2017
Upper air variables (dew point, mixing ratio, and precipitable water (PW))	Radiosonde	1978 to 2017

Some potential instrumental problems and environmental factors may affect the quality and representativeness of the measurements from the radiosonde, particularly in the lowest layer of the troposphere (Connel and Miller, 1995; Free et al., 2002; Parlange and Brutsaert, 1990). There are also many missing and outlier values in radiosonde measurements, and generally, the observation period is very short in many countries. In addition, radiosondes are installed in very few areas of Japan. Hence, this study focused on reanalysis data to compensate for the limitations of the measurements.

Atmospheric reanalysis is a meteorological and climate data assimilation project, with an aim of assimilating historical atmospheric observational data spanning an extended period, using a single consistent assimilation scheme throughout. In Japan, a Japanese 25-year reanalysis was jointly conducted by the JMA and Central Research Institute of Electric Power Industry (Onogi et al., 2007). Then, based on the improvements, the JMA conducted a second Japanese global atmospheric reanalysis, i.e., JRA-55. JRA-55 produced a high-quality homogeneous climate dataset covering the last half-century during which regular radiosonde observations began on a global basis (Kobayashi et al., 2015). Many of the deficiencies of JRA-25 are alleviated in JRA-55, as the data assimilation system used for the project featured a variety of improvements introduced after JRA-25. In this study, to analyze the deviations between the actual and estimated variables, the SDP and total PW extracted from the JRA-55 data from 1960 to 2017 were utilized.

The SDP is the 12-hour persisting SDP, and the total PW is the daily maximum PW, as integrated from the surface to 300 hPa (Table 3-1).

In this study, the 30 points in Japan were selected for evaluating the assumption for PMP estimation, as shown in Figure 3-1(a). As Japan is surrounded by the sea, the inflow of moisture is likely to be a condition in high-moisture cases, and heavy rainfall events are frequent. It is also possible to analyze various local climatic characteristics, owing to the widely established topographic characteristics

3.2 JRA-55 Verification

The USWB (1947) previously argued that abundant upper-air data are required to sufficiently examine PMP estimations. In this study, JRA-55 reanalysis data was utilized to obtain the actual atmospheric PW and SDP data for all Japanese points. Using the reanalysis data, a large number of analyses could have been performed over a long-term period (60 years) at any point. In addition, atmospheric and surface data could be directly extracted. However, it was necessary to evaluate the availability of the JRA-55 data before utilizing JRA-55 in this study. This is because reanalysis-based data are simulation data obtained through data assimilation. This study verified JRA-55 using atmospheric PW radiosonde data, along with the dew points of the AMeDAS data at 10 points with radiosondes (Figure 3-1(b)).

Figures 3-2 and 3-3 show comparisons of the observed values with the JRA-55 data shown in Table 3-2. Table 3-2 shows the correlation coefficient (CC), root mean square error (RMSE). This study verified the data quality of JRA-55 for the 12-hour persisting SDP and atmospheric PW between the observed data and JRA-55 data based on the CC and RMSE values presented in Table 3-2. Consequently, most of the points show high correlations for the SDP and PW. Most of the points have CCs greater than 0.7 for the SDP and atmospheric PW. Additionally, the RMSE values were estimated. Most of the points indicated low RMSE values that were less than 10 (Table 3-2). From these results, this study determined that the accuracy of the JRA-55 data was sufficient for conducting further analysis.

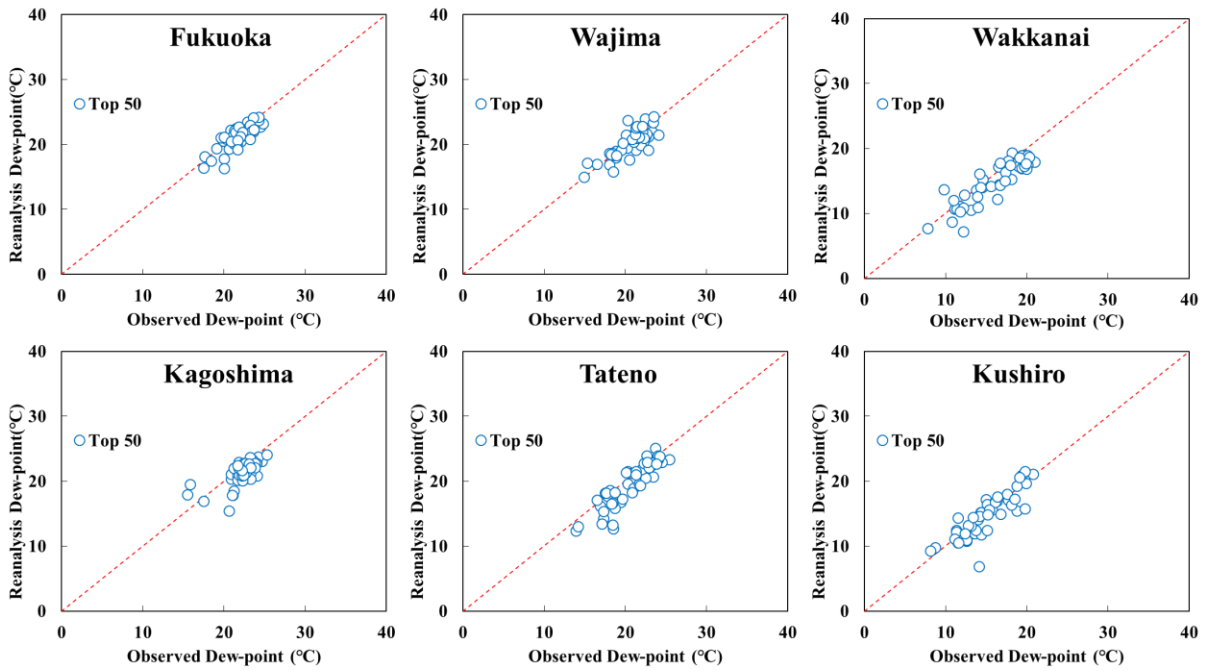


Figure 3-2. Comparison of observed SDP with SDP of JRA-55 for approximately 50 rainfalls at Fukuoka, Wajima, Wakkanai points, Kagoshima, Tateno, and Kushiro points.

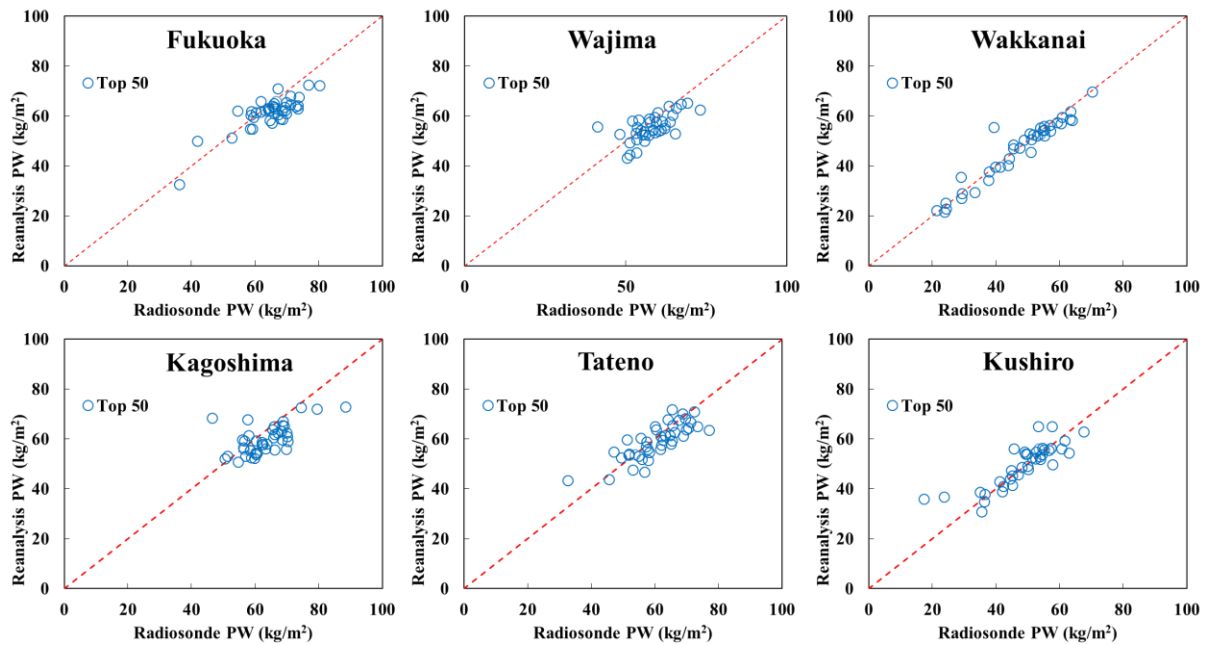


Figure 3-3. Comparison of observed PW with PW of JRA-55 for approximately 50 rainfalls at Fukuoka, Wajima, Wakkanai, Kagoshima, Tateno, and Kushiro points.

Table 3-2. Validation of reanalysis data by using CC and RMSE.

Station	SDP		Actual PW	
	CC	RMSE	CC	RMSE
Kagoshima	0.69	1.70	0.61	7.05
Fukuoka	0.77	1.23	0.83	5.56
Matsue	0.82	1.17	0.79	4.44
Shionomisaki	0.69	2.13	0.70	10.44
Wajima	0.77	1.44	0.64	5.48
Tateno	0.90	1.84	0.80	5.33
Akita	0.80	2.17	0.81	6.83
Sapporo	0.82	2.09	0.88	4.35
Kushiro	0.86	1.74	0.84	5.48
Wakkanai	0.88	2.09	0.96	3.63

3.3 Deviation Estimation of PMP Variables

In this study, to quantify the deviation of each PMP variable, errors between three PMP variables (event PW, maximum PW, and MMR) estimated using the two approaches were estimated (Equation 3-1). In this analysis, both the actual PW values in the UAD and the SDPs for estimating the PMP variables were extracted from JRA-55. To evaluate the pseudo-adiabatic assumption with a focus on heavy rainfall days, three rainy days based on the heaviest three daily rainfall periods (0–24 h) for each point from 1960 to 2017 were selected. This is because previous studies showed reasonable results regarding the moisture-maximization method based on the pseudo-adiabatic assumption for days of heavy rainfall (USWB, 1954, 1960, 1963). In this study, three daily rainfall events were extracted from the AMeDAS data.

$$Error (\%) = (variable_{SDP} - variable_{UAD}) / variable_{UAD} \quad (3-1)$$

Variable SDP refers to the variables (event PW, maximum PW, and MMR) of the PMP, as estimated using SDP data extracted from JRA-55 under the pseudo-adiabatic assumption. *Variable* UAD refers to the actual variables of the PMP, as estimated using the actual PW data in the UAD extracted directly from JRA-55. The errors were estimated using *variable* SDP and *variable* UAD . The errors are divided into positive and negative errors. A positive error indicates that the SDP-based estimation is greater than the UAD-based estimation. Meanwhile, a negative error indicates that the SDP-based estimation is lower than the UAD-based estimation.

3.3.1 Event PW

Before estimating the error of the event PW, the actual event PW (using the directly extracted actual PW) was compared with the event PW as estimated using the SDP under the pseudo-adiabatic assumption. As shown in Figure 3-4, this study analyzed the deviations between the UAD-based event PWs (using the actual PW) and the SDP-based event PWs (using the SDP)

Table 3-3. SDPs for the top three rainfalls (°C)

Points	Top 1 rainfall	Top 2 rainfall	Top 3 rainfall
Fukuoka	23.14	21.41	20.96
Kumamoto	22.37	21.08	22.29
Wajima	17.73	20.57	19.88
Kyoto	15.79	20.61	21.26
Wakkanai	17.05	12.84	13.81
Obihiro	16.37	17.76	10.13

for the top one, top three, and top 50 rainfalls, focusing on the heavy rainfalls at points in Fukuoka, Kumamoto, Wajima, Kyoto, Wakkanai, and Obihiro.

The Kumamoto and Fukuoka points show that the assumption is relatively reasonable, as the deviation between the SDP-based event PW and UAD-based event PW is very low for the top three rainfall events. However, the deviations between the two approaches at the Wajima, Kyoto, Wakkanai, and Obihiro points are greater. In particular, the SDP-based event PWs are underestimated more severely than the UAD-based event PWs for the top 50 rainfalls at the Wakkanai and Obihiro points (located in the Hokkaido area). Table 3-3 shows the SDPs for the heavy rainfall events. The SDPs for the top three rainfalls at the Wakkanai and Obihiro points are relatively low as compared with other points. These results indicate that the low event PWs using the SDP approach at the Wakkanai and Obihiro points might be caused by the low SDPs for the top three rainfalls. These results also imply that rainfalls indicating low SDPs may cause high deviations between the actual event PW and estimated event PW values.

To quantify the deviation between the two approaches, the event PW errors were estimated for 30 points in Japan. The results are shown in Figure 3-5, and express positive errors at the points in Fukuoka, Kumamoto, Kagoshima, Kochi, and Shionomisaki; the remaining 25 points show negative errors. Points with positive errors show a low error margin (within 15%). However, the points with negative errors show high error margins at some points, and in particular, the Hokkaido points show a very high error margin. High negative errors were also found at the Hiroshima and Osaka points in the western and central parts of Japan, as shown in Figure 3-5. As such, the SDPs for the top three rainfalls at all of the Hokkaido points may also be relatively low, along with the Obihiro and Wakkanai points. This indicates that the high deviation of event PW between the two approaches may be significantly related to the SDPs of heavy rainfalls at some points with negative errors. These results will be examined more closely in Chapters 4.

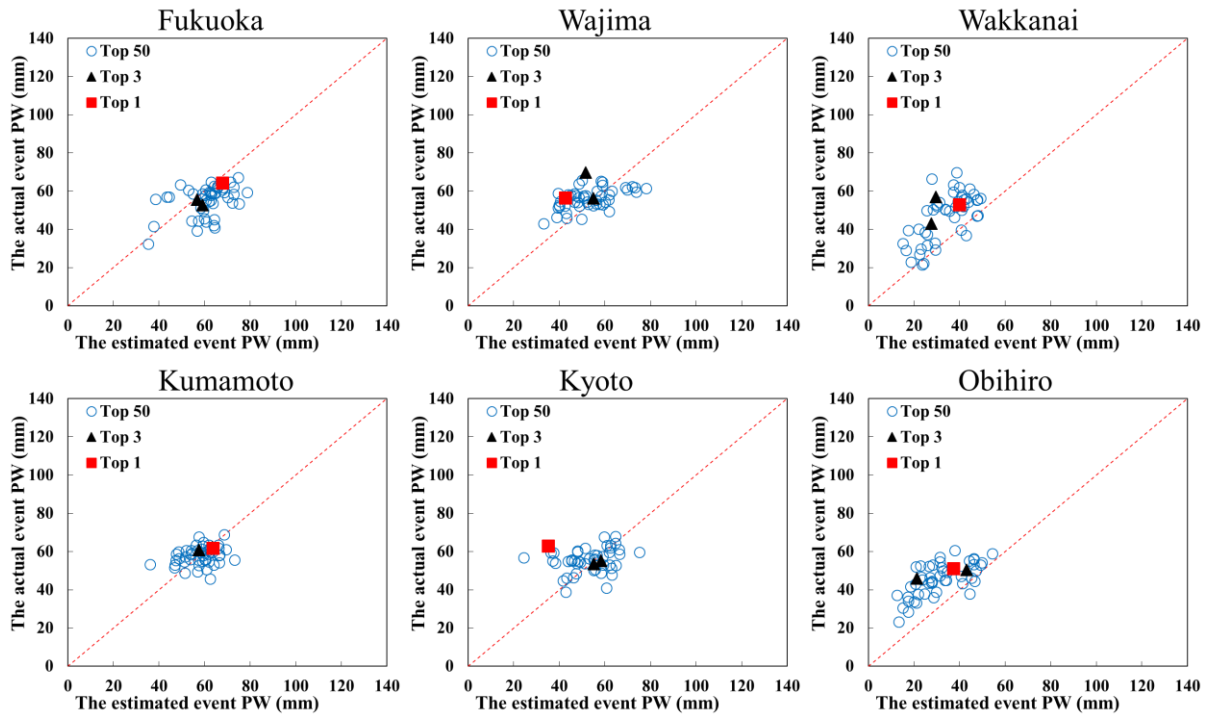


Figure 3-4. Actual event PW versus event PW estimated using the SDP under the pseudo-adiabatic assumption.

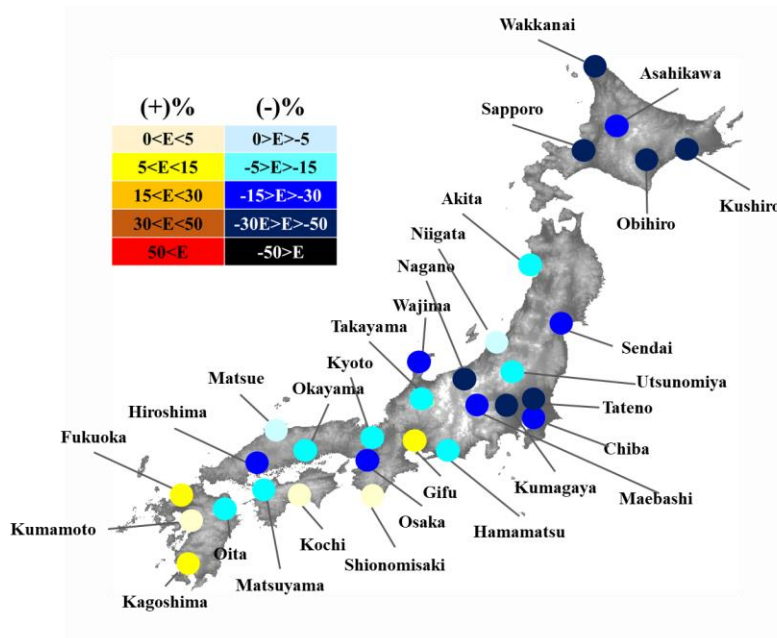


Figure 3-5. Resulting map of the average errors between the actual event PW values and estimated event PW values for the top three rainfalls at 30 points in Japan.

3.3.2 Maximum PW

The errors of the maximum PW values were estimated for 30 points in Japan. Before estimating the errors, the maximum PWs estimated using the SDP approach were compared with the maximum PWs estimated using the UAD approach, as shown in Figure 3-6. Unlike the event PW results, it is difficult to identify the regional characteristics of deviation. The maximum PWs using the SDP approach are overestimated than the UAD approach for the top three rainfalls in most areas. This is because the maximum PW is estimated using historical SDPs obtained from a survey of long records for both rainy and non-rainy days. The maximum PW is also estimated through a frequency analysis of the historical SDPs. Thus, if the frequency analysis includes data for both rainy and non-rainy days, the maximum PW is not sensitive to the individual selected rainfall event. These results are shown more clearly in Figure 3-7.

Figure 3-7 shows the errors of the maximum PW values at the 30 points. Other than the Wakkanai and Takayama points, all of the points show positive errors. This means that the maximum PW using the SDP approach is overestimated than the UAD approach in most areas. Although the errors at the Takayama and Wakkanai points are negative, their errors are close to 0%. In Figures 3-5 and 3-7, it is difficult to find the relationship between the results of the event PW errors and those of the maximum PW errors. Additionally, it is difficult to find the relationship of the maximum PW with the regional characteristics and Table 3-3. This may imply that the maximum PW errors are more affected by the frequency analysis and UAD or SDP data for non-rainy days than by the impact on the characteristics of the individual selected rainfall event.

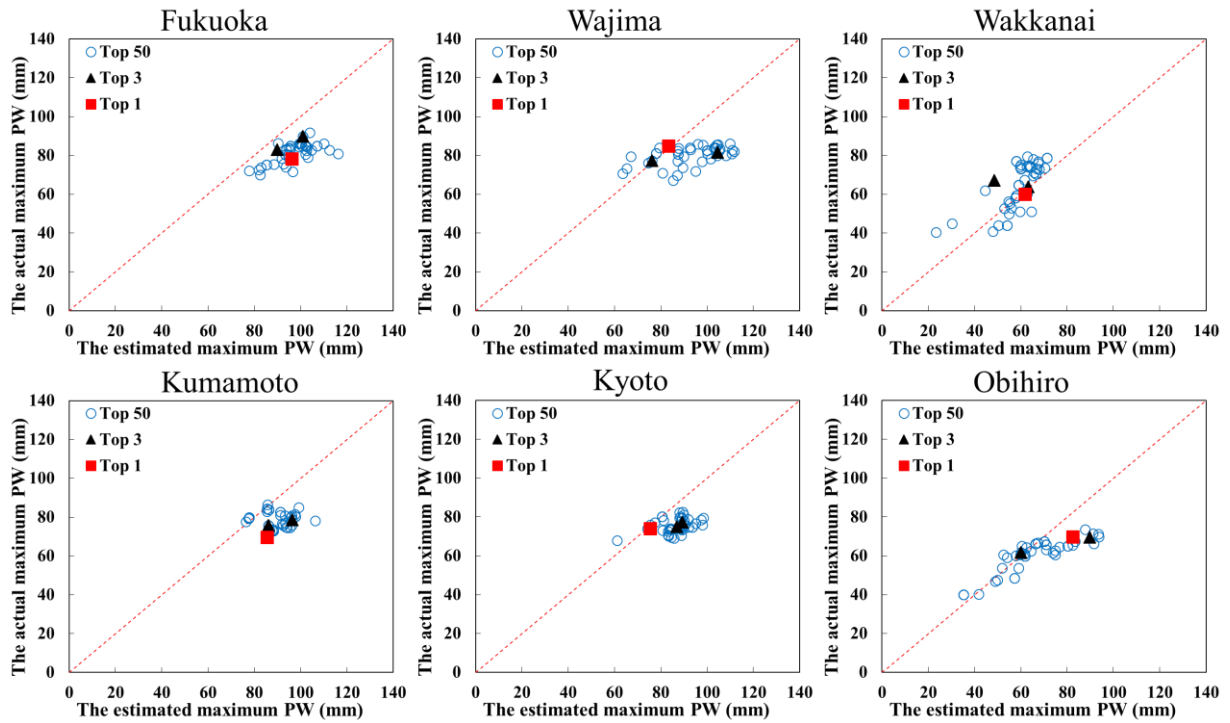


Figure 3-6. Actual maximum PW values using the actual PWs of the UAD versus maximum PW values estimated using the SDPs under the pseudo-adiabatic assumption.

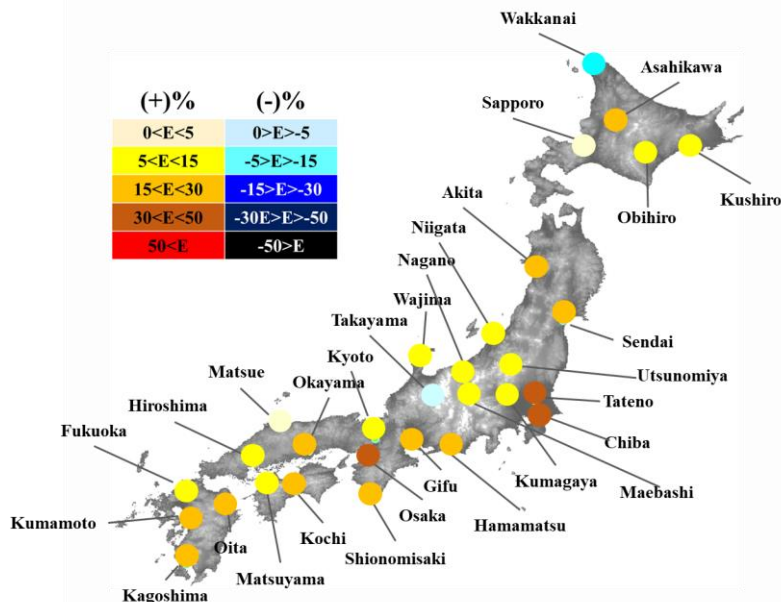


Figure 3-7. Resulting map of the average errors between the actual maximum PW values and estimated maximum PW values for the top three rainfalls at 30 points in Japan.

3.3.3 Moisture Maximizing Ratio

The MMRs were analyzed for the 30 points in Japan. Figure 3-8 shows the result of the comparison of the MMRs estimated using the two approaches at the Fukuoka, Kumamoto, Wajima, Kyoto, Wakkanai, and Obihiro points. At Fukuoka and Kumamoto points, although the MMRs estimated using the SDP approach are slightly overestimated than the UAD approach for the top three rainfalls, the points in Figure 3-8 for the top three rainfalls are very close to the dashed line. This means that the SDP approach can estimate the MMRs with a low deviation for the UAD approach at Fukuoka and Kumamoto points. However, the deviation between the two approaches increased for the top three rainfalls at Wajima, Kyoto, Obihiro, and Wakkanai points. In particular, the deviation is highest at Wakkanai and Obihiro points, located in the Hokkaido area. This result is similar to that of the event PW. This means that the deviation of the event PW may be related to the deviation of the MMR.

These results can be analyzed more clearly using Figure 3-9. As with the event PW and maximum PW, the errors of the MMRs are estimated for the 30 points and top three rainfalls, to quantitatively indicate the deviation between the two approaches. The MMRs show positive errors at all points, and the MMRs at 18 out of 30 points show error rates of more than 30%. The reasons for the high errors at some points are that the denominators (event PW values) mostly represent negative errors, and the numerators (maximum PW values) mostly represent positive errors.

Similar to the results for the event PW, significant errors in the MMR occurred in the eastern and northern parts of Japan, and the Osaka and Hiroshima points also showed high positive errors, i.e., greater than 50%. Therefore, the MMR may be significantly related to the SDP and event PW. However, the influence of the maximum PW cannot be ignored because all points have positive MMR errors, such as the maximum PW. Therefore, it is necessary to confirm the biggest source of error in the PMP variables in establishing the MMR error, to reduce the deviation of the MMR. This is because the PMP is estimated by directly using the MMR, but precipitation is a stabilized variable. In this study, to analyze the variables that influenced the MMR errors, the relationships between the PMP variables were also analyzed.

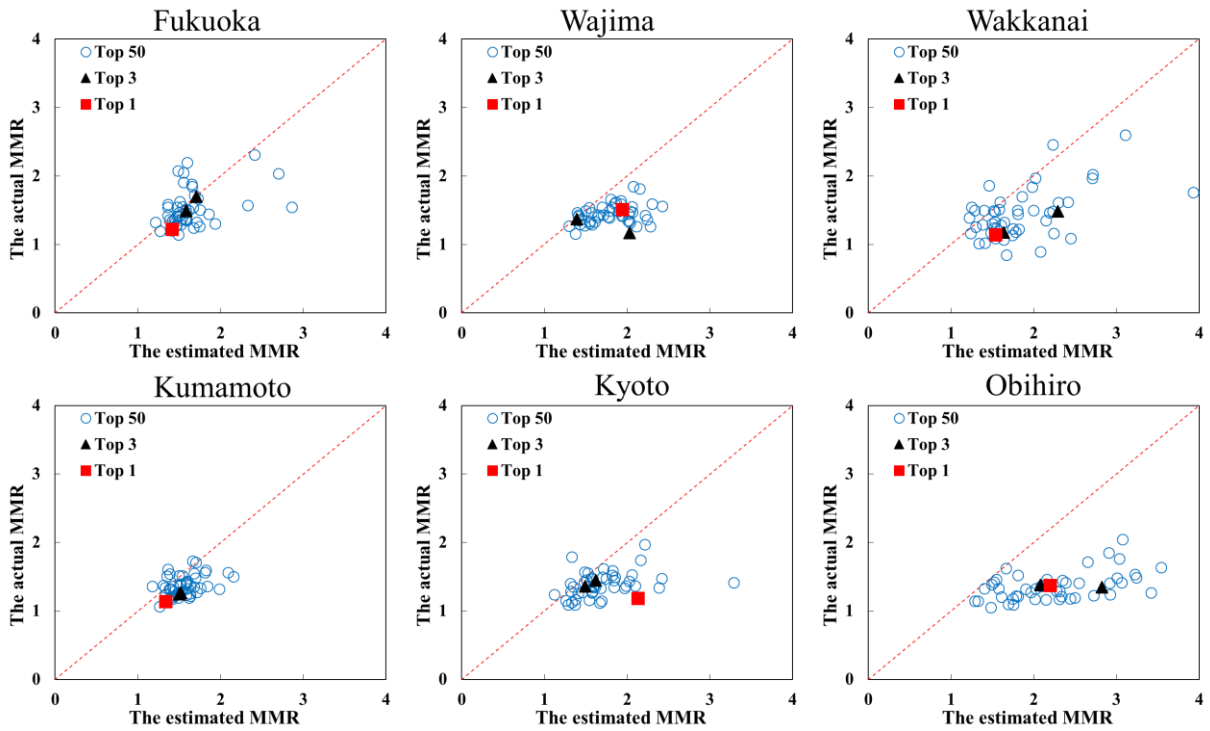


Figure 3-8. Actual moisture-maximizing ratio (MMR) using actual PWs of the UAD versus MMR estimated using the SDPs under the pseudo-adiabatic assumption.

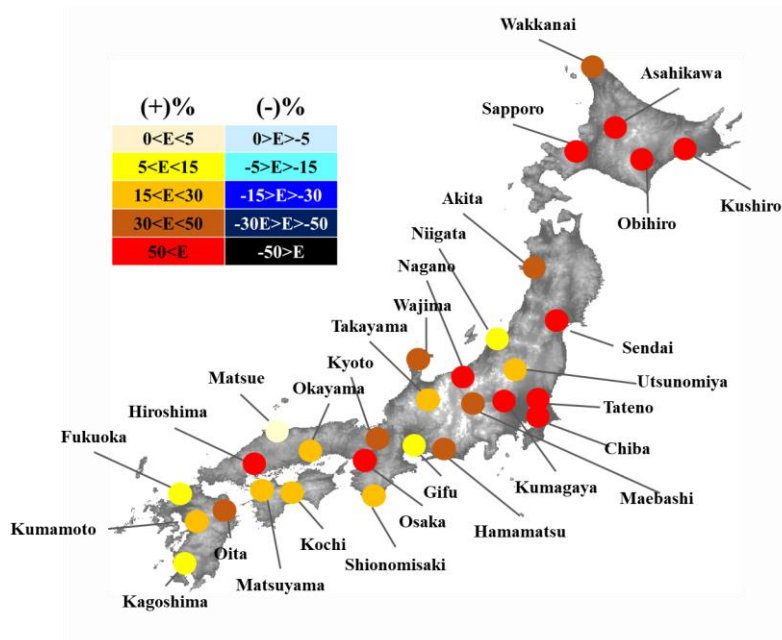


Figure 3-9. Resulting map of the average error between the actual MMR and estimated MMR for the top three rainfalls at 30 points in Japan.

3.4 Relationship of PMP Variables

If the MMRs are overestimated, it is also highly possible to overestimate the PMP. To prevent the overestimation of the PMP, it is necessary to determine the cause of the MMR overestimation. In this study, the relationships of PMP variables were analyzed. Figure 3-10 shows the event PW, maximum PW, and MMR for the top three rainfall events at all points. Unlike the case in the previous chapter, all of the points are not divided.

The range of the maximum PW errors is relatively small, from -10% to 40%, and the points of error are concentrated in the range of 10% to 30% (Figure 10(a)). Meanwhile, as shown in Figure 10(b), the event PW error shows a relatively large range as compared with the maximum PW error, and the points of the event PW error are evenly distributed in all areas from -50% to 10%. The MMR errors are widely distributed from 0% to 110%. Based on these results, this study analyzed the relationship of the maximum PW and event PW with the MMR. When the MMR error is close to 0%, a more reasonable PMP can be estimated. As the MMR error increases in the positive direction, the possibility of overestimating the PMP also increases. Therefore, a variable that allows for the MMR errors to be close to 0% finds.

In regards to the relationship between the maximum PW and MMR (Figure 3-10(a)), it is difficult to determine the tendency of the two variables or to determine a noticeable pattern between them. In contrast, the event PW and MMR show a high relationship, as illustrated in Figure 10(b). As the error of the event PW increases in the negative direction, the error of the MMR increases in the positive direction. In particular, if the event PW errors are less than -20%, MMR errors greater than 50% are found.

As a result, a high relationship between the event PW and MMR was determined. If the event PW error increases, the MMR error will also increase. This high relationship between the event PW and MMR can be also predicted from the methodology of the moisture-maximization method. The event PW is generally sensitive to the characteristics of the individual selected rainfall event such as the SDP and UAD during the rainfall. However, the maximum PW is not sensitive to the individual selected rainfall event because it is estimated via frequency analysis using the historically observed PWs or SDPs obtained from a survey of long records for rainy or non-rainy days, as mentioned in Chapter 3.2. Therefore, MMR exhibits a stronger relationship with the event PW than with the maximum PW.

Consequently, to determine the cause of the deviations of the MMR and PMP, it is necessary to identify the cause of the event PW error. The deviation between the actual event PW and estimated event PW may be related to the SDPs of the heavy rainfalls. In the next chapter, the relationship between the actual event PW values and SDPs will be analyzed for the top three rainfalls at all 30 points.

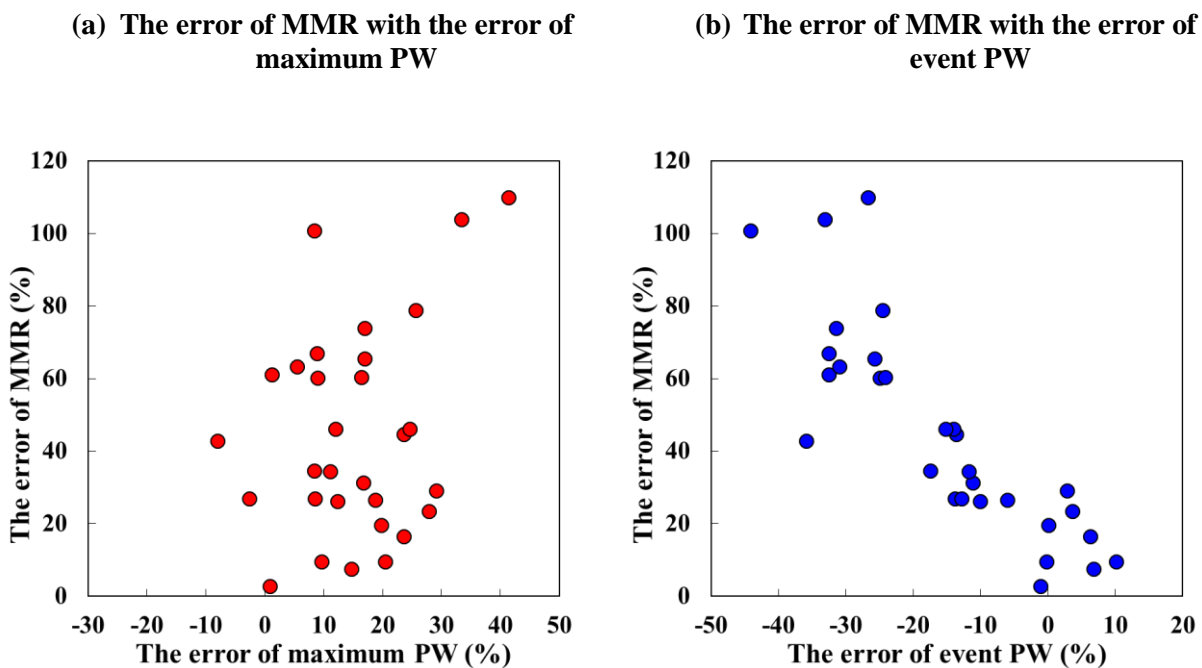


Figure 3-10. Relationship between the probable maximum precipitation (PMP) variable errors.

3.5 Conclusion

In this study, the PMP estimation methodology using the moisture-maximization method was evaluated to analyze the uncertainty of using the pseudo-adiabatic process. This chapter analyzed the deviation between the PMP variables estimated using the SDP and UAD approaches at 30 points across Japan. This study employed and verified the reanalysis data from “Japanese 55-year Reanalysis” (JRA-55) to consider abundant atmospheric data spanning a long-term period. The JRA-55 data showed good reliability, based on verification with observed SDPs and actual PW values at 10 points across Japan.

Then, using the JRA-55 data, the deviations were analyzed. To quantify the deviation, the errors between the PMP variables estimated using the SDP and UAD approaches were analyzed. The event PWs estimated using the SDP were more overestimated than the event PWs estimated using the UAD. In particular, the Hokkaido points with a relatively low SDP show a very high error margin. This indicates that the high deviation may be significantly related to the SDPs of heavy rainfalls at some points with negative errors.

The MMRs using the SDP were more underestimated than the MMRs using the UAD, especially in the northern parts of Japan with a relatively low SDP. This result is similar to the results for the event PW. To analyze the relationship between the event PW and MMR, the errors of event PW were compared with the errors of MMR. The event PW showed a high relationship with the MMR; if the event PW error increases, the MMR error will also increase. From these results, to figure out the cause of the deviations of the MMR and PMP, it is necessary to identify the cause of the event PW error.

Chapter 4

Evaluation on the Pseudo-adiabatic Process using Atmospheric Profiles

The deviation issues between PMP variables estimated using the SDP- and UAD-based approaches might be owing to the difficulty in reflecting the actual moisture in the air column using only the SDP, i.e., the limited information on the atmospheric surface, and the assumption for the saturated moisture conditions in the air column (Abbs, 1999; Minty et al., 1996; Papalexidou and Koutsoyiannis, 2006; Rouhani and Leconte, 2020). For example, the actual dew point profile in the air column as observed from a radiosonde (UAD approach) may fluctuate according to the altitude, without a constant pattern. Meanwhile, the estimated dew point profile from the pseudo-adiabatic process in the air column (SDP approach) is uniformly reduced according to the altitude. This is because the pseudo-adiabatic lapse rate, which is the rate of decrease in temperature with altitude under the saturated moisture conditions of the pseudo-adiabatic assumption, is used to estimate the dew points in the air column. In comparing the two profiles, the deviation would occur in the air column. Therefore, it is difficult to reflect the actual atmospheric conditions and profiles as opposed to using an estimated profile by the SDP approach.

It is necessary to systematically analyze why the deviation between the PW estimated using the SDP and the actual PW occurs in the air column. Previous deviation-related studies have focused on the fact that the deviation between the two approaches affects the result of the PMP estimation, but hardly any analysis has been conducted on how the pseudo-adiabatic assumption affects the deviation for the actual profiles in the air column and upper-air. For an in-depth analysis of the deviation as described in the previous paragraph, it is necessary to compare the observed atmospheric profile (UAD-based profile) to an atmospheric profile estimated using the SDP (SDP-based profile) in the air column and upper-air. In addition, the relationship between the SDP and

actual PW may vary significantly with climatic characteristics (Reber and Swope 1972; Robinson 2000; Viswanadham 1981). To evaluate the various deviation results with the climatic characteristics, the analysis should include identifying the climatic characteristics in each region and country.

To better understand the underlying assumption of the PMP methodology, this chapter analyzed the relationships between the SDPs and the actual PW values of the UAD for the top three rainfalls at all points selected in Chapter 3. An analysis was performed by integrating the 30 points into a single one, to thereby analyze the relationship between the actual PW values and SDPs commonly occurring in Japan. In addition, this chapter identified the impact on the deviation between the actual observed upper atmospheric condition, and the upper atmospheric condition estimated by the pseudo-adiabatic assumption in the air column.

Accordingly, this study analyzed and compared the profiles of the atmospheric variables observed from radiosondes (UAD approach) with those estimated by the pseudo-adiabatic assumption (SDP approach) according to the atmospheric pressure layers from the surface to 300 hPa, where the saturated air parcel is very thin. In general, the total PW was estimated by integrating the mixing ratio from the atmospheric surface to 300 hPa. The mixing ratio was estimated using the water vapor, as converted from the dew point at each atmospheric vertical layer. Hence, the dew point, water vapor, and mixing ratio were highly related to each other in the process of the total PW estimation. Thus, to identify the problems or limitations of using the assumption in the upper air, this study decided to analyze the dew point, mixing ratio, and PW integrated at each atmospheric vertical layer. The results make it possible to more clearly analyze the deviations resulting from fluctuations of the atmospheric variables, by analyzing deviations of the actual atmospheric conditions alongside the assumed atmospheric conditions.

4.1 Data and Target Area

To compare the observed atmospheric profile to an atmospheric profile estimated using the SDP in the air column, this chapter utilized the data observed from the radiosonde station. Radiosonde data provides the atmospheric profiles for each atmospheric vertical pressure in the

air column. This makes it possible to analyze the deviation between the actual observed atmospheric variables (UAD-based variables) and the atmospheric variables estimated through the pseudo-adiabatic process (SDP-based variables). This was based on the atmospheric vertical pressure layers from the surface to 300 hPa, i.e., where the saturated air parcel is very thin.

In general, the total PW is estimated by integrating the mixing ratio from the atmospheric surface to 300 hPa, and the mixing ratio is estimated using the water vapor converted from the dew point at each atmospheric vertical layer. The dew point, water vapor, and mixing ratio are highly related to each other in the process of the total PW estimation. In this study, to identify the deviation for the estimation PW in the air column, it decided to analyze the dew point, mixing ratio, and PW as integrated at each atmospheric vertical layer.

Target areas are selected based on the station installed radiosonde; which are Kagoshima, Fukuoka, Shionomisaki, Sapporo, Kushiro, and Wakkanai (Figure 4-1). The atmospheric data used were the dew point, mixing ratio, and accumulated PW from 1978 to 2017, based on a heavy rainfall day. The variables at the time of the highest total PW in one day were extracted. One of the top three rainfalls at each of the six points was selected to analyze the deviation. The selected rainfall locations were as follows: SDPs below 18 °C at the Sapporo, Kushiro, and Wakkanai points, and above 18 °C at the Kagoshima, Fukuoka, and Shionomisaki points.

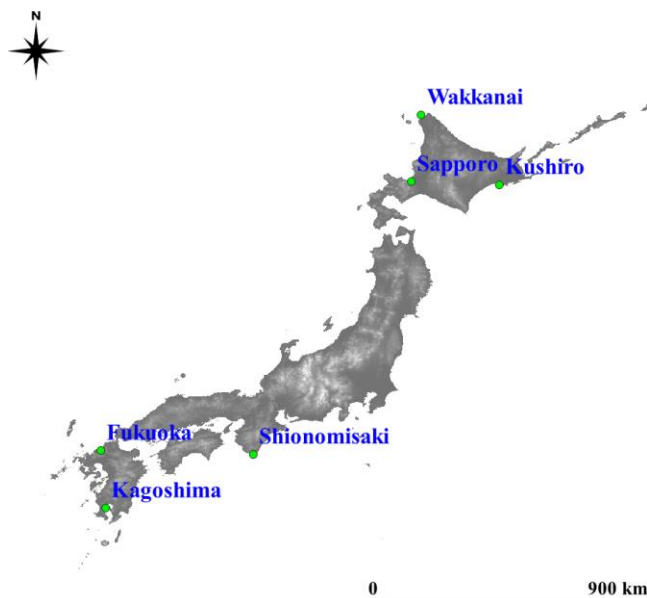


Figure 4-1. Target areas based on station installed the radiosonde.

4.2 Relation between Event PW and Surface Dew Point

As discussed in Chapter 3, there is a need to more thoroughly analyze the event PW to estimate an accurate PMP under the pseudo-adiabatic assumption. The high deviation between the actual PW (UAD-based PW) and estimated PW (SDP-based PW) may be highly related to the SDPs of heavy rainfalls at some points. Before analyzing the actual atmospheric profiles, the relationships between the actual PWs and SDPs were analyzed, using the estimated PW values for the top three rainfalls at all points (Figure 4-2). Unlike our approach in Chapter 3, the analysis was performed by integrating the SDPs and PW values at all 30 points, to determine the characteristics of the SDPs that can occur universally in Japan under the assumption.

Figure 4-2 shows the actual PW values and SDPs for the top three rainfalls at all 30 points. Each point represents the actual PW and SDP of the day at the same rainfall; the SDP is independent of the actual PW. The dashed line indicates the ideal curve when the total PW is pseudo-adiabatically estimated according to each SDP (pseudo-adiabatic curve). Therefore, if the points are close to the dashed line, the deviation between the SDP-based PW and UAD-based PW will decrease, and the PW will be more reasonably estimated under this assumption.

As shown in Figure 4-2, the points are close to the pseudo-adiabatic curve at the SDPs of 18 to 23 °C. This means that it is possible to more reasonably estimate the PW using the SDP approach within this range and that the deviation between the SDP and UAD approaches will decrease. In contrast, when the SDP is lower than 18 °C, the deviations will continue to increase, and the SDP approach will underestimate the PW more severely than the actual PW. An underestimated PW value can lead to an overestimation of the MMR, as mentioned in Chapter 3. This means that in terms of Japan's data, estimating the PMP using heavy rainfall events with SDPs below 18 °C may involve a significant deviation for the SDP-based approach

Chen and Bradley (2006) also reported that a pseudo-adiabatic process provides a more reasonable estimate of the atmospheric moisture conditions at SDPs above 20 °C than those using SDPs below 20 °C. Likewise, this study showed different magnitudes of deviations at each SDP for certain degrees. In particular, the PW as estimated by the pseudo-adiabatic process at the SDP below 18 °C showed a large deviation relative to the actual PW.

However, it is difficult to determine why different deviations occur at each SDP of specific degrees. The PW refers to the total humidity in the air column, but the SDP indicates limited humidity on the surface. It is difficult to analyze the phenomena occurring in the air column with limited information on the surface. Thus, it is necessary to analyze how the pseudo-adiabatic assumption and SDP affect the deviations of the actual profiles in the air column.

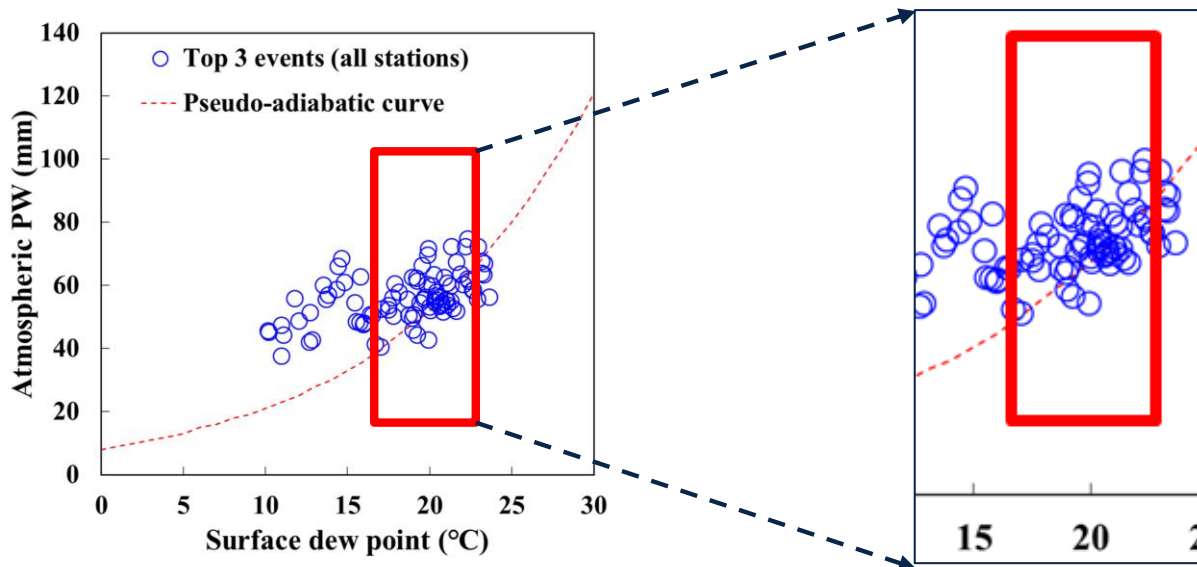


Figure 4-2. Actual PW values and SDPs for all of the top three rainfalls at 30 points. The dashed line refers to the ideal curve when the PW is pseudo-adiabatically estimated according to each SDP.

4.3 Atmospheric Profiles and Pseudo-adiabatic Profiles

To identify the deviation between the atmospheric variables observed in the air column (based on the UAD approach) and those estimated by the pseudo-adiabatic process (based on the SDP approach), the profiles of atmospheric variables observed from radiosondes were compared with those estimated by the pseudo-adiabatic assumption. In this study, to identify the deviation for the estimation PW in the air column, it decided to analyze the dew point, mixing ratio, and total PW integrated at each atmospheric vertical layer as these factors are highly related to each other in the process of the total PW estimation.

One of the top three rainfalls at each of the six points was selected. The selected rainfall locations were as follows: SDPs below 18 °C at the Sapporo, Kushiro, and Wakkanai points, and above 18 °C at the Kagoshima, Fukuoka, and Shionomisaki points. Rather than using the JRA-55 data as in the previous chapter, it used the actual data observed from the radiosondes to analyze the actual profiles of the atmospheric data at the radiosonde stations. This study directly obtained the actual observed atmospheric profiles for the upper air based on the selected heavy rainfalls and selected the SDPs of the AMeDAS data for the same heavy rainfall. The assumed atmospheric profiles were also estimated from the SDP by the pseudo-adiabatic process in the air column; specifically, the dew points in the upper atmospheric layers were estimated using the pseudo-adiabatic lapse rate.

4.3.1 Dew Point Profile from Surface to Upper-air

The degrees of the dew points represent the temperatures at which a given air mass is saturated with water vapor and is proportional to the amount of water vapor in the air column. The dew point can indirectly indicate the atmospheric moisture conditions in the upper-air; a higher dew point represents more moisture in the air column.

Figures 4-3 and 4-4 show the observed and estimated profiles of the dew point according to the atmospheric vertical pressures at the points in Kagoshima, Fukuoka, Shionomisaki, Sapporo, Kushiro, and Wakkanai. As shown in Figure 4-3, the Sapporo, Kushiro, and Wakkanai points show relatively low SDPs below 18 °C (points with low SDP). The Kagoshima, Fukuoka, and Shionomisaki points show relatively high SDPs of more than 20 °C, as shown in Figure 4-4 (points with high SDP).

The red dashed line indicates that the dew point profile was estimated in consideration of the pseudo-adiabatic lapse rate with the atmospheric vertical pressure. The blue line indicates that the dew point profile was observed directly from a radiosonde at the atmospheric vertical pressure. In Figures 4-3 and 4-4, all of the red dashed lines of the estimated dew point profiles show a constant reducing pattern. This indicates that the pseudo-adiabatic assumption allows the vertical profiles of atmospheric variables to have constant patterns, as the constant pseudo-adiabatic lapse rate is applied under saturated atmospheric conditions.

In Figure 4-3, the areas representing the low SDPs show that the red dashed line is below the blue line at most atmospheric vertical pressures. In particular, the deviation is very high from the surface to 500 hPa, and this deviation affects the underestimation of the total PW as estimated under the pseudo-adiabatic assumption. This is because the deviation is high in a range of atmospheric vertical pressure that can indicate a high atmospheric moisture content (i.e., the surface to 500 hPa). The actual dew point profiles also fluctuate according to the altitude, without a constant pattern. However, the dew point profiles estimated by the pseudo-adiabatic assumption show a constant tendency according to the altitude.

As a result, the actual atmospheric conditions in the upper air appear moister and fluctuate more than the atmospheric conditions estimated by the pseudo-adiabatic process at the low SDPs (Figure 4-3). It was also found that the observed dew point profile has a temporary increasing pattern near the surface, as shown in Figure 4-3. The atmospheric dew points temporarily increase with increasing altitude from the surface to 900 hPa in the estimated dew point profile. In particular, at points with a low SDP, the increasing pattern of the dew point profile is noticeable, as shown in Figure 4-3. This pattern may even affect the deviation of the PW estimation.

Figure 4-4 shows the points with high SDPs as a red dashed line above the blue line, but the deviation between the two lines is very low from the surface to 500 hPa, where there is higher

atmospheric moisture content. The deviation increases relatively slowly above 500 hPa, where there is relatively less atmospheric moisture content. Even though the dew point profile under the assumption was slightly overestimated than the observed dew point profile (especially above 500 hPa), the estimated dew point profile adequately follows the observed dew point profile in the upper air. Thus, the points with high SDPs might allow for a more reasonable estimation of the total PW. At points with high SDPs, the actual observed dew point profiles also show a constant tendency according to the altitude, similar to the estimated dew point profiles.

To find out the reason for the increasing pattern at low SDPs, this study analyzed the dew point profiles with the actual observed temperature profile in the northern areas (Figure 4-5). The purple line refers to the actual observed temperature profile in Figure 4-5. The temperature profile pattern is similar to the observed dew point profile pattern. This is because the relative humidity is almost 100% during the rainfall periods. The temperature profile also showed the temporarily increasing pattern near the surface only in the northern areas with low SDPs. This means that the surface is relatively cooler than near the surface if the temperature and SDP are lower than a specific value in the actual atmosphere.

It further analyzed the estimated dew point profile by focusing on the pseudo-adiabatic profiles described in Figures 4-3 and 4-4. In Figure 4-6(a), the difference between the SDP and dew point at 300 hPa increases, as the SDP is low. As the SDP is lower, the pseudo-adiabatic lapse rate (i.e., the decrease in the temperature of the air parcels undergoing a pseudo-adiabatic process as associated with elevation change) is higher. In other words, the pseudo-adiabatic lapse rates at points with high SDPs are relatively low, and the pseudo-adiabatic lapse rates at points with low SDPs are relatively large (Figure 4-6(a)). However, if only the observed profiles are analyzed, it can find different results from Figure 4-6(b). The differences in the actual observed dew point lapse rates between the low SDP points and the high SDP points are relatively smaller than the differences in the pseudo-adiabatic lapse rates between them, except at the Kushiro point. From these results, it can be inferred that the actual observed dew point profile is not significantly affected by the SDP. In particular, at points with low SDPs, the observed profile does not follow the estimated profile. As a result, a dew point profile estimated using the pseudo-adiabatic process in an air column cannot reflect the actual observed profile at points with low SDPs. Further, the estimated dew point profiles could not catch increasing pattern occurring near the surface because the only surface information is used to estimate PW in the pseudo-adiabatic assumption.

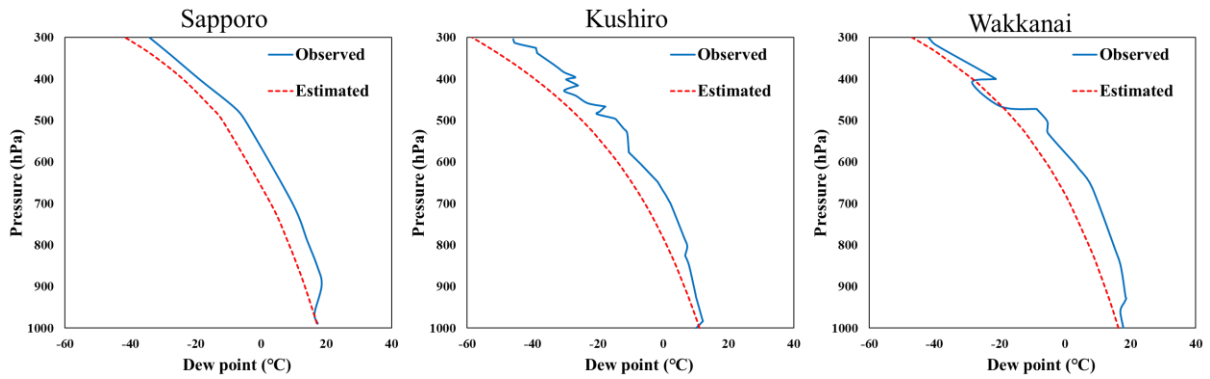


Figure 4-3. The dew point profiles observed from the radiosonde stations and those estimated using the pseudo-adiabatic lapse rate (Southern areas of Japan).

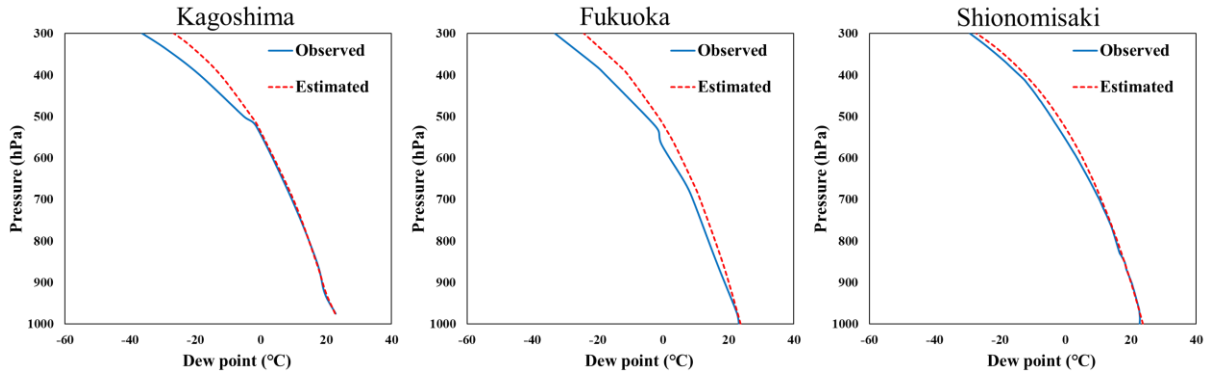


Figure 4-4. The dew point profiles observed from the radiosonde stations and those estimated by the pseudo-adiabatic lapse rate (Northern areas of Japan).

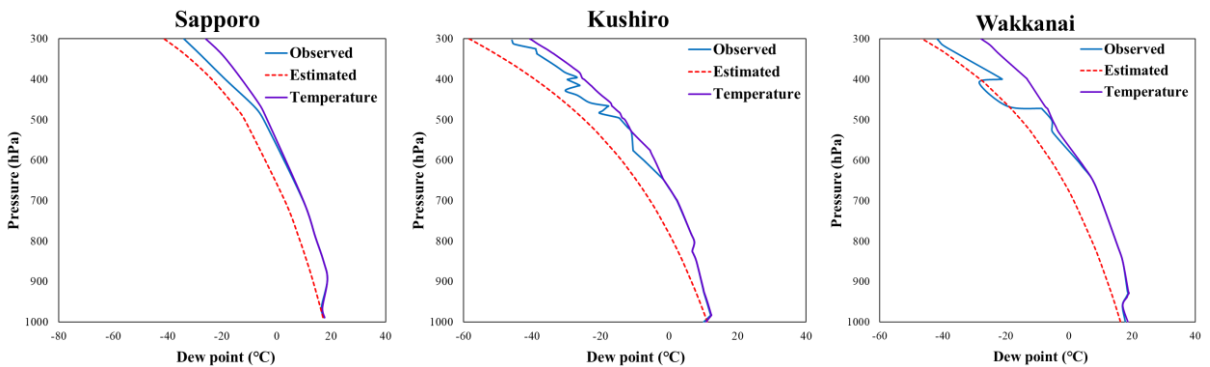


Figure 4-5. The dew point profiles observed from the radiosonde stations and those estimated by the pseudo-adiabatic lapse rate with the actually observed temperature profiles (Northern areas of Japan).

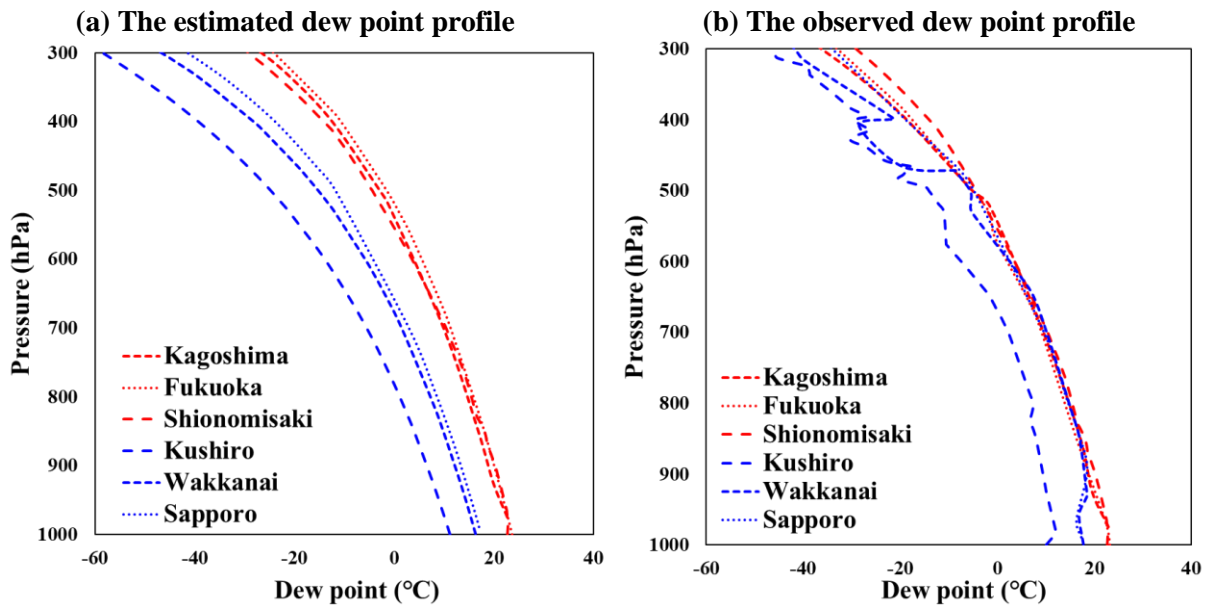


Figure 4-6. All of the dew point profiles from the surface to 300 hPa at the Kagoshima, Fukuoka, Shionomisaki, Kushiro, Wakkanai, and Sapporo points.

4.3.2 Mixing Ratio Profile from Surface to Upper-air

The mixing ratio is defined as the ratio of the mass of the water vapor to the mass of the dry air and functions well as a tracer of the movements of air parcels in the atmosphere. The water vapor is an essential factor for estimating the mixing ratio, and the mixing ratio is highly related to the dew point, as the water vapor can be estimated using the dew point. This study analyzes the mixing ratio and dew point in the air column.

Figures 4-7 and 4-8 show the mixing ratio profiles observed and estimated according to the atmospheric vertical pressures. Similar to the previous graph, the red dashed line refers to the mixing ratio profile as estimated using the dew point, and considering the pseudo-adiabatic lapse rate for each atmospheric vertical pressure. The blue line refers to the mixing ratio profile (hereafter, observed mixing ratio), as obtained using the observed dew point for each atmospheric vertical pressure.

Figures 4-7 and 4-8 show a pattern of deviation between the observed mixing ratio and estimated mixing ratio. The observed mixing ratios are mostly higher than the estimated mixing ratios at points with low SDPs, as shown in Figure 4-7. In particular, the total deviation from the surface to 700 hPa is higher than the total deviation from 700 hPa to 300 hPa. This indicates that the deviation increases from the surface to the middle of the atmosphere, rather than to the upper air (more than approximately 700 hPa).

This is also found that the increasing pattern of the dew point profile affects the mixing ratio near the surface. The observed mixing ratio profile does not decrease in a constant pattern as the altitude increases from the surface to the upper-air but shows a different pattern, in which the observed mixing ratio temporarily increases in a section between the surface and 900 hPa. This pattern will significantly affect the deviation of the mixing ratio, as it is generated near the surface, where moisture is concentrated. This could be easily observed at points with a low SDP; specifically, this pattern in Sapporo was more easily found, as shown in Figure 4-7. This pattern might also lead to a deviation of the event PW at low SDPs.

Figure 4-8 shows the points with a high SDP; the observed mixing ratios are slightly lower than the estimated mixing ratios, but the pseudo-adiabatic profile is reasonable, as the deviation is very low. The estimated mixing ratio profile lines follow the observed mixing ratio profile lines

very well. Similar to the observed dew point profiles at points with a high SDP, the observed mixing ratio profile shows a relatively constant tendency at points with a high SDP (Figure 4-8).

Therefore, the pseudo-adiabatic process can lead to a more reasonable estimation of the mixing ratio at points with a high SDP. Moreover, in the analysis of the mixing ratio, at points with a low SDP, the profile estimated by the pseudo-adiabatic process cannot reflect the observed profile. The deviation is highly related to the magnitude of the SDP.

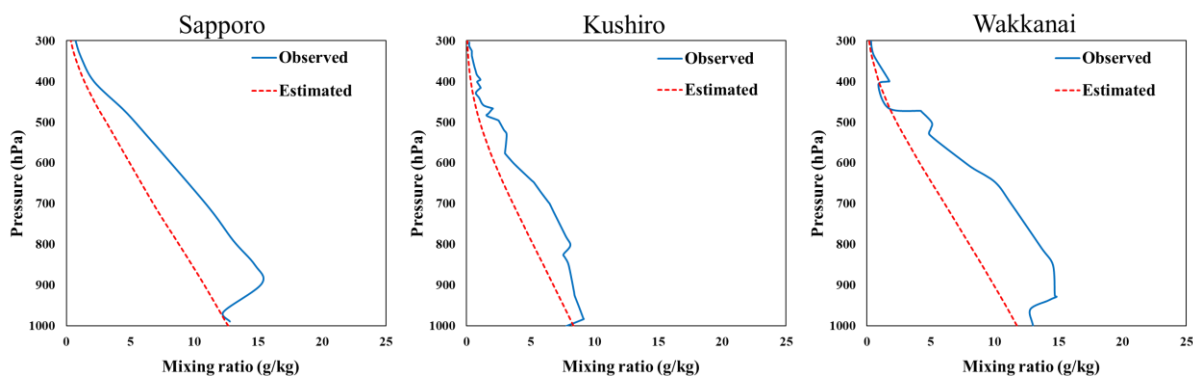


Figure 4-7. The mixing ratio profiles observed from the radiosonde stations and those estimated using the pseudo-adiabatic lapse rate.

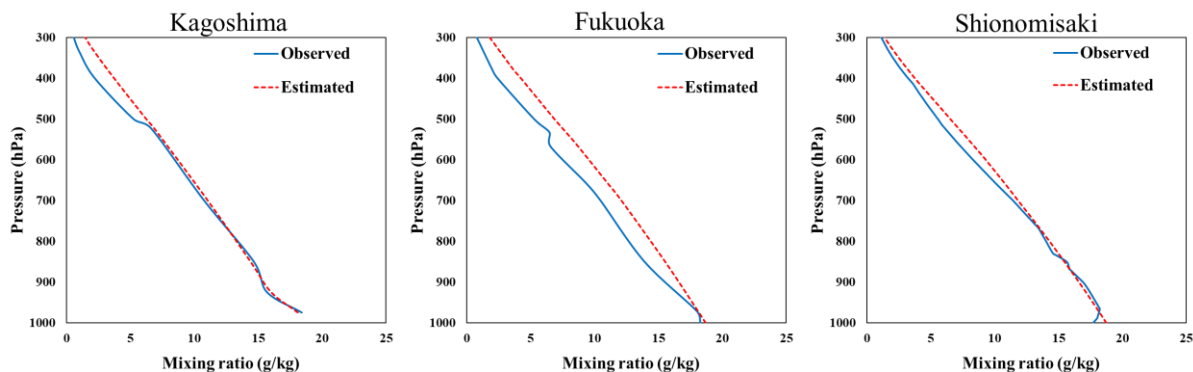


Figure 4-8. The mixing ratio profiles observed from the radiosonde stations and those estimated by the pseudo-adiabatic lapse rate.

4.3.3 Total PW Profile from Surface to Upper-air

Figures 4-9 and 4-10 show the accumulated PW profiles according to the atmospheric vertical pressure. The red line shows the PW profile estimated by integrating the estimated mixing ratio according to the rising altitude; this PW profile refers to the event PW as estimated using the SDP approach under the assumption. The blue line shows the PW profile obtained by integrating the observed mixing ratio according to the rising altitude; this PW profile refers to the actual event PW in the atmosphere as the PW obtained using the UAD approach.

To analyze whether the observed PW lines fit into the estimated PW for each dew point, dashed reference lines were drawn. The dashed lines show the PW values as estimated using SDPs of 17 to 22 °C under the pseudo-adiabatic assumption according to the atmospheric vertical layer, as with the red line. The reference PW profiles show a higher growth rate of the PW as the SDP increases. As mentioned in Chapter 4.3.1, this is because the pseudo-adiabatic lapse rate is relatively small at the points with a high SDP. If the SDP is higher, the PW will be highly estimated, as the high dew point can be maintained up to the upper air, owing to the low pseudo-adiabatic lapse rate.

Figure 4-10 indicates the points with high SDPs; the red line of the estimated PW follows the blue line of the observed PW very well. Figure 4-9 indicates the points with low SDPs; the red line of the estimated PW does not follow the blue line of the observed PW. The blue line of the observed PW profile is also analyzed in the context of the dashed lines. Although the SDP is less than 18 °C at the Sapporo and Wakkanai points, the blue line follows the dashed line of the SDP at values over 22 °C. This high deviation is probably due to an increasing pattern of the dew point near the surface (Figure 4-3). Even though the SDP was lower than 18 °C, the observed profile follows the reference line of the SDP higher than the actual SDP because the observed profiles start from the dew point increased near the surface.

The Kushiro point has different results from the Sapporo and Wakkanai points regarding the estimated PW. Even the actual observed PW is lower than the dashed line at 17 °C. This is because the rainfalls of the Kushiro point have a very low SDP of approximately 10 °C. However, even the Kushiro point confirmed that the observed PW was higher than the pseudo-adiabatically estimated PW at all atmospheric pressures.

As a result, the deviation between the observed dew point and estimated dew point from the surface to the upper air affects the mixing ratio and accumulated total PW. At points with a high SDP, the dew points, mixing ratios, and PW profiles estimated by the assumption can follow the actual observed profiles in the air column. In contrast, at points with low SDPs, the dew points, mixing ratios, and PW profiles estimated by the assumption cannot align with the profiles observed from the radiosonde in the air column. This means that the SDP may not reflect the actual atmospheric conditions in the upper air at a location with low SDPs and that the deviation between the observed and estimated profiles is highly related to the SDP.

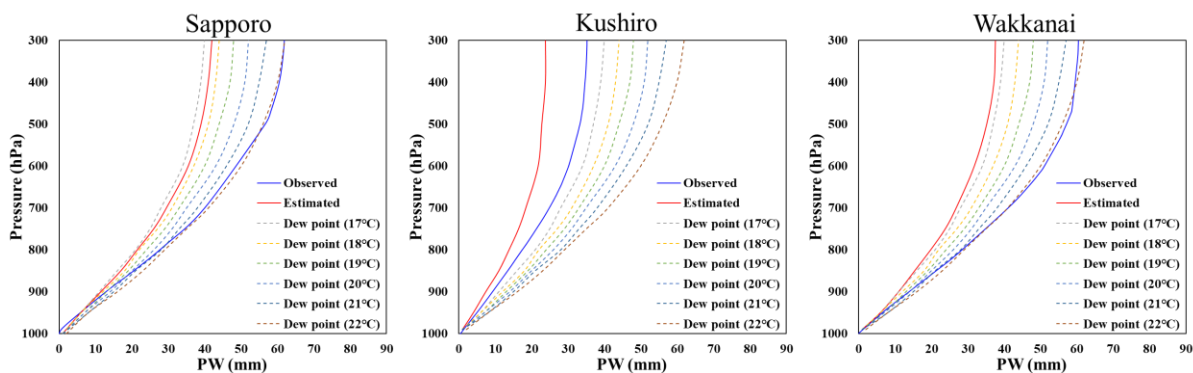


Figure 4-9. Accumulative PW profiles according to the atmospheric vertical pressure at Sapporo, Kushiro, and Wakkanai points.

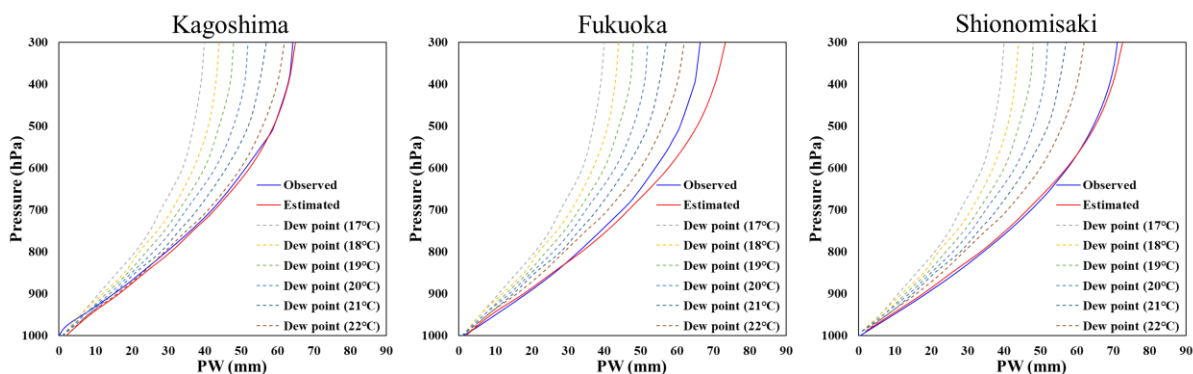


Figure 4-10. Accumulative PW profiles according to the atmospheric vertical pressure at Kagoshima, Fukuoka, and Shionomisaki points.

4.4 Discussion

The relationships between the actual PWs and SDPs were analyzed for the top three rainfalls at all points. As a result, this study found a high deviation from the actual PW when the event PW is estimated by the pseudo-adiabatic assumption at SDPs below 18 °C. Meanwhile, when the event PW is estimated by the assumption at SDPs of 18 to 23 °C, the deviation from the actual PW is very low. This means that it is possible to more reasonably estimate the PW using the SDPs within this range under the pseudo-adiabatic assumption. This also implies that the SDP approach estimates the event PW with a high deviation for the UAD approach at SDPs below 18 °C.

In addition, this analyzed the cause of high deviation between the two approaches occurring at SDPs below 18 °C by using the atmospheric profiles in the air column, The atmospheric profiles estimated by the assumption at SDPs below 18 °C do not reflect the actual atmospheric profiles observed in the air column. The actual dew point profiles fluctuate according to the altitude, without a constant pattern. Meanwhile, the dew point profiles estimated by the pseudo-adiabatic process show a constant tendency according to the altitude. As a result, the actual atmospheric conditions in the upper air appear moister and fluctuate more than the atmospheric conditions estimated by the pseudo-adiabatic process at relatively low SDPs below 18 °C. It was also found that the observed dew point profile has a temporary increasing pattern between the surface and 900 hPa. This pattern affected the deviation between PW estimations using the SDP and UAD approaches.

4.5 Conclusion

The pseudo-adiabatic process was used within the range of relatively high SDPs from 18 °C to 23 °C, the estimated dew point profiles adequately followed the observed dew point profile in the air column. The estimated PW with a significantly low deviation could be estimated. From these results, if the pseudo-adiabatic process is applied to estimate the PWs within the range of SDPs from 18 °C to 23 °C, a PMP with a significantly low deviation can be estimated. Hence, an assumption using only the SDP will make it difficult to estimate a reasonable PW for heavy

rainfalls with low SDPs. To reduce the deviation when using the pseudo-adiabatic assumption, a PMP estimation based on the moisture-maximization method should be carefully considered in regions and events with relatively low SDPs (e.g., lower than 18 °C).

Chapter 5

Evaluation on the Moisture-maximization method using Large Ensemble Climate Simulation Outputs

This study closely evaluated the PMPs estimated using the moisture-maximization method based on the SDP and UAD approaches. To obtain the abundant extreme rainfall events, the SDPs, and the actual PWs obtained in the UAD, we utilized the d4PDF data based on a large ensemble climate simulation outputs with the high-resolution. We extracted the rainfall, SDP, and UAD (actual PW) data from 1951 to 2010 for each area and each ensemble. This study focuses on the eight areas located in the southern and northern parts of Japan with clearly different climatic characteristics. This study did not consider climate change simulation; however, it used the d4PDF database for historical climate simulation. This study is divided into four parts to evaluate PMP estimation using the moisture-maximization method.

First, to examine the bias of the d4PDF data from the observed data, this study compares the daily rainfall, SDP, and actual PW in one ensemble of the d4PDF data with the observed data. A total of 50 rainfall cases obtained from the top 50 events in an ensemble are analyzed. This analysis was conducted in the Kagoshima, Fukuoka, Sapporo, and Kushiro areas where the radiosonde was installed to examine the PW.

Second, the deviation between the PMP variables (event PW, MMR, and PMP) estimated using the SDP and UAD approaches was analyzed for the top daily rainfall event per ensemble of d4PDF, and the deviation was estimated for a total of 50 rainfall events (50 ensembles). Here, the PMP variables estimated using the SDP were indirectly estimated under the pseudo-adiabatic assumption using the SDP data extracted from d4PDF. The PMP variables obtained using the UAD were estimated directly using the actual PW values obtained from the UAD of d4PDF. To quantify the deviation between SDP and UAD-based estimations, the average errors of 50 deviations for

each PMP variable were estimated, and the estimated PMP variables were represented as a box plot.

Third, the estimated PMPs were evaluated with empirically determined extreme-scale reference precipitation. The aforementioned analysis cannot evaluate the possibility of PMP over- and underestimation accurately because the method that more reasonably estimates the PMP cannot be identified. Therefore, there is a need to check if SDP and UAD approaches propose reasonable PMP estimates and to identify which method is more reasonable for PMP estimation. To assess the reasonability of the two approaches, the largest precipitation estimated without statistical models or methods by collecting annual maximum precipitation values for 3,000 years from the d4PDF database (50 ensembles and 60 years) is proposed as the reference value. This reference value corresponds to a 3,000-years return period in terms of the frequency of probable rainfall. This value was used to determine whether the SDP- and UAD-based PMPs of 50 ensembles were overestimated or underestimated. Errors between the PMPs and reference values were estimated to represent the deviation. The lower the average error between each PMP and reference value, the more reasonably is PMP estimated by avoiding the over- and underestimation possibility in this study.

Finally, this study applies an alternative in the northern areas of Japan with relatively low SDPs to avoid the possibility of PMP overestimation when the SDP approach is applied. This alternative is limiting the upper bound of MMRs estimated using the SDP. This study checks the limit of the upper bound of MMR by considering the tendency of MMRs in each area through the box plot. The SDP-based PMPs are estimated with the limited upper bound of MMR, and the average errors between the estimated PMPs and reference value are estimated. The average error is checked to identify whether the SDP-based approach can reduce the possibility of PMP overestimation.

Consequently, this study analyzes how much the SDP-based PMP estimation shows the deviation compared to the UAD-based PMP estimation. Then, the SDP and UAD approaches are evaluated focusing on the possibility of PMP over- and underestimation. Further, an alternative is applied to reduce this possibility, and the availability of an alternative is examined. These results allow more clearly analyzing the reasonability of PMP estimation based on the moisture-maximization method by evaluating it with a reference value estimated using a large ensemble simulation output called d4PDF.

5.1 Data and Target Area

5.1.1 d4PDF

The Meteorological Research Institute (MRI) of Japan recently produced a large ensemble climate simulation with a high-resolution atmospheric model—the “Database for Policy Decision-Making for Future Climate Change” (d4PDF) (Mizuta et al., 2017). To overcome the limitation of the length of extreme weather cases and meteorological factors, this study utilized the d4PDF database based on the large-scale ensemble climate simulation. The large ensemble simulations provide a large number of variables including temperature, dew point, and precipitation (Mizuta et al., 2017). The d4PDF shows promise for PMP evaluation as a dataset to perform a reliable extreme flood risk assessment. The d4PDF database is applied to a wide range of climate change impact assessments and to the current risk assessment of very-low-frequency phenomena such as floods and droughts (Doll et al., 2018; Faye et al., 2018; Kay et al., 2015; Lavender et al., 2018; Mori et al., 2019; Yang et al., 2018). The d4PDF is thus used in this study because its good applicability and reliability have been reported in many previous studies (Hanittinan et al., 2019; Tanaka et al., 2018; Tanaka et al., 2020).

This study uses the d4PDF database of dynamical downscaling around Japan with a 20-km-resolution nonhydrostatic regional climate model (NHRCM). The horizontal grid size is 211×175 , which covers Japan, the Korean Peninsula, and the eastern part of the Asian continent. The d4PDF database provides hourly weather data from 1951–2010 for 50 ensemble simulations, and this makes it possible to overcome the shortage of radiosonde data and estimate 50 PMPs. The precipitation, SDP, and actual PW were estimated from the d4PDF.

This study selected eight areas in Japan, as indicated in Figure 5-1. Japan is surrounded by the sea and it experiences a high-moisture condition through moisture inflow and frequent heavy rain events. Japan is useful for analyzing the deviation of local climatic characteristics because of the widely established geographical characteristics from the northern to the southern latitudes. The southern and northern areas of Japan with clearly different climatic characteristics were selected

to analyze the deviation between the two PW approaches and evaluate the possibility of over- and underestimation under different climatic conditions. Kagoshima, Fukuoka, Kochi, and Matsue are located in the southern part of Japan; these areas have relatively higher surface temperatures and SDPs than Sapporo, Obihiro, Asahikawa, and Kushiro, which are located in the northern part of Japan.

Table 5-1. Average precipitation and 12-hr persisting surface dew point (SDP) for the top rainfall events for each ensemble of 50 ensembles.

Area	Precipitation (mm)	Surface dew point (°C)	Location
Kagoshima	248.90	24.02	Southern part of Japan
Fukuoka	297.43	22.36	
Kochi	357.68	23.61	
Matsue	217.49	21.23	
Sapporo	162.76	14.79	Northern part of Japan
Obihiro	204.08	17.09	
Asahikawa	162.21	12.67	
Kushiro	173.13	16.57	

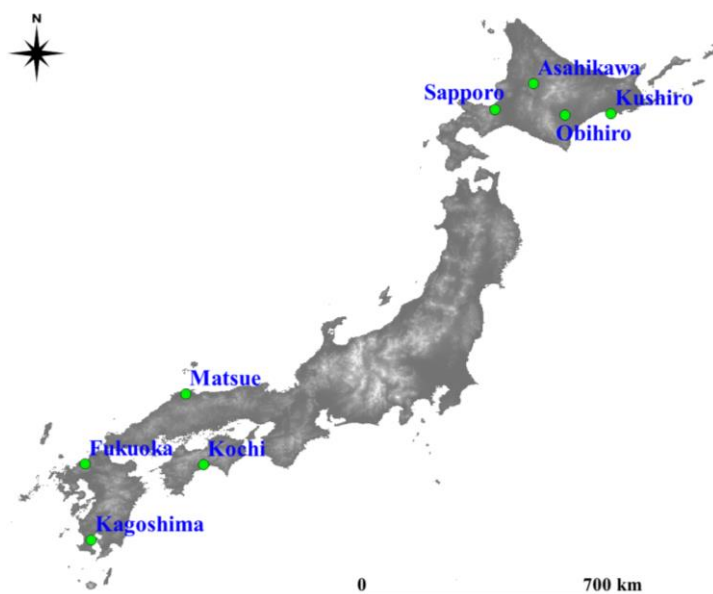


Figure 5-1. Target areas. Kagoshima, Fukuoka, Kochi, and Matsue are located in the southern part of Japan; Sapporo, Obihiro, Asahikawa, and Kushiro are located in the northern part of Japan.

Rainfall events are more frequent, and the magnitude of rainfall events in the southern areas is larger than that in the northern areas. Table 5-1 lists the average amount of precipitation and the average SDP for the top daily rainfall per ensemble of 50 ensembles. Kagoshima, Fukuoka, Kochi, and Matsue areas are located in the southern part of Japan, and they are adjacent to the coast. These areas have high SDPs and the magnitudes of rainfall, as listed in Table 5-1. Sapporo, Obihiro, Asahikawa, and Kushiro are located in the northern part of Japan. These areas have relatively low SDPs and rainfall magnitudes.

5.1.2 Comparison of the d4PDF Data and Observed Atmospheric Variables

To examine the availability of d4PDF data, the rainfall, SDP, and PW in one ensemble of the d4PDF database are compared with those of the observed data. The observed rainfall and SDPs are extracted from the Automated Meteorological Data Acquisition System (AMeDAS), and the observed PW is the value in the UAD extracted from the radiosonde. This analysis was conducted for Kagoshima, Fukuoka, Sapporo, and Kushiro areas where the radiosonde was installed to examine the PW.

Figures 5-2, 5-3, and 5-4 shows the histograms of daily rainfall, SDP, and PW for the top 50 rainfall events between June and September from 1973–2010. The first row shows the results of the comparison for rainfall. The second row shows the result of the SDP, and the third row shows the result of PW in the UAD. In all figures, the red bars refer to the data extracted from d4PDF, and the blue bars refer to the observed data. This comparison result can be confirmed more closely by the average values of the top 50 events for the d4PDF and the observed data, which are listed in Table 5-2. The error refers to the deviation of the average value of the d4PDF data for the average value of the observed data.

Although the d4PDF data in Kagoshima and Sapporo showed a slight bias for the observed rainfall, other areas show a relatively low error between the two data sets for the rainfall. The SDP shows a relatively low error between the two data sets in all areas. The PW data in Kushiro and

Kagoshima showed a slight bias between the d4PDF and observed data, but other areas show a relatively low error between the two data sets.

Even if there was a slight bias in some areas, the histograms of d4PDF and the observed data showed a very similar tendency. In Kagoshima and Fukuoka located in the southern part of Japan, the rainfall, SDP, and PW data for both the d4PDF and observed data showed high density with a relatively high magnitude of variables (e.g., average rainfall higher than 120 mm, average SDP close to 22 °C, average PW close to 60 mm). In Sapporo and Kushiro located in the northern part of Japan, the rainfall, SDP, and PW of both the d4PDF and observed data showed high density with a relatively low magnitude of variables (i.e., rainfall lower than 80 mm, SDP close to 15 °C, and average PW close to 40 mm).

Consequently, although there are slight biases between the two datasets, the biases are not significant, and the d4PDF data reflect local climatic characteristics well in the southern and northern areas of Japan, as indicated in Figures 5-2, 5-3, and 5-4 and Table 5-2. In addition, the d4PDF data are reliable and have been continuously applied to the analysis of very-low-frequency extreme rainfall (Hanittinan et al., 2018; Tanaka et al., 2018; Tanaka et al., 2020). This study determined that the d4PDF database is sufficient for conducting further analysis.

Table 5-2. Average rainfall, SDP, and PW of the top 50 events for the d4PDF and observed data.

Area	Rainfall (mm)			Surface dew point (°C)			PW (mm)			
	d4PDF	Observed	Error (%)	d4PDF	Observed	Error (%)	d4PDF	Observed	Error (%)	
Southern area	Kagoshima	120.0	166.6	-27.9	23.6	22.2	6.3	64.42	55.2	16.7
	Fukuoka	140.5	131.6	6.7	22.3	21.5	3.9	58.62	56.9	3.0
Northern area	Sapporo	60.6	75.0	-19.2	15.0	17.1	-12.2	39.86	40.1	-0.6
	Kushiro	81.2	75.3	7.9	14.7	14.4	2.2	46.99	38.8	21.0

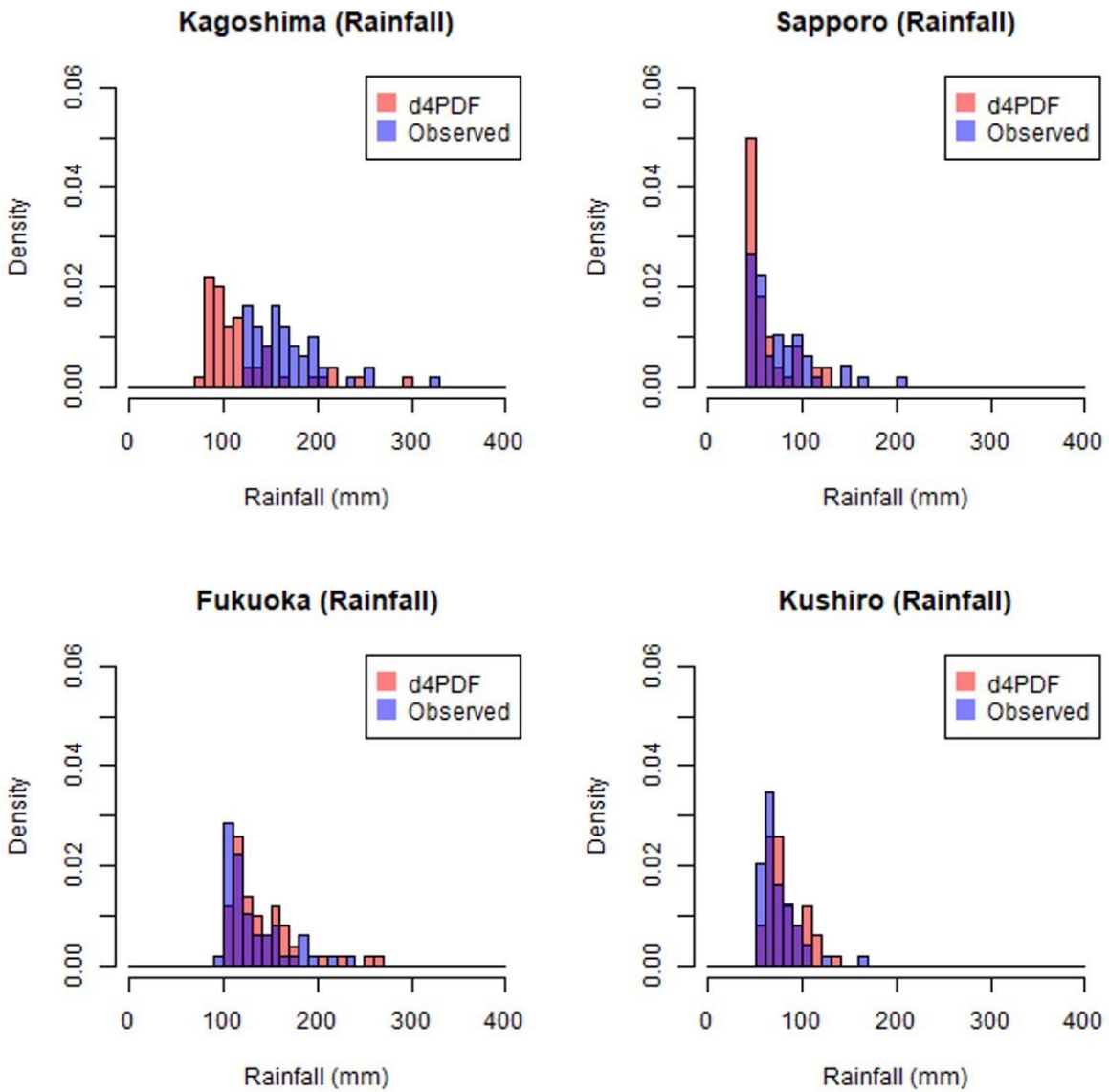


Figure 5-2. Histograms of daily rainfall extracted from d4PDF and from observed data.

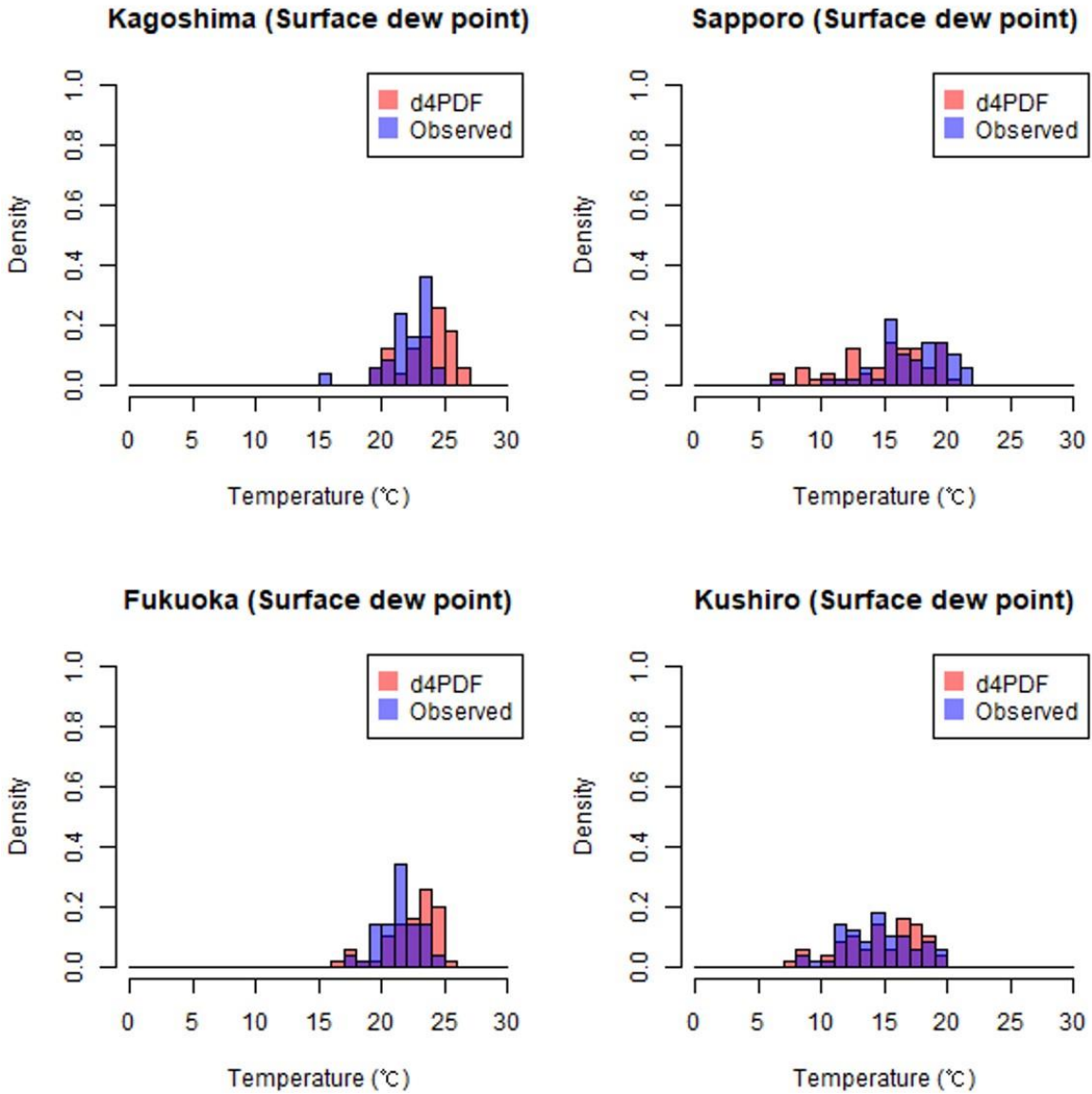


Figure 5-3. Histograms of daily surface dew point (SDP) extracted from d4PDF and from observed data.

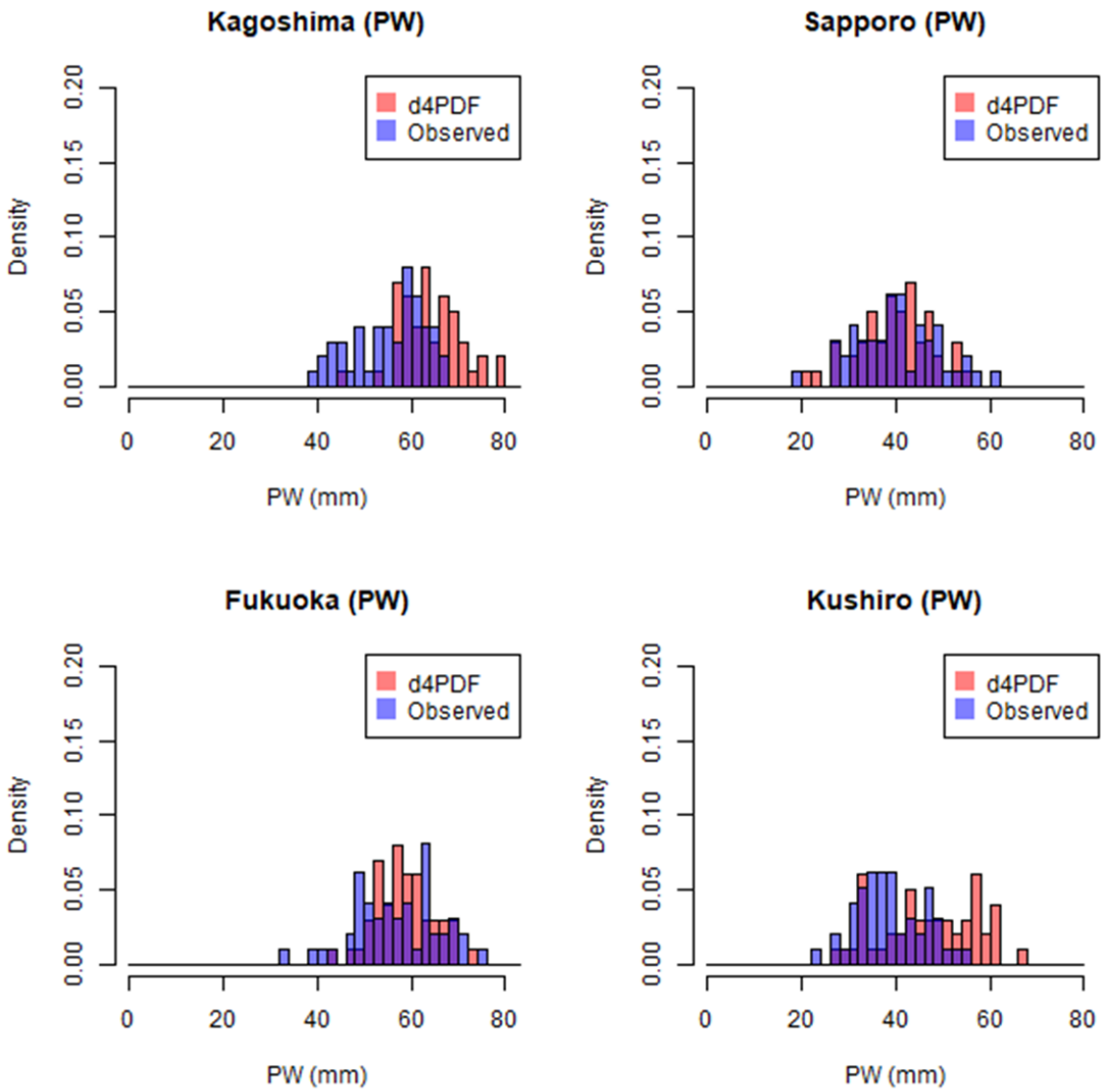


Figure 5-4. Histograms of daily precipitable water (PW) extracted from d4PDF and from observed data.

5.2 PMP Estimation and Comparison

In this study, PMP variables (event PW, MMR, and PMP) of the moisture-maximization method estimated using the SDP approach were compared with those estimated using the UAD approach. The deviation of the PMP variables between the two approaches was analyzed based on the top daily rainfall per ensemble (50 events) in the eight target areas. The deviation was estimated for a total of 50 rainfall of 50 ensembles (each top rainfall per ensemble). Further, this study estimated the average error values to quantify the deviation. The average error refers to the average deviation of the PMP variables estimated using the SDP for the PMP variables estimated using the UAD. The average errors are divided into positive and negative errors. A positive error indicates that the PMP variables using the SDP are greater than those using the UAD. Meanwhile, a negative error indicates that the PMP variables using the SDP are lower than those using the UAD.

5.2.1 Deviation of Event PW

Figure 5-5 shows the event PWs estimated using the SDP and UAD approaches for 50 rainfalls of 50 ensembles (each top daily rainfall). The upper figures show the result in the southern areas of Japan with high SDPs and a high magnitude of rainfall events. The bottom figures show the results in the northern areas of Japan with relatively low SDPs and a low magnitude of rainfall events. The position of each circle in Figure 5-5 indicates the deviation between the event PWs estimated using the SDP and UAD for each area. Table 5-3 lists the average errors for event PW in the eight target areas.

In Figure 5-5 and Table 5-3, the event PW demonstrated considerably low positive errors within 10% between the SDP and UAD approaches in the southern areas (Kagoshima, Fukuoka, Kochi, and Matsue). The northern areas (Sapporo, Obihiro, Asahikawa, and Kushiro) had high negative errors of over 15%, and the event PWs estimated using the SDP were more underestimated than the event PWs estimated using the UAD. These results indicate that the SDP approach could estimate the event PW similar to the UAD approach in southern Japan; however, the SDP approach may underestimate the event PW in the northern part of Japan.

To analyze the deviation closely, this study analyzed the deviation using the box plot for the event PWs, as shown in Figure 5-6. In the box plots, the upper/lower limit of the box represents the 75/25th percentile of the values; the upper/lower whisker represents the maximum/minimum values, and the outliers are denoted by a circle sign. The centerline of the box displays the median value. The range between the upper and lower limits of the box (75th percentile minus 25th percentile) indicates the variability and spread of the estimated values.

In the southern areas, the box of the SDP is located higher than the box of the UAD. This implies that event PWs using the SDP tend to be overestimated than that of UAD in the southern areas. However, in northern areas, the box of SDP is located lower than the box of UAD, which implies the SDP approach showed a tendency of underestimated event PWs compared to the UAD approach, especially in Kushiro.

Table 5-3. Average errors of the SDP-based event PWs to the UAD-based event PWs.

Area	Average error (%)	Location
Kagoshima	10.76	Southern part of Japan
Fukuoka	6.35	
Kochi	8.93	
Matsue	-2.31	
Sapporo	-20.12	Northern part of Japan
Obihiro	-20.70	
Asahikawa	-16.00	
Kushiro	-28.21	

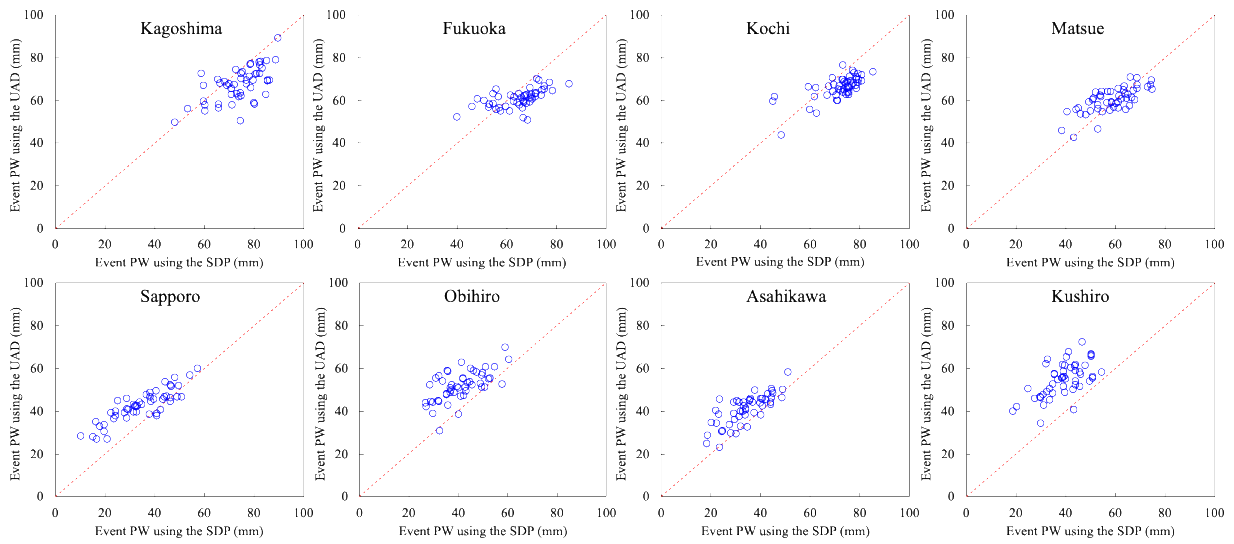


Figure 5-5. The SDP-based event PWs versus the UAD-based event PWs in Kagoshima, Fukuoka, Kochi, Matsue, Sapporo, Obihiro, Asahikawa, and Kushiro.

(a) Southern areas of Japan

(b) Northern areas of Japan

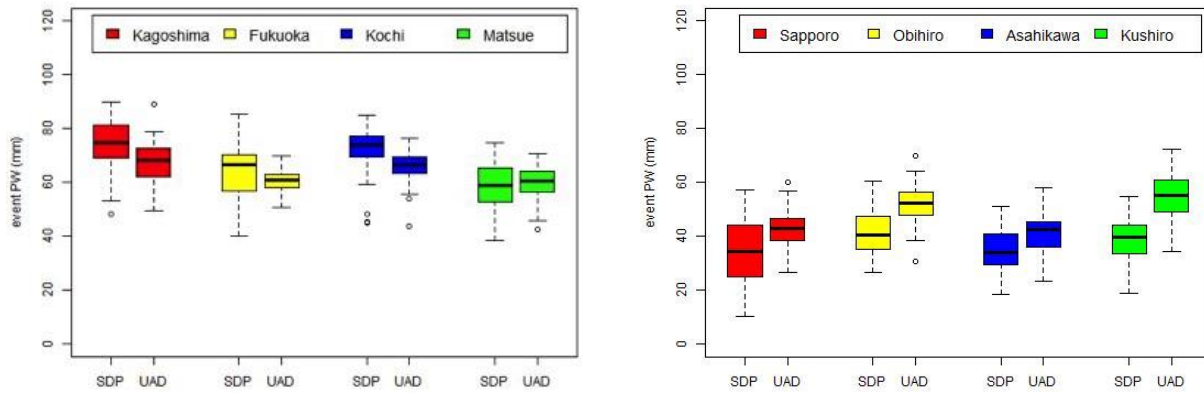


Figure 5-6. Box plots of event PWs estimated using SDP and UAD in eight areas.

5.2.2 Deviation of MMR

Figure 5-7 shows the MMRs estimated using the UAD and SDP for each top rainfall per ensemble (50 values of 50 ensembles). The position of each circle represents the deviation between the MMRs estimated using the SDP and UAD in each area.

In Figure 5-7, the SDP approach overestimates the MMR compared to the UAD approach in the northern area. The SDP approach slightly underestimated MMR in the southern area; however, the deviation between the two approaches was very low. Table 5-4 lists the average errors of the MMRs in each area. The average errors were considerably low in the southern area, but the northern areas showed relatively high average errors. These results indicate that the SDP approach overestimates the MMR in the northern region compared to the UAD approach.

Figure 5-8 shows the box plots of the MMRs estimated using the SDP and UAD approaches. In the southern areas, similar box plots were formed for an MMR of 2 or less in both SDP-and UAD-based estimations; the median value was between 1 and 1.5. The spread of the box plot was considerably similar in both approaches. These results suggest that the deviation of MMR is considerably small between the SDP and UAD approaches in the southern areas with high SDPs; MMRs estimated using the SDP approach have a tendency similar to that using the UAD approach.

However, in the northern areas, the box plots of the two approaches are considerably different. The spreads of MMRs using the SDP is considerably large, and the upper whisker showed an MMR of 2 or more. Meanwhile, in the UAD approach, the upper whisker showed an MMR of 2 or less, and most MMRs of the box plot are located at 2 or less. This implies MMRs estimated using the SDP had a tendency to considerably overestimate compared to the UAD. In this analysis, the tendency of overestimated MMRs for the SDP approach was recognized only in the northern areas with relatively low SDPs. Hence, the MMRs overestimated based on the SDP, and the deviation for both approaches may be significantly related to low SDPs.

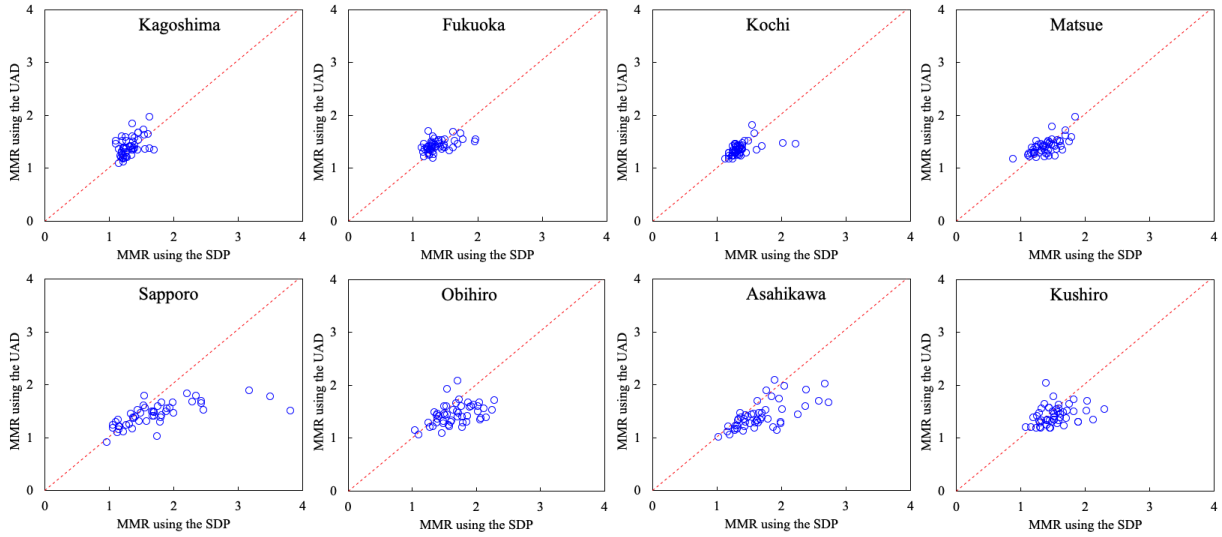
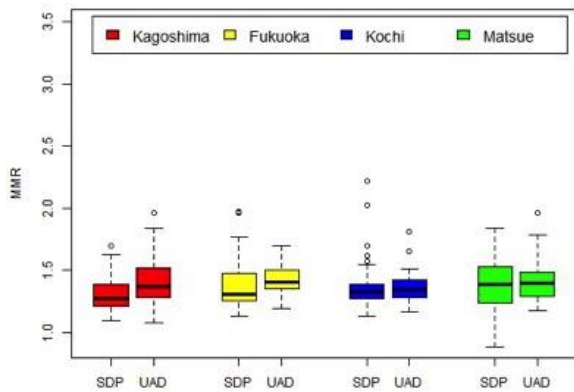


Figure 5-7. The SDP-based MMRs versus the UAD-based MMRs in Kagoshima, Fukuoka, Kochi, Matsue, Sapporo, Obihiro, Asahikawa, and Kushiro.

(a) Southern areas of Japan



(b) Northern areas of Japan

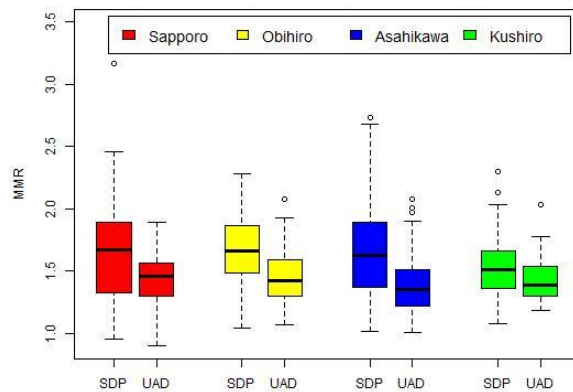


Figure 5-8. Box plots of MMRs estimated using the SDP and UAD in eight areas.

Table 5-4. Average errors of the SDP-based MMRs to the UAD-based MMRs.

Area	Average error (%)	Location
Kagoshima	-5.22	Southern part of Japan
Fukuoka	-2.58	
Kochi	0.93	
Matsue	-0.43	
Sapporo	19.08	Northern part of Japan
Obihiro	16.37	
Asahikawa	19.49	
Kushiro	8.98	

5.2.3 Deviation of PMP

Figure 5-9 shows the PMPs estimated using the UAD and the SDP for the top daily rainfall per ensemble (50 values of 50 ensembles). In the southern areas, the points are close to the dashed line. This means that the deviations are very low between the two approaches, and the SDP approach can estimate the PMP similar to the UAD approach. However, the deviations of PMP were relatively high between the two approaches in the northern areas, and the SDP approach overestimated the PMPs compared to the UAD based PMPs. These overestimated PMPs are due to overestimated MMRs in the northern areas. These results are more detailed in Table 5-5. Most average errors of PMP showed higher than 10% in the northern areas, but the average errors showed less than 5% in the southern areas.

Figure 5-10 shows box plots of the PMP values using MMRs estimated from the SDP and UAD. The results of PMP showed different deviations in the southern and northern areas as indicated in the MMR results. In the southern areas, the box plots of SDP and UAD were quite similar at similar PMP locations (y-axis). The median, spread, maximum, and minimum values of

SDP showed similar results with the UAD approach. In the northern area, the box plot of SDP was located above the box plot of UAD. This implies that in the northern areas with a low SDP, PMPs estimated using the SDP tend to be overestimated than that estimated using the UAD. These high deviations of PMP may be attributed to the SDP approach underestimating the event PW compared to the UAD approach in the northern areas.

Figure 5-11 shows the average errors for event PW and PMP. In the southern areas, both the event PW and PMP showed low average errors. Meanwhile, in the northern areas with low SDPs, the event PW showed high negative errors, and the PMP showed high positive errors. This implies the SDP approach underestimates the event PW and overestimates the PMP rather compared to that for the UAD approach, in the northern areas of Japan with low SDPs. In addition, Figure 5-11 indicates that the error of event PW may be related to the error of PMP.

This relationship was indicated by Kim et al. (2020); they suggested that high negative errors of the event PW affect the high positive errors of PMP. Further, they identified the relationship between the high error of event PW and low SDP by comparing the vertical profiles of atmospheric variables (dew point, mixing ratio, and PW). The estimated profiles (SDP-based estimated variables in the air column) were underestimated compared to the observed profiles (UAD-based observed variables in the air column) for all vertical atmospheric pressures in the areas with low SDPs. This deviation caused a high error of the event PW in areas with low SDPs. Consequently, the high deviation of the SDP-based PMP for the UAD-based PMP was highly related to the event PW and low SDP.

Then, the possibility of PMP overestimation or underestimation should be evaluated to determine whether the SDP- and UAD-based PMP estimations are reasonably estimated, and to identify which method is more reasonable to estimate PMP. However, based on only the aforementioned analysis, it is difficult to evaluate the possibility of PMP over- and underestimation for the SDP and UAD approaches because the method that more reasonably estimates the PMP cannot be identified. If the UAD approach underestimated the PMP, the SDP approach may be able to reasonably estimate PMP in the northern areas. Hence, a reasonable extreme-scale reference value is required to evaluate the possibility of PMP over- and underestimation for each approach.

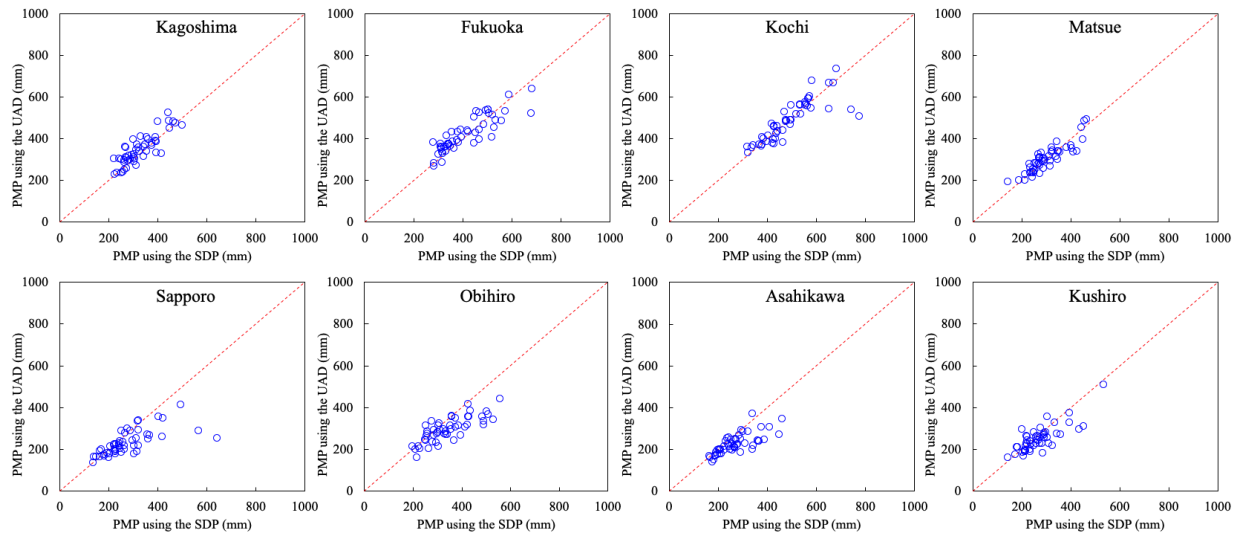


Figure 5-9. The SDP-based PMPs versus the UAD-based PMPs in Kagoshima, Fukuoka, Kochi, Matsue, Sapporo, Obihiro, Asahikawa, and Kushiro.

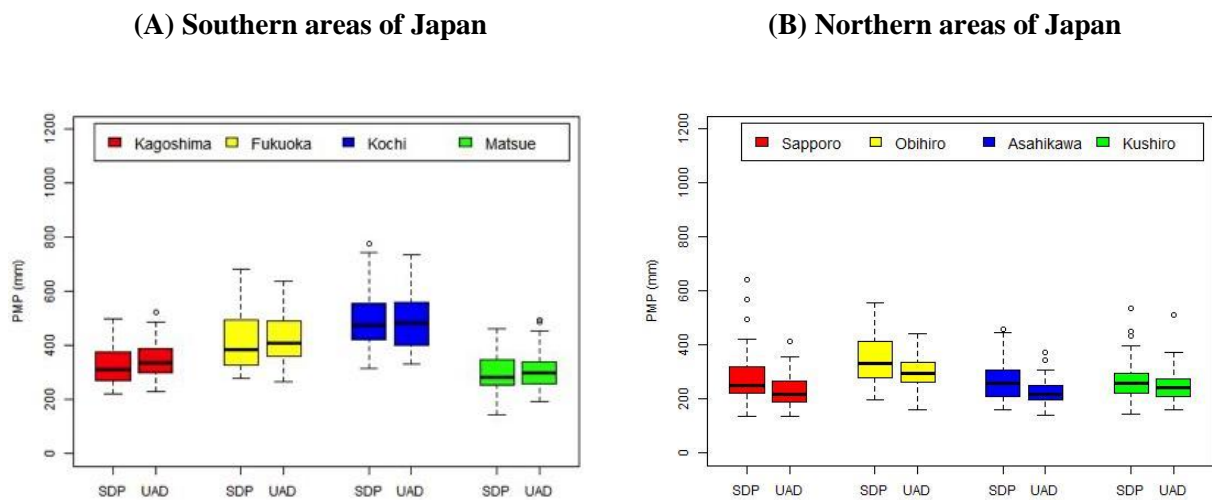


Figure 5-10. Box plots of PMPs estimated using the SDP and UAD in eight areas. (a) Areas located in the southern part of Japan with a relatively high SDP.

Table 5-5. Average errors of the SDP-based PMPs to the UAD-based PMPs.

Area	Average error (%)	Location
Kagoshima	-5.22	Southern part of Japan
Fukuoka	-2.58	
Kochi	0.93	
Matsue	-0.43	
Sapporo	19.08	Northern part of Japan
Obihiro	16.37	
Asahikawa	19.49	
Kushiro	8.98	

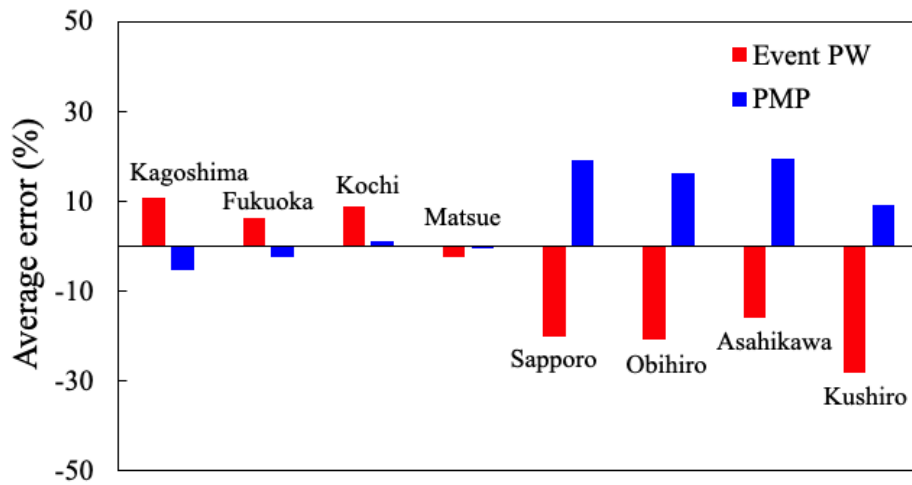


Figure 5-11. Average errors between PMP variables estimated using the SDP and UAD approach in eight areas. Red bars refer to the average error of event PW, and blue bars refer to the average error of PMP.

5.3 Evaluation of the PMP Estimation with a Reference Precipitation

5.3.1 Estimation of the Largest Precipitation using d4PDF

In this study, a reference value was proposed to evaluate the possibility of PMP over- and underestimation for the SDP and UAD approaches. To propose a reasonable reference precipitation value, two conditions were considered: (1) The reference value should have a very long return period that can correspond to the upper limit of rainfall. (2) The reference value should be estimated from a vast amount of rainfall data without any statistical model or method. To satisfy the two conditions, the reference value was estimated without statistical models or methods by collecting annual maximum precipitation values for 3,000 years from the d4PDF database (60 years and 50 ensembles).

The largest precipitation corresponds to a 3,000-years return period in terms of the frequency of probable rainfall. As shown in Figure 5-12, the cumulative density function (CDF) was estimated based on the nonparametric method without using any statistical method or model. Figure 5-12 shows the CDF of the 3,000 events extracted from the annual maximum rainfall for 3,000 years in each area. The largest precipitation values of the CDF were used as a reference value for evaluating the PMP. The magnitude of the largest values was different for each study area as the largest precipitation values were estimated for a grid of d4PDF representing each area. In Figure 5-12, all of the largest values in the southern areas were considerably higher than those in the northern areas. Kushiro shows that the largest value is relatively higher than those in the other northern areas, and it was very close to the largest value in Matsue, as located in the southern area.

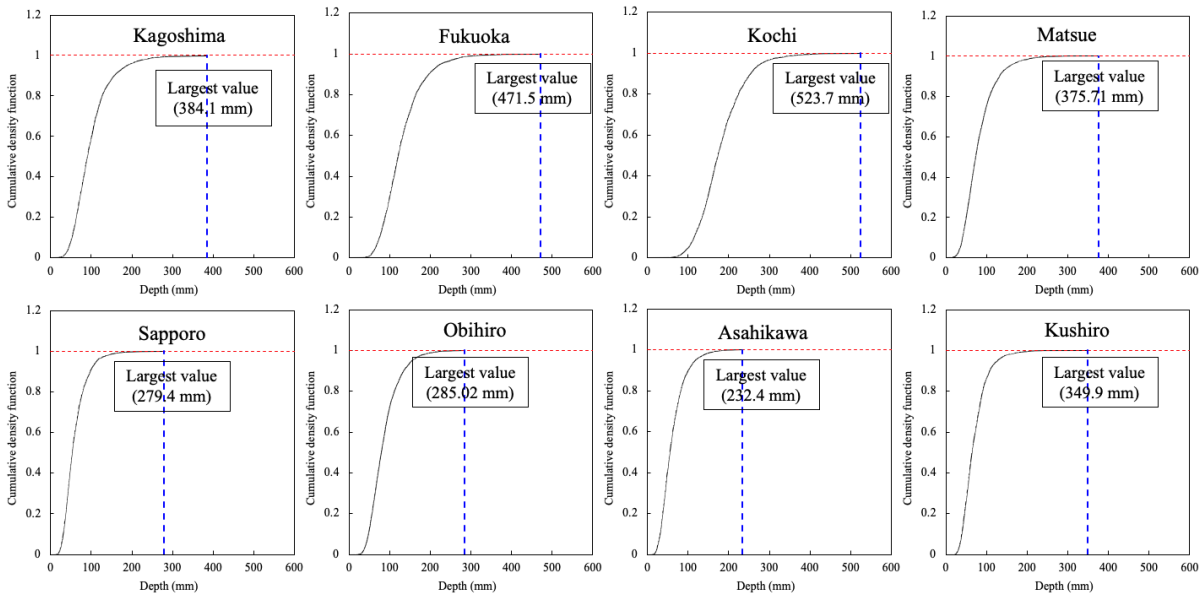


Figure 5-12. Cumulative density function estimated from the d4PDF database (60 years \times 50 ensembles) and the largest value has a 3,000-years return period in term of the probable frequency of rainfall.

5.3.2 Evaluation of the PMPs Estimated using the SDP and UAD

In this study, the PMPs of each ensemble estimated using the SDP and UAD approaches were evaluated using the largest precipitation estimated in Figure 5-12 as a reference value. Unlike that in Chapter 4, where the top rainfall of each ensemble was analyzed, this study was based on the largest PMP value per ensemble. Figure 5-13 shows the results of the 50 PMPs of 50 ensembles estimated using the SDP and UAD approaches. The left figure shows Kagoshima with high SDPs, and the right figure shows Asahikawa with low SDPs. In Figure 5-13, the red circles refer to PMPs estimated using the UAD approach; the blue squares refer to PMPs using the SDP approach; the black dashed line refers to the largest precipitation corresponding to the 3,000-years return period as a reference value; the red line refers to the average value of 50 PMPs estimated using the UAD approach; the blue line refers to the average value of 50 PMPs estimated using the SDP. If the largest precipitation (black dashed line) exceeds the red or blue line, it implies that the PMP is relatively underestimated; if the largest precipitation does not reach the red or blue line, it implies

the PMP is relatively overestimated. The lower the deviation between the black dashed line and the line of the average PMP, the more reasonably the PMP can be estimated.

Both areas show a very low deviation between PMPs estimated using the UAD approach and the reference value in Figure 5-13. Even in Asahikawa that has a low SDP, the PMPs using the UAD showed a low deviation. This indicates that the UAD approach makes it possible to estimate PMP in the northern and southern areas reasonably. Meanwhile, the deviation for PMPs estimated using the SDP is different from the result of the UAD approach. Kagoshima showed a considerably low deviation for PMPs using the SDP; however, Asahikawa showed a very high deviation of PMPs using the SDP to the reference value rather than that in the Kagoshima area. Similar to that in Section 4, this implies that the area with low SDPs may show an overestimated PMP in the SDP approach.

Figure 5-14 shows the average error of the PMPs estimated using the SDP and UAD approaches for the reference value in the eight areas. The red bars refer to the average error between the PMPs using the UAD and reference value; the Blue bars refer to the average error between the PMPs using the SDP and reference value. As shown in Figure 5-14, the SDP-based PMPs indicate a low average error within 10% in Kagoshima, Fukuoka, Kochi, and Matsue. Meanwhile, most northern areas with low SDPs show high positive average errors for the reference value. This means that the northern areas with low SDPs have a high possibility of PMP overestimation. However, the UAD-based PMPs showed low average errors with the reference value in most southern and northern areas, even if the PMPs were slightly underestimated compared to a reference value in most areas of Japan.

In the Kushiro area, the average PMPs estimated using the SDP and UAD approaches were all underestimated compared to the reference value. As shown in Figure 5-12, this may be attributed to the magnitude of the reference value in Kushiro being larger than the reference values in other northern areas. Hence, the result for Kushiro could not help determine which method would estimate a reasonable PMP. Meanwhile, in most northern areas except Kushiro, the UAD-based estimation showed a very low average error compared to that for the SDP-based method.

These results imply that the UAD approach may reasonably estimate PMP even in northern areas with low SDPs. However, it is difficult to use the UAD approach in practice because it remains difficult to construct an abundant number of actual PWs of the UAD observed from the

radiosonde. The actual PWs in the UAD have very short observation periods and contain corrupted values in many cases. In addition, it is difficult to use actual PWs observed in areas where a radiosonde is not installed. Meanwhile, the SDP approach is relatively easy to use in practice because the SDP data is well established even in areas where the radiosonde is not installed. Therefore, there is a need for an alternative approach that can help estimate the PMP using the SDP approach reasonably, even in northern areas with relatively low SDPs.

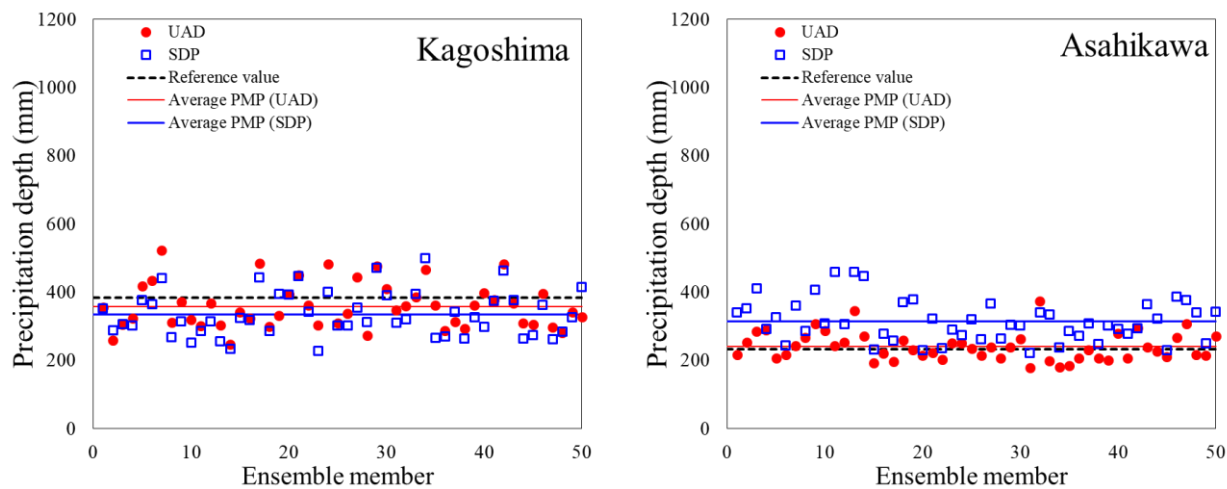


Figure 5-13. Comparison between the PMPs estimated using the SDP and UAD approaches and the largest precipitation obtained from the d4PDF.

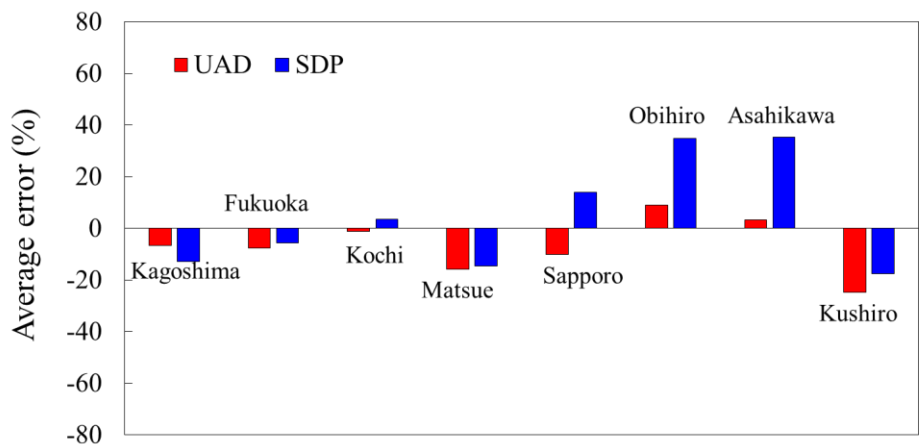


Figure 5-14. Average errors of the PMPs using the SDP and UAD for the largest precipitation in the eight areas.

5.4 Limiting MMR in SDP-based Estimation

In this study, the upper bound of MMR was limited to reduce and control the possibility of the PMP overestimation for the SDP approach in the northern area. Many previous studies have used this alternative approach and limited the upper bound of MMR from 1.5 to 2.0 to prevent PMP overestimation and to maintain storm dynamics characteristics (CEHQ and SNC-Lavalin, 2003; Hansen et al., 1988; Minty et al., 1996; Rousseau et al., 2014; Schreiner and Riedel, 1978; Walland et al., 2003; WMO, 2009). Various limits have been subjectively proposed (Jakob et al., 2009). The upper bound of the MMR, which is most used, is 2.0. However, the limit for the upper bound of MMR to 2 has yet to be answered in terms of specific sites and climatic conditions (Rouhani and Leconte, 2016). Hence, the limit of 2.0 should be checked whether this is a proper limit for Japan. In this study, the tendency of MMRs for 50 rainfall events in each area were analyzed, and the limiting value of 2.0 is examined based on the tendency of MMRs.

To analyze the tendency of MMRs in each area, the box plots of MMRs in Figure 5-8 were checked again. The MMRs estimated using the SDP approach show a different tendency to those using the UAD approach in Figure 5-8. The SDP-based MMRs are located higher than the UAD-based MMRs. The maximum value of SDP-based MMRs is quite higher than 2.0 in the northern areas, and it is close to 2.5 in Sapporo and Obihiro. The SDP-based approach relatively overestimated the PMP to the reference value in most northern areas (Figure 5-14). Meanwhile, MMRs estimated using the UAD were mostly lower than 2.0 in the northern areas in Figure 5-8. The PMPs estimated using the UAD showed low deviations to the reference value in most areas, as indicated in Figure 5-14. These results imply that the limit of 2.0 may be proper in Japan because the UAD approach could estimate a reasonable PMP, and most MMRs of the UAD approach are lower than 2.0. Thus, it was assumed that if the upper bound of MMR is limited to 2.0 in the SDP approach, this approach also may be able to reduce the possibility of PMP overestimation. To reduce the possibility of PMP overestimation of the SDP approach, this study decided to limit the upper bound of MMR to 2.0 in the SDP approach (Figures 5-15 and 5-16).

Figure 5-15 shows the results of the 50 PMPs of 50 ensembles estimated using the SDP approach by limiting the upper bound of MMR to 2.0 with Figure 5-13. The left figure shows Kagoshima with high SDPs, and the right figure shows Asahikawa with low SDPs. In Figure 5-15, the green circles refer to PMPs estimated using the SDP approach with limiting the upper bound of MMR; the green line refers to the average value of 50 PMPs estimated using the SDP

approach with the limiting the MMR to 2.0. In Figure 5-16, the PMPs are estimated using the SDP approach with limiting the upper bound of MMR to 2.0, and the average error between the estimated PMPs and the reference value is estimated. The green bars show the average error between the reference value and PMPs estimated using the limited upper bound of MMRs. The estimated PMPs with limiting MMR show still a low average error to the reference value in the southern areas (Kagoshima, Fukuoka, Kochi, and Matsue). Sapporo, Obihiro, and Asahigawa all reduced the average error. In particular, the average error of Sapporo and Asahikawa decreased by nearly 15%. Thus, it was possible to reduce the average error by limiting the upper bound of MMR in the northern areas with low SDPs. This implies that if the upper bound of MMR is limited to a specific value, the SDP approach can reduce the possibility of PMP overestimation in the northern areas of Japan with the low SDPs.

Based on these results, in practice, the SDP approach with the limited MMR may be able to show very high applicability even in the northern areas with low SDPs. Therefore, this study indicates that it would be possible to estimate a reasonable PMP using the SDP approach by limiting the upper bound of MMR for each area instead of using the UAD approach, which is difficult to utilize in practice.

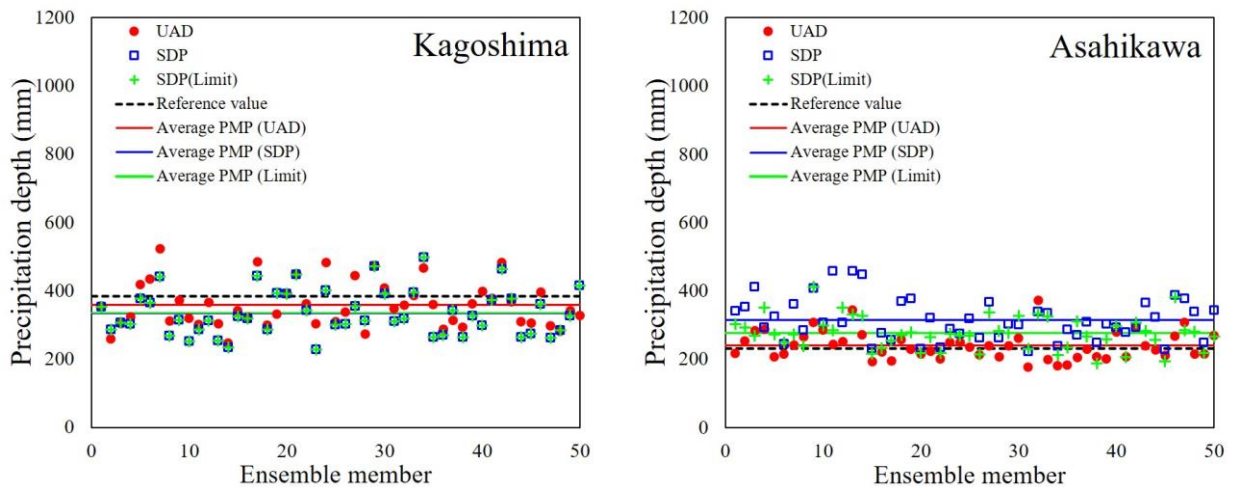


Figure 5-15. Comparison between the PMPs estimated using the SDP approach with limiting the upper bound of MMR and the largest precipitation obtained from the d4PDF.

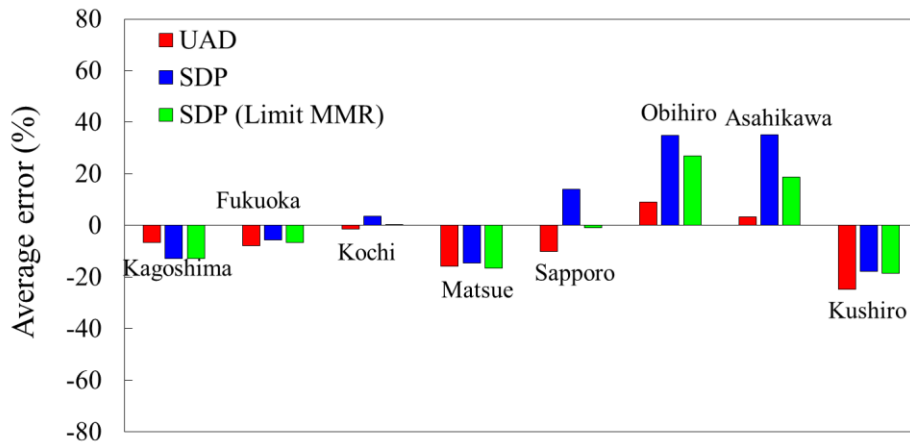


Figure 5-16. Average errors of the PMPs using the SDP when limiting the upper bound of MMR with Figure 12. Green bars show the average error between the reference value and PMPs estimated using the limited upper bound of MMR to 2.0.

5.5 Conclusion

For event PW, MMR, and PMP, the deviation between the SDP and UAD approaches was relatively low in the southern areas with high SDPs. The deviation of the PMP variables was relatively high between the two approaches in the northern areas with low SDPs. In particular, the SDP approach underestimated the event PWs compared to the UAD approach. In contrast, the SDP approach overestimated the MMRs compared to the UAD approach in the northern areas. Kim et al. (2020) mentioned that the events PW and MMRs showed a high correlation. As the error of the event PW increases in the negative direction, the error of the MMR increases in the positive direction (Kim et al., 2020). The significantly overestimated MMRs obtained using the SDP approach in the northern areas are caused by the tendency that event PWs estimated using the SDP were underestimated compared to those estimated using UAD.

Extreme-scale reference precipitation was proposed to evaluate the PMP over- and underestimations. The suggested reference value was compared with the PMPs of 50 ensembles of d4PDF. The SDP approach showed high average errors in the northern areas. The UAD approach showed very low average errors in most southern and northern areas. This implies that the UAD approach can reasonably estimate PMP, unlike the SDP approach. However, it is difficult to use the UAD approach in practice because it is difficult to construct the actual observed PW from the UAD such as the radiosonde. Meanwhile, the SDP approach is relatively easy to use in practice because the SDP data is well established even in areas where the radiosonde is not installed.

To reduce the possibility of PMP overestimation when the SDP approach is applied, the upper bound of MMR is limited to 2.0, similar to one of the methods that are widely used to control the PMP. The PMPs estimated using the SDP approach could reduce the possibility of PMP overestimation by limiting the upper bound of MMR. Consequently, the SDP approach that limits the MMR may be able to reasonably estimate PMP by reducing the possibility of PMP overestimation.

In this paper, the PMP estimation based on the moisture-maximization method was evaluated from the extreme-scale reference precipitation under sufficient extreme events by utilizing the d4PDF. To date, there are no reliable guidelines for evaluating PMP estimates. However, because the reference precipitation estimated using d4PDF can exhibit a considerably

longer reproducibility than historical observation data, it may be possible to evaluate the PMP by estimating a reliable extreme-scale reference value from d4PDF.

Chapter 6

Analyzing Dominant Meteorological Factors in Extreme Rainfall Events

A physical basis for the moisture-maximization and numerical approach to estimate PMP has still not been thoroughly established for the key meteorological factors. In the moisture-maximization method, the linearity between the precipitation and PW is not valid for various target areas and storms. Furthermore, the numerical approach has not been widely validated for various meteorological factors (Chen et al., 2017). One important issue concerning such techniques for estimating the PMP is that there has been no comprehensive study investigating the key meteorological factors that affect extreme precipitation estimation (Chen and Hossain, 2018). This is because there is no consensus on how to physically “maximize” the historical storms for PMP estimation (Chen and Hossain, 2018). In addition, studies related to the numerical model have focused on storm maximization to estimate the “upper bound” of the precipitation. Accordingly, it is necessary to identify the dominant meteorological factors in extreme precipitation and validate them for the PMP estimation methods.

As a further study, this chapter aims to find the most suitable and dominant meteorological factors for extreme precipitation. This analysis is based on historical heavy rainfall events and some meteorological factors in the target areas. This study focused on identifying the factors that appear dominant during heavy rainfall, without consideration for their time-lagged relationship. An analysis of whether the most dominant meteorological factor in one area is also dominant in another area is conducted by selecting multiple target areas; geographic and climatic characteristics vary between areas, affecting extreme precipitation.

This study selected meteorological factors that have been frequently utilized to estimate the PMP via the numerical approach and moisture-maximization method. To collect the abundant meteorological factors, the reanalysis data from the Japanese 55-year Reanalysis (JRA-55) was utilized. The historical rainfall events were obtained from AMeDAS (Automated Meteorological Data Acquisition System) to collect the observed daily rainfall data. The top 50 rainfall events, from 1960 to 2019, were selected for eight target areas in Japan to focus on the “large magnitude” of the rainfall events.

This study applied the cumulative density function (CDF) to determine the dominant meteorological factors. The CDF allows direct analysis of the correlation between the factors and rainfall by representing as the percentile, without considering the actual extent of factor values. This chapter identified where the 50 values of each factor are located on the CDF curve and if more of the top 50 event values are located near 1 on the CDF, then the correlation with the magnitude of extreme precipitation is higher. To quantify how many of the top 50 rainfall events were correlated to the selected factors, the number of rainfall events exceeding 0.95 on the CDF was counted.

6.1 Data and Target Area

In this study, several meteorological factors were selected, based on these previous studies, to analyze the relationship between extreme events and meteorological factors. The selected factors are the precipitable water (PW), surface dew point (SDP), temperature, relative humidity (RH), vertical wind velocity at the 700 hPa (VVEL), and convective available potential energy (CAPE), as presented in Table 6-1.

PW is the depth of water in a column of the atmosphere if all the water in that column were precipitated as rain. PW is highly correlated with the moisture content in the air column such as water vapor and mixing ratio. CAPE is the integrated amount of work that the upward (positive) buoyancy force would perform on a given mass of air (called an air parcel) if it rose vertically through the entire atmosphere. Positive CAPE will cause the air parcel to rise, while negative CAPE will cause the air parcel to sink (Paquin, 2010). Nonzero CAPE is an indicator of

atmospheric instability in any given atmospheric sounding, a necessary condition for the development of cumulus and cumulonimbus clouds with attendant severe weather hazards. Vertical wind velocity is directly taken from reanalysis fields, presented as the velocity between pressure levels. From the mass balance perspective, the strength of vertical velocity is also an approximation of the large-scale horizontal convergence.

As shown in Figure 6-1, this study selected eight target areas of Japan, focusing on locations with an installed radiosonde (six areas, discounting the Maebashi and Kyoto areas). The Kyushu and Hokkaido areas were mainly selected to analyze the dominant factors of two areas with clearly different characteristics. The meteorological factors were extracted from JRA-55 from June to September 1960 – 2019, at selected areas.

The dependence of CAPE and SDP for extreme precipitation has been analyzed in a climatological study in the U.S., demonstrating that both parameters are of similar importance (Lepore et al., 2020). A further study proposed that the CAPE and atmospheric moisture might be potential indicators of extreme events and the stronger events are highly correlated with large-scale vertical wind velocity (Loriaux et al., 2016).

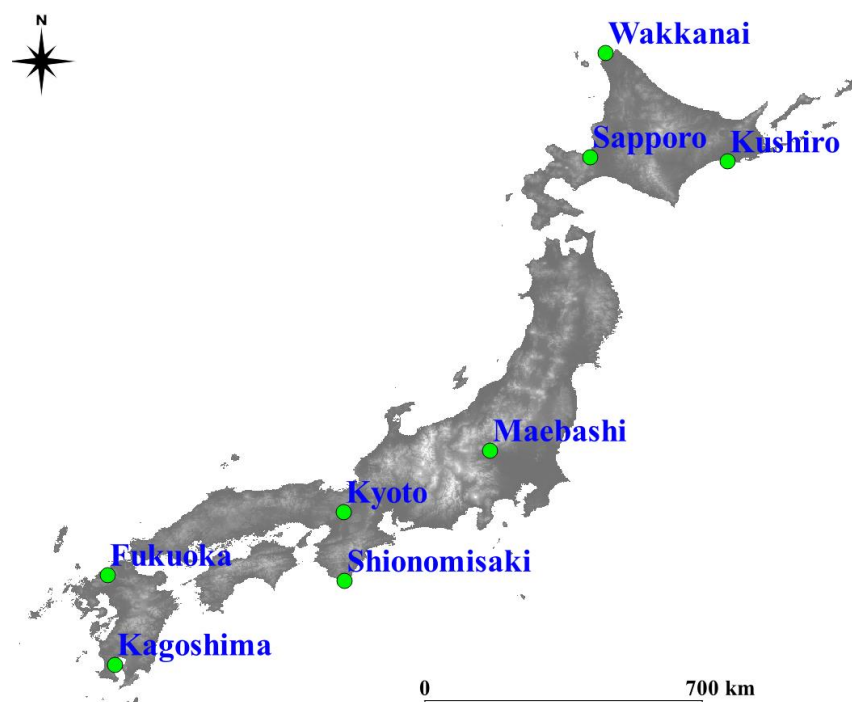


Figure 6-1. The eight target areas in Japan.

Table 6-1. The selected meteorological factors and description.

Factor	Description	Reference
PW	refers to the total water vapor in the air column and has used to estimate moisture availability in the air column	WMO (2009) Chen and Hossain (2018)
Dew point	refers to the saturate moisture availability at the atmospheric surface and has used to estimate PMP	WMO (2009) Lepore et al. (2015)
Temperature	related to the precipitation intensity and widely utilized in the numerical simulation	Yu et al. (2018) Ishida et al. (2018)
RH	widely utilized to estimate extreme precipitation in the numerical simulation	Ohara et al. (2011) Ohara et al. (2018)
CAPE	Convective available potential energy and widely used to indicate atmospheric instability	Chen and Hossain (2018) Lepore et al. (2015) Loriaux et al. (2016)
VVEL	Vertical wind velocity at 700 hPa and triggers moisture condensation and implies large-scale horizontal convergence.	Loriaux et al. (2016) Davies et al. (2013) Dorrestijn et al. (2014)

The other studies showed a strong correlation between tropical precipitation and vertical wind velocity (Davies et al., 2013; Dorrestijn et al, 2014). The dependence of the precipitation characteristics on air temperature was also analyzed (Yu et al., 2018). Another study analyzed the correlation between extreme events and CAPE, PW, and VVEL and noted that a VVEL at 700 hPa had the greatest impact on extreme precipitation (Chen and Hossain et al., 2018).

In the PMP estimation method, WMO estimated the PMP using the PW and SDP, based on the moisture-maximization method (WMO, 2009). In the physical model-based numerical simulation, some studies maximized the RH by 100% and increased the air temperature uniformly by 0.0–8.0 °C (Ishida et al., 2018; Ohara et al., 2011). The PW represents the total moisture availability in the air column. The SDP represents the temperature at which air is saturated with

water vapor. The RH is the ratio of the partial water vapor pressure to the equilibrium water vapor pressure at a given temperature. The SDP, temperature, and RH can be obtained from the JRA-55 surface analysis fields; the height of these data is 2 m from 1000 hPa. The CAPE is widely used to indicate atmospheric instability and is useful in severe weather prediction. The VVEL can be obtained directly from the JRA-55 at each pressure level. This factor triggers moisture condensation and implies large-scale horizontal convergence.

6.2 Analysis Design

Based on the selected meteorological factors, this study analyzed the correlation between the historical rainfall events and factors in the same duration when a heavy rainfall happens. Figure 6-2 shows the analysis procedures to find the dominant meteorological factors and to estimate the extreme ratio for a representative area in Figure 6-1. Figure 6-2 (a) depicts the daily rainfall from June to September from 1960 to 2019 in a representative area. Black bars refer to the daily rainfall. Purple squares indicate the top 50 rainfall events. In Figure 6-2 (b), the daily maximum PWs for the top 50 rainfall events which are selected in Figure 6-2 (a) were extracted. The red points refer to the daily maximum PWs when the top 50 rainfall events have occurred. The blue bars in Figure 6-2 (b) were represented as the blue CDF curve in Figure 6-2 (c). The red points indicate the 50 daily maximum PWs selected in Figure 6-2 (b). A higher correlation with extreme precipitation magnitude is indicated by more of the top 50 events located near 1 in the CDF.

To quantify how many of the top 50 rainfall events were correlated to the selected factors, this study was conducted on the assumption that more values exceeding 0.95 on the CDF curve indicate a higher correlation between the factor and rainfall events. This assumption applied to all meteorological factors as the values of the top 50 events are concentrated above 0.95 on the CDF curve for most meteorological factors. This correlation is represented as an extreme ratio. Equation 6-1 represents the extreme ratio. In Equation 6-1, the number of rainfall events exceeding 0.95 on the CDF is counted. The extreme ratio is estimated as the ratio of the counted events exceeding 0.95 on the CDF among the total selected events. For instance, based on Figure 6-2 (c), if the total

rainfall events are 50 events and the number of events exceeding 0.95 on the CDF is 22 events, the extreme ratio is estimated at 44%.

$$\textit{Extreme ratio} = \frac{\textit{Event} > 0.95 \textit{ on the CDF}}{\textit{Total Events}} \times 100 (\%) \quad (6-1)$$

Although $\text{CDF} > 0.95$ was set arbitrarily in this study, the objective is not to analyze the sensitivity between the rainfall events and the meteorological factors but to find the most dominant factors in historical rainfall events. To identify the dominant factor in all areas of Japan, this procedure was applied to all of the areas shown in Figure 6-1. In the next section, the correlations between the historical events and PW, CAPE, surface temperature, RH, VVEL, and SDP are analyzed. In addition, this study is focusing on the 50 events.

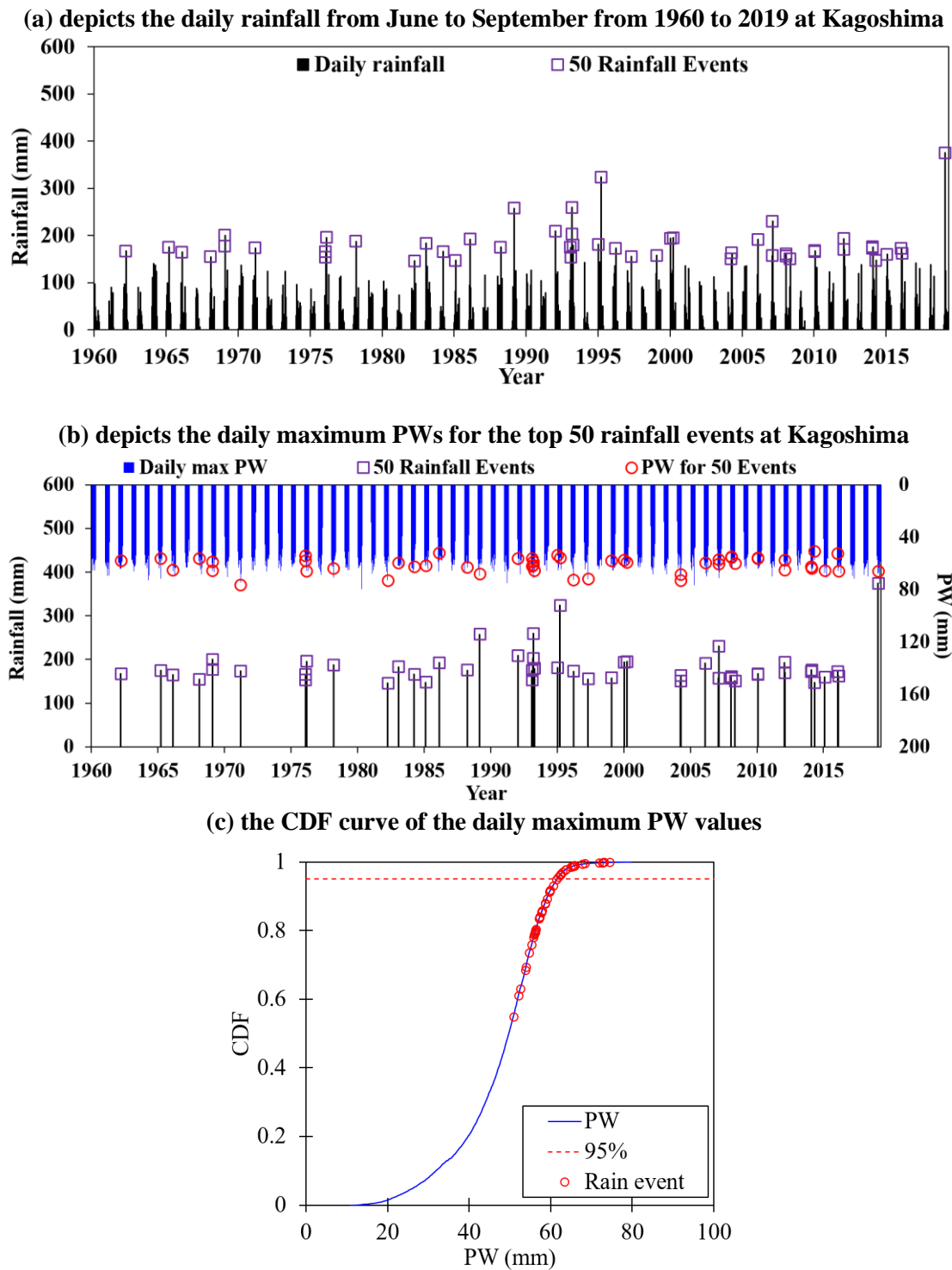


Figure 6-2. The procedure to find the dominant meteorological factors with historical rainfall event.

6.3 Correlation Analysis between Storm Events and Meteorological Factors

According to the analysis process illustrated in Figure 6-2, this study was conducted on six meteorological factors for eight areas of Japan. The CDF curves were represented for the six factors, and the extreme ratios were estimated by counting the number of events exceeding 0.95 on the CDF. Figure 6-3 shows the result for the Kagoshima area; many red points of the CAPE, PW, SDP, and RH were located close to a CDF of 1 and distributed over a CDF of 0.4. In the VVEL, although 50 events were distributed from 0 to 1, many red points showed a CDF of 0.95 or more. However, the temperature results were different from those of other factors. Most red points were located on the CDF of 0.4 or less. The top 50 events for each factor, except for temperature, were concentrated above 0.95 on the CDF curve, shown in Figure 6-3. Thus, this study was conducted on the assumption that if more values exceed 0.95 on the CDF curve, the correlation between the factors and rainfall events is higher.

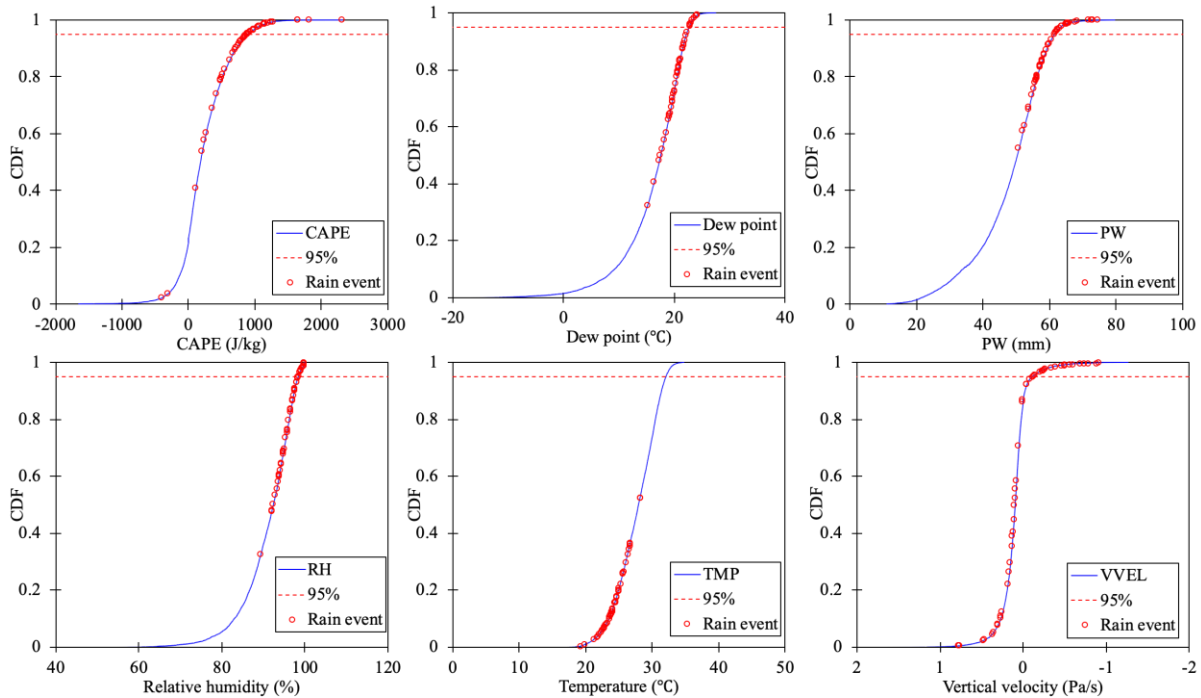


Figure 6-3. CDF curves for 8 meteorological factors at Kagoshima. The red points show the CDF of the factors at top 50 rainfall events.

6.3.1 Results for the Top 50 Rainfall Events

Figure 6-4 and Table 6-2 show the result of counting the events exceeding a CDF of 0.95 out of 50 events, as a percentage for eight areas of Japan. The larger this value, the higher the relation between the factor and the heavy rainfall event.

As shown in Figure 6-4, the temperature showed an extreme ratio of less than 5% in all areas, unlike the results of other factors. This indicates that the historical rainfall events have a low correlation to the magnitude of temperature at the time of daily maximum rainfall occurrence. However, there could be a time-lagged relationship between extreme events and temperature, which would be investigated in a future study. This study focused on identifying what are the meteorological factors that appear dominant at the time of the daily maximum rainfall occurrence.

The CAPE refers to the highest value of 42% at Kagoshima. The PW refers to the highest value of 46% at Wakkanai. The dew point refers to the highest value of 40% at Fukuoka. The RH refers to the highest value of 44% at Fukuoka. The VVEL refers to the highest value of 44% at Kagoshima. These factors showed a high correlation of over 40%.

Then, this study checked which factors were most dominant with the historically observed top 50 rainfall events for each area. This analysis focused on the Hokkaido and Kyushu areas with clearly different climatic characteristics. In the Hokkaido area, the extreme ratio of PW was highly estimated, and rainfall events had a high correlation for PW. However, the extreme ratios of the other factors were relatively low. On the other hand, in the Kyushu area, the extreme ratios of all factors except temperature showed high values of more than 20% as shown in Table 6-2. This implies that rainfall events occurring in the Kyushu were highly affected by not only the PW as well as other factors at the time of the daily maximum rainfall occurrence, unlike the Hokkaido area.

This study also noticed the VVEL factor. The VVEL was more dominant in the Kyushu area than the Hokkaido area. In Hokkaido, the extreme ratio of VVEL is relatively lower than that in the Kyushu area. Thus, the VVEL was the more dominant factor with the historical rainfall events in the Kyushu area than the Hokkaido area. This result implies that the VVEL may be highly related to the magnitude of rainfall as the events in the Kyushu area had a higher magnitude than the Hokkaido area.

The top 50 events

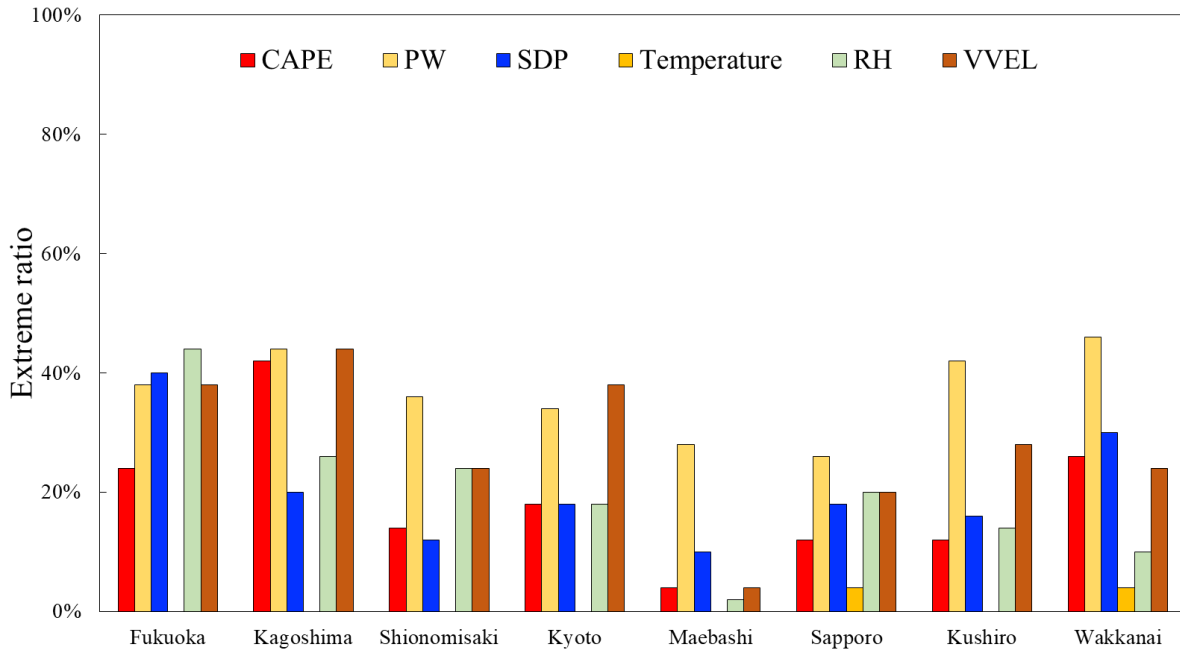


Figure 6-4. The result of counting the events exceeding the CDF of 0.95 out of 50 events.

Table 6-2. The result of the extreme ratio of each meteorological factor for the top 50 rainfall events in all areas.

Points	CAPE	PW	SDP	Temperature	RH	VVEL	Highest factor
Fukuoka	24%	38%	40%	0%	44%	38%	RH
Kagoshima	42%	44%	20%	0%	26%	44%	PW, VVEL
Shionomisaki	14%	36%	12%	0%	24%	24%	PW
Kyoto	18%	34%	18%	0%	18%	38%	VVEL
Maebashi	4%	28%	10%	0%	2%	4%	PW
Sapporo	12%	26%	18%	4%	20%	20%	PW
Kushiro	12%	42%	16%	0%	14%	28%	PW
Wakkanai	26%	46%	30%	4%	10%	24%	PW
Total average	19%	37%	21%	1%	20%	28%	PW

Consequently, in the analysis for the top 50 rainfall events, the dominant meteorological factors were different from each other in the Hokkaido and Kyushu areas. The PW showed a high extreme ratio in all areas. In particular, the PW was the most dominant factor for the top 50 events that occurred in the Hokkaido area. The VVEL was one of the dominant factors in the Kyushu area. This is because each area has distinctly different geographic and climatic characteristics, such as the rainfall event magnitude, atmospheric temperature, and SDP.

6.4 Discussion

In the analysis using the top 50 rainfall events, those that occurred in the Hokkaido area had a lower extreme ratio with the VVEL than those in the Kyushu area. This may be because the magnitudes of the top 50 events in the Kyushu area are higher than those in the Hokkaido area. The past study indicated that extreme precipitation is more related to the VVEL than the PW as the VVEL implies large-scale horizontal convergence, which brings in moisture from the surrounding areas during precipitation (Chen and Hossain, 2018). Therefore, the Kyushu area, which has a high magnitude of rainfall events, exhibited a higher extreme ratio with the VVEL than the Hokkaido areas.

Most areas showed very high extreme ratios of PW for the top 50 events. This result implies that PW was a considerable dominant meteorological component of historical heavy rain events observed throughout the region. From this result, the moisture-maximization method, with PW as a key factor, may be useful for estimating extreme precipitation; this study demonstrated that historical rainfall events in all areas were highly correlated with PW.

6.5 Conclusion

This study identifies PW that is a key factor in estimating the reasonable extreme precipitation in the moisture-maximization method. This study may help to establish a guideline for selecting the key meteorological factors in the numerical approach. From these results, a sufficient correlation analysis between historical rainfall events and meteorological factors may be useful in supporting the physical basis and estimating the reasonable extreme precipitation via the numerical model simulation, as well as various other extreme precipitation methods, such as the moisture-maximization method proposed by the WMO.

An investigation into how historical extreme rainfall events are controlled by certain meteorological factors may help to estimate extreme precipitation. This analysis makes it possible to re-evaluate the use of the SDP or PW in the moisture-maximization method and helps to establish guidelines for selecting the key meteorological factors in the numerical approach. Hence, this analysis will be of great significance in supporting a physical basis for the study of extreme precipitation.

In this study, dominant factors were found based on the time point when the daily maximum rainfall occurred. As a result, the meteorological factor such as temperature, which is characterized by a decrease in magnitude after heavy rain, have an extremely low extreme ratio. Therefore, it is necessary to analyze the climatic conditions before the time when the daily maximum rainfall occurs. Therefore, as a follow-up study, the dominant factors will be figured out for climatic conditions before the daily maximum rainfall occurs. The next study will find dominant factors that can help predict extreme rainfall as well as estimation of extreme rainfall by calculating the extreme ratio for the change of factors between the time of the daily maximum rainfall occurrence and before.

Chapter 7

Concluding Remarks

This study evaluated the moisture-maximization method for the PMP estimation by analyzing the deviation of each PMP variable estimated through the SDP and UAD approaches. To utilize abundant data for a long-term period, JRA-55 data were employed. The JRA-55 data showed good reliability, based on verification with observed SDPs and actual PW values at 10 points across Japan. Subsequently, by using the JRA-55 data, the deviations between the two approaches were analyzed for 30 points in Japan. The event PW and MMR estimated using the SDP approach showed a high deviation from those estimated using the UAD approach in some areas. In particular, the Hokkaido points with a relatively low SDP show a very high error margin. This indicates that the high deviation may be significantly related to low SDPs of heavy rainfalls at some points. Further, the relationship of the PMP variables was analyzed to identify the main cause of MMR overestimation. Consequently, this study identified a high relationship between the event PW and MMR. If the event PW error increases in the negative direction, the MMR error continues to increase.

By focusing on the event PW, this study analyzed the relationship between the actual PW values and SDPs for the top three rainfall events at all 30 points to evaluate the reasonability of using the SDP approach under the pseudo-adiabatic assumption. This assumption could reasonably estimate the PW when using the SDP from 18 to 23 °C. As the SDP became lower than 18 °C, the deviations continued to increase, and the PW values were underestimated more severely. This study showed different magnitudes of deviation at each SDP for certain degrees. However, the reason for the occurrence of this phenomenon was difficult to determine.

To identify the effect of the pseudo-adiabatic assumption and the SDP on the deviations of actual atmospheric profiles in the air column, the profiles of the dew point, mixing ratio, and accumulated PW as observed from radiosondes were compared with those estimated through the

pseudo-adiabatic process according to the atmospheric vertical pressure layers from the surface to 300 hPa (i.e., where the saturated air parcel is very thin). One of the top three rainfall events at each of the six points was selected to analyze the deviation. The selected rainfall locations were as follows: SDP was below 18 °C at the Sapporo, Kushiro, and Wakkanai points, and it was above 18 °C at the Kagoshima, Fukuoka, and Shionomisaki points. The points with high SDPs indicated that the estimated profiles (SDP approach) follow the observed profiles (UAD approach) in the air column. However, the points with low SDPs showed a high deviation between the estimated and observed profiles. The actual dew point profiles fluctuate according to the altitude, without a constant pattern. Whereas, the dew point profiles estimated through the pseudo-adiabatic assumption exhibit a constant tendency according to the altitude. Consequently, the actual atmospheric conditions in the upper air appear moister and fluctuate more than the atmospheric conditions estimated through the pseudo-adiabatic process at SDPs below 18 °C. A large deviation occurred at SDPs below 18 °C, and a significantly low deviation could be estimated within the range of the SDPs from 18 to 23 °C. This implies that the SDP approach using the pseudo-adiabatic assumption could not estimate a reasonable PW value for events and points with low SDPs. Therefore, the estimation of PMP using the SDP in the moisture-maximization method can enable the estimation of a rational PMP in areas where the SDP is high (e.g., higher than 18 °C). To reduce the deviation when using the pseudo-adiabatic assumption, a PMP estimation based on the moisture-maximization method should be carefully considered in regions and events with relatively low SDPs (e.g., lower than 18 °C).

By using the d4PDF based on a large ensemble simulation output, this study was able to closely evaluate PMP estimation approaches using the SDP and UAD based on the moisture-maximization method by satisfying the following three conditions: (1) By using 50 events with a total of 50 ensembles, the deviation between the two approaches could be analyzed closely under sufficient rainfall events. (2) By using climate simulation-based data, abundant PWs and SDPs could be obtained. (3) Finally, the possibility of PMP over- and underestimation could be evaluated by estimating the extreme-scale reference value without any statistical model and method from the data period corresponding to 3,000-years. The SDP approach exhibited high average errors to the reference value in the northern areas, as in Chapters 3 and 4. The UAD approach exhibited very low average errors to the reference value in most southern and northern areas. This implies that the UAD approach can reasonably estimate PMP, and the SDP approach overestimates PMPs to the reference value in the northern areas. To reduce the possibility of PMP overestimation for the

SDP approach, the upper bound of the MMR is limited to 2.0. The PMPs estimated using the SDP approach could reduce the possibility of PMP overestimation by limiting the upper bound of MMR. Consequently, this SDP approach may be able to reasonably estimate PMP. It is difficult to use the UAD approach in practice because it is difficult to construct the actual observed PW from the UAD such as the radiosonde. Meanwhile, the SDP approach is relatively easy to use in practice because the SDP data is well established even in areas where the radiosonde is not installed. The SDP approach can be utilized to estimate reasonable PMP by limiting the upper bound of MMR for each area instead of using the UAD approach, which is difficult to utilize in practice.

Finally, the correlation between meteorological factors and historical heavy rainfall events was analyzed to determine the most dominant factors in the extreme rainfall events. This study selected multiple target areas in Japan, and six meteorological factors were analyzed in historical heavy rainfall events to identify whether the dominant factors vary according to the area. In this study, the CDF was applied to determine the dominant meteorological factors. The extreme ratio was estimated for the top 50 events using the CDF. In the Hokkaido area, with a relatively lower magnitude of rainfall, atmospheric temperature, and SDP, PW is considered the most dominant factor in historical rainfall events. In the western areas of Japan, with higher magnitudes of rainfall, atmospheric temperature, and SDP, the VVEL and PW were determined as the dominant factors in the historical rainfall events. Consequently, this study identified that PW is a key factor in estimating reasonable extreme precipitation by using the moisture-maximization method, and the VVEL is highly correlated with the high magnitude of the rainfall event. According to these results, an investigation into the control of historical extreme rainfall events by certain meteorological factors may help estimate extreme precipitation. This analysis allows the re-evaluation of the use of the SDP or PW in the moisture-maximization method and helps establish guidelines for selecting the key meteorological factors using a numerical approach. Hence, the proposed analysis could be of great significance in supporting a physical basis for the study of extreme precipitation.

References

- Abbs, D. J. (1999). A numerical modeling study to investigate the assumptions used in the calculation of Probable Maximum Precipitation. *Water Resources Research*, 35(3), 785–796. <https://doi.org/10.1029/1998WR900013>
- Allan, R. P. & Soden, B. (2008). Atmospheric warming and amplification of precipitation extremes. *Science*, 321(5895), 1481-1484. <https://doi.org/10.1126/science.1160787>
- Beauchamp, J., Leconte, R., Trudel, M., & Brissette, F. (2013). Estimation of the summer-fall PMP and PMF of a northern watershed under a changed climate. *Water Resources Research*, 49, 3852–3862. <https://doi.org/10.1002/wrcr.20336>
- Ben Alaya, M. A., & Zwiers, F. (2019). Evaluation and Comparison of CanRCM4 and CRCM5 to Estimate Probable Maximum Precipitation over North America. *Journal of Hydrometeorology*, 20, 2069-2089, <https://doi.org/10.1175/JHM-D-18-0233.1>
- Ben Alaya, M. A., Zwiers, F. W., & Zhang, X. (2018). Probable maximum precipitation: Its estimation and uncertainty quantification using bivariate extreme value analysis. *Journal of Hydrometeorology*, 19, 679–694, <https://doi.org/10.1175/JHM-D-17-0110.1>
- Casas, M. C., Rodríguez, R., Prohom, M., Gázquez, A. & Redaño, A. (2011). Estimation of the probable maximum precipitation in Barcelona (Spain), *International Journal of Climatology*, 31(9), 1322–1327, <https://doi.org/10.1002/joc.2149>
- CEHQ, & SNC-Lavalin (2003). Estimation des conditions hydrometeorologiques conduisant aux crues maximales probable (CMP) au Quebec. *Pluies*, SNC-Lavalin, Div. Energie.
- Chen, L. C., & Bradley, A. A. (2006). Adequacy of using surface humidity to estimate atmospheric moisture availability for probable maximum precipitation, *Water Resources Research*, 42(9), W09410. <https://doi.org/10.1029/2005WR004469>

- Chen, X. & Hossain, F. (2018). Understanding model-based probable maximum precipitation estimation as a function of location and season from atmospheric reanalysis, *Journal of Hydrometeorology*, 19(2), 459-475, <https://doi.org/10.1175/JHM-D-17-0170.1>
- Chen, X., Hossain, F., & Leung, L. R. (2017). Probable maximum precipitation in the U.S. Pacific Northwest in a changing climate. *Water Resources Research*, 53(11), 9600-9622. <https://doi.org/10.1002/2017WR021094>
- Choudhury, B. J. (1996). Comparison of two models relating precipitable water to surface humidity using globally distributed radiosonde data over land surfaces, *International Journal of Climatology*, 16(6), 663 – 675. [https://doi.org/10.1002/\(SICI\)1097-0088\(199606\)16:6<663::AID-JOC29>3.0.CO;2-O](https://doi.org/10.1002/(SICI)1097-0088(199606)16:6<663::AID-JOC29>3.0.CO;2-O)
- Chow, K. C. A., & S. B. Jones (1994), Probable Maximum Floods in Boreal Regions, prepared by Atria Engineering Hydraulics Inc for Canadian Electrical Association, Can. Electr. Assoc., Ottawa, Ont.
- Connel, B. H., & Miller, D. R. (1995). An interpretation of radiosonde errors in the atmospheric boundary layer, *Journal of Applied Meteorology*, 34(5), 1070–1081. <https://doi.org/10.1175/1520-0450%281995%29034<1070%3AAIOREI>2.0.CO%3B2>
- Davies, L., Jakob, C., May, P., Kumar, V. V. & Xie, S. (2013). Relationships between the large-scale atmosphere and the small-scale convective state for Darwin, Australia, *Journal of Geophysical Research Atmospheres*, 118(11), 534–545, <https://doi.org/10.1002/jgrd.50645>
- Doll, P., Trautmann, T., Gerten, D., Muller Schmied, H., Ostberg, S., et al. (2018). Risks for the global freshwater system at 1.5 degrees C and 2 degrees C global warming. *Environmental Research Letters*, 13(4), 1-15, <https://doi.org/10.1088/1748-9326/aab792>
- Dorrestijn, J., Crommelin, D. T., Siebesma, A. P., Jonker, H. J. J. & Jakob, C. (2014). Stochastic parameterization of convective area fractions with a multcloud model inferred from observational data, *Journal of Atmospheric Science*, 72(2), 854–869, <https://doi.org/10.1175/JAS-D-14-0110.1>
- Easterling, D. R., Evans, J. L., Groisman, P. Y., Karl, T. R., Kunkel, K. E., & Ambenje, P.

- (2000). Observed variability and trends in extreme climate events: a brief review, *Bulletin of the American Meteorological Society*, 81(3), 417–425. [https://doi.org/10.1175/1520-0477\(2000\)081<0417:OVATIE>2.3.CO;2](https://doi.org/10.1175/1520-0477(2000)081<0417:OVATIE>2.3.CO;2)
- Faye, B., Webber, H., Naab, J., MacCarthy, D. S., Adam, M., Ewert, F., et al. (2018). Impacts of 1.5 versus 2.0 degrees C on cereal yields in the West African Sudan Savanna. *Environmental Research Letters*, 13(3), 1-13, <https://doi.org/10.1088/1748-9326/aaab40>
- Fletcher, R. D. (1951). Hydrometeorology in the United States, in *Compendium of Meteorology*, edited by T. F. Malone, American Meteorological Society, Boston, Mass, 1033 – 1047. https://doi.org/10.1007/978-1-940033-70-9_83
- Free, M., et al., (2002). Creating climate reference datasets: CARDS workshop on adjusting radiosonde temperature data for climate monitoring, *Bulletin of the American Meteorological Society*, 83(6), 891–899. [https://doi.org/10.1175/1520-0477\(2002\)083<0891:CCRDCW>2.3.CO;2](https://doi.org/10.1175/1520-0477(2002)083<0891:CCRDCW>2.3.CO;2)
- Hanittinan, P., Tachikawa, Y., & Ram-Indra, T. (2020). Projection of hydroclimate extreme indices over the Indochina region under climate change using a large single-model ensemble, *International Journal of Climatology*, 40(6), 2924-2952. <https://doi.org/10.1002/joc.6374>
- Hansen, E. M., Fenn, D. D. Schreiner, L. C., Stodt, R. W. & Miller, J. F. (1988). Probable maximum precipitation estimates, United States between the Continental Divide and the 103rd meridian. *Hydrometeorological Report*.
- Hershfield, D. M. (1965). Method for estimating probable maximum rainfall. *Journal of the American Water Works Association*, 57(8), 965–972. <https://doi.org/10.1002/j.1551-8833.1965.tb01486.x>
- Hershfield, D. M. (1981). The magnitude of the hydrological frequency factor in maximum rainfall estimation/Valeur du facteur de fréquence hydrologique dans l'estimation de la hauteur maximale de précipitations, *Hydrological Sciences Journal*, 26(2), 171-177, <https://doi.org/10.1080/02626668109490874>
- Huffman, K., Schaefer, M., & Bowles, D. (2014). *Local Precipitation-Frequency Studies*:

- Development of 1-hour/1-square mile precipitation-frequency relationships for two example nuclear power plant sites. Electric Power Research Institute, Palo Alto, CA. 3002004400. Retrieved from <https://www.epri.com/#/pages/product/3002004400/>
- Ishida, K., Kavvas, M. L., Jang, S., Chen, Z.Q., Ohara, N., & Anderson, M. L. (2015a). Physically based estimation of maximum precipitation over three watersheds in Northern California: atmospheric boundary condition shifting, *Journal of Hydrological Engineering*, 20(4), 04014052. [https://doi.org/10.1061/\(ASCE\)HE.1943-5584.0001026](https://doi.org/10.1061/(ASCE)HE.1943-5584.0001026)
- Ishida, K., Kavvas, M. L., Jang, S., Chen, Z.Q., Ohara, N., & Anderson, M. L. (2015b). Physically based estimation of maximum precipitation over three watersheds in Northern California: Relative humidity maximization method, *Journal of Hydrological Engineering*, 20(10), 04015014. [https://doi.org/10.1061/\(ASCE\)HE.1943-5584.0001175](https://doi.org/10.1061/(ASCE)HE.1943-5584.0001175)
- Ishida, K., Ohara, N., Kavvas, M. L., Chen, Z.Q., & Anderson, M. L. (2018). Impact of air temperature on physically-based maximum precipitation estimation through change in moisture holding capacity of air, *Journal of Hydrology*, 556, 1050-1063. <https://doi.org/10.1016/j.jhydrol.2016.10.008>
- Jakob, D., Smalley, R., Meighen, J., Taylor, B., & Xuereb, K. (2009), *Climate Change and Probable Maximum Precipitation*, Australian Government, Bureau of Meteorology, Melbourne.
- Kay, J. E., & Coauthors, (2015). The Community Earth System Model (CESM) Large Ensemble project: A community resource for studying climate change in the presence of internal climate variability. *Bull. Amer. Meteor. Soc.*, 96, 1333–1349, <https://doi.org/10.1175/BAMS-D-13-00255.1>
- Kim, Y. K., Kim, S. M., Tachikawa, Y. (2019). Analyzing the uncertainty of using surface humidity for PMP estimation. *Journal of Japan Society of Civil Engineers*, 75(2), I_19-I_24, https://doi.org/10.2208/jscejhe.75.2_I_19**
- Kim, Y. K., Kim, S. M., Tachikawa, Y. (2020). Correlation analysis between storm events and meteorological conditions. *Journal of Japan Society of Civil Engineers*, 76(2), I_397-I_402.**

- Kim, Y. K., Kim, S. M., Tachikawa, Y. (2020). Analyzing uncertainty in probable maximum precipitation estimation with pseudoadiabatic assumption. *Water Resources Research*, 56(9), 1-24, <https://doi.org/10.1029/2020WR027372>**
- Klemes, V. (1986) Dilettantism in hydrology: Transition or destiny? *Water Resources Research*, 22(9S), 177S–188S, <https://doi.org/10.1029/WR022i09Sp0177S>.
- Klemes, V. (1987) Hydrological and engineering relevance of flood frequency analysis. *Hydrologic Frequency Modeling*, Springer, 1–18, https://doi.org/10.1007/978-94-009-3953-0_1
- Klemes, V. (2000) Tall tales about tails of hydrological distributions. *Journal of Hydrological Engineering*, 5(3), 227–231, [https://doi.org/10.1061/\(ASCE\)1084-0699\(2000\)5:3\(227\)](https://doi.org/10.1061/(ASCE)1084-0699(2000)5:3(227))
- Kobayashi, S., Ota, Y., Harada, Y., Ebita, A., & Moriya, M. (2015). The JRA-55 Reanalysis: General specifications and basic characteristics. *Journal of the Meteorological Society of Japan*, 93, 5–48. <https://doi.org/10.2151/jmsj.2015-001>
- Koutsoyiannis, D. (1999). A probabilistic view of Hershfield's method for estimating probable maximum precipitation, *Water Resources Research*, 35(4), 1313-1322, <https://doi.org/10.1029/1999WR900002>
- Kunkel, K. E., Karl, T. R., Easterling, D. R., Redmond, K., Young, J., Yin, X., & Hennon, P. (2013). Probable Maximum Precipitation and climate change. *Geophysical Research Letters*, 40, 1402–1408. <https://doi.org/10.1002/grl.50334>
- Lavender, S. L., Walsh, K. J., Caron, L. P., King, M., Monkiewicz, S., et al. (2018). Estimation of the maximum annual number of North Atlantic tropical cyclones using climate models. *Science Advance*, 4(8), <https://doi.org/10.1126/sciadv.aat6509>
- Lepore, C., Veneziano, D., & Molini, A. (2015). Temperature and cape dependence of rainfall extremes in the eastern United States, *Geophysical Research Letters*, 42(1), pp. 74–83, 2015, <https://doi.org/10.1002/2014GL062247>
- Loriaux, J. M., Lenderink, G. & Siebesma, A. P. (2016). Peak precipitation intensity in relation to atmospheric conditions and large-scale forcing at midlatitudes, *Journal of Geophysical*

- Research Atmospheres, 121(10), 5471-5487, <https://doi.org/10.1002/2015JD024274>
- M. Abdel Wahab, M. A., & Sharif, T. A. (1995). Estimation of precipitable water at different locations using surface dew point, *Theoretical and Applied Climatology*, 51(3), 153-157. <https://doi.org/10.1007/BF00867441>
- Micovic, Z., Schaefer, M. G., & Taylor, G. H. (2015). Uncertainty analysis for Probable Maximum Precipitation estimates. *Journal of Hydrology*, 521, 360–373. <https://doi.org/10.1016/j.jhydrol.2014.12.033>
- Minty, L. J., Kennedy, M. R., & Meighen, J. (1996). Development of the Generalised Southeast Australia Method for Estimating Probable Maximum Precipitation, edited by L. J. Minty, J. Meighen, and M. R. Kennedy, Hydrology Unit, Bureau of Meteorology, Melbourne, Australia.
- Mizuta, R., Murata, A., Ishii, M., Shiogama, H., Hibino, K., Mori, N., et al. (2017). Over 5000 years of ensemble future climate simulations by 60-km global and 20-km regional atmospheric models. *Bulletin of the American Meteorological Society*, 98(7), 1383–1398. <https://doi.org/10.1175/BAMS-D-16-0099.1>
- Mori, N., Shimura, T., Yoshida, K., Mizuta, R., Okada, Y., et al. (2019). Future changes in extreme storm surges based on mega-ensemble projection using 60-km resolution atmospheric global circulation model. *Coastal Engineering Journal*. 61(3), 295–307. <https://doi.org/10.1080/21664250.2019.1586290>.
- Ohara, N., Kavvas, M. L., Kure, S., Chen, Z. Q., Jang, S., & Tan, E. (2011). Physically based estimation of maximum precipitation over American river watershed, California, *Journal of Hydrological Engineering*, 16(4), 351-361. [https://doi.org/10.1061/\(ASCE\)HE.1943-5584.0000324](https://doi.org/10.1061/(ASCE)HE.1943-5584.0000324)
- Onogi, K., Tsutsui, J., Koide, H., Sakamoto, M., & Kobayashi, S. (2007). The JRA-25 reanalysis. *Journal of the Meteorological Society of Japan*, 85, 369–432. <https://doi.org/10.2151/jmsj.85.369>
- Plana-Fattori, A., Legrand, M., Tanré, D., Devaux, C., Vermeulen, A., 1998. Estimating the atmospheric water vapor content from sun photometer measurements. *J. Appl. Meteor.* 37 (8),

790–804.

- Papalexiou, S., & D. Koutsoyiannis (2006), A probabilistic approach to the concept of Probable Maximum Precipitation, *Advances in Geosciences*, 7(7), 51–54. <http://doi.org/10.5194/adgeo-7-51-2006>
- Paquin, D. (2010), Evaluation du MRCC4 en pass e r ecent (1961–1999), Internal report-Climate simulation group, Ouranos. Parlange, M. B., & Brutsaert, W. (1990). Are radiosonde time scales appropriate to characterize boundary layer wind profiles?, *American Meteorological Society*, 29(3), 249–255. [https://doi.org/10.1175/1520-0450\(1990\)029<0249:ARTSAT>2.0.CO;2](https://doi.org/10.1175/1520-0450(1990)029<0249:ARTSAT>2.0.CO;2)
- Rakhecha, P. R., & Kennedy, M. R. (1985). A generalised technique for the estimation of Probable Maximum Precipitation in India. *Journal of Hydrology*, 78(3), 345–359. [https://doi.org/10.1016/0022-1694\(85\)90112-X](https://doi.org/10.1016/0022-1694(85)90112-X)
- Rakhecha, P. R., & Singh, V. P. (2009). *Applied hydrometeorology*. Berlin, Germany: Springer.
- Reber, E. E., & Swope, J. R. (1972). On the correlation of the total precipitable water in a vertical column and absolute humidity at the surface. *Journal of Applied Meteorology*, 11, 1322–1325. [https://doi.org/10.1175/1520-0450\(1972\)011<1322:OTCOTT>2.0.CO;2](https://doi.org/10.1175/1520-0450(1972)011<1322:OTCOTT>2.0.CO;2)
- Reitan, C. H. (1963). Surface dew point and water vapor aloft. *Journal of Applied Meteorology*, 2, 776 – 779. [https://doi.org/10.1175/1520-0450\(1963\)002<0776:SDPAWV>2.0.CO;2](https://doi.org/10.1175/1520-0450(1963)002<0776:SDPAWV>2.0.CO;2)
- Robinson, P. J. (2000). Temporal trends in United States dew point temperatures. *International Journal of Climatology*, 20, 985–1002, [https://doi.org/10.1002/1097-0088\(200007\)20:9<985::AID-JOC513>3.0.CO;2-W](https://doi.org/10.1002/1097-0088(200007)20:9<985::AID-JOC513>3.0.CO;2-W)
- Rouhani, H., & Leconte, R. (2016). A novel method to estimate the maximization ratio of the Probable Maximum Precipitation (PMP) using regional climate model output. *Water Resources Research*, 52, 7347–7365. <https://doi.org/10.1002/2016WR018603>
- Rouhani, H., & Leconte, R. (2020). Uncertainties of precipitation water calculations for PMP estimates in current and future climates. *Journal of Hydrologic Engineering*, 25(3), [https://doi.org/10.1061/\(ASCE\)HE.1943-5584.0001877](https://doi.org/10.1061/(ASCE)HE.1943-5584.0001877)

- Rousseau, A. N., Klein, I. M., Freudiger, D., Gagnon, P., Frigon, A., & Ratt e-Fortin, C. (2014). Development of a methodology to evaluate Probable Maximum Precipitation (PMP) under changing climate conditions: Application to southern Quebec, Canada. *Journal of Hydrology*, 519, 3094–3109. <https://doi.org/10.1016/j.jhydrol.2014.10.053>
- Schaefer, M.G. (1994). PMP and other extreme storms: concepts and probabilities. In: ASDSO National Conference, Baltimore, MD, USA, pp. 61–73.
- Schaefer, M.G., & Barker, B.L. (2005). Stochastic Modeling of Extreme Floods on the American River at Folsom Dam: Flood-Frequency Curve Extension. MGS Engineering Consultants for US Army Corps of Engineers, Hydrologic Engineering Center, Davis, CA, USA.
- Schreiner, L. C., & Riedel, J. T. (1978). Probable maximum precipitation estimates, United States east of the 105th meridian, Silver Spring, MD: Department of Commerce, National Oceanic and Atmospheric Administration.
- Sheffield, J., Barrett, A. P., Colle, B., Fernando, D. N., Fu, & R. (2013). North American climate in CMIP5 experiments. Part I: Evaluation of historical simulations of continental and regional climatology. *Journal of Climate*, 26(23), 9209–9245. <https://doi.org/10.1175/JCLI-D-12-00592.1>
- Sinha, S., & Sinha, S. K. (1981). Precipitable water and dew point temperature relationship during the indian summer monsoon. *Pure and applied geophysics*, 119(5), 913-921. <https://doi.org/10.1007/BF00878959>
- Tan, E. (2010). Development of a methodology for Probable Maximum Precipitation estimation over the American river watershed using the WRF model. Davis: University of California, Davis.
- Tanaka T., Kiyoharo, K., & Tachikawa, Y. (2020). Comparison of fluvial and pluvial flood risk curves in urban cities derived from a large ensemble climate simulation dataset: A case study in Nagoya, Japan. *Journal of Hydrology*, 584, 1-11, <https://doi.org/10.1016/j.jhydrol.2020.124706>

- Tanaka T., Tachikawa, Y., Ichikawa, Y., & Yorozu, K. (2018). Flood risk curve development with probabilistic rainfall modelling and large ensemble climate simulation data: a case study for the Yodo River basin. *Hydrological Research Letters*, 12(4), 28-33. <https://doi.org/10.3178/hrl.12.28>
- Trenberth, K. E., Dai, A., Rasmussen, R. M., & Parsons, D. B. (2003). The changing character of precipitation, *Bulletin of the American Meteorological Society.*, 84(9), 1205–1217, doi:<http://doi.org/10.1175/BAMS-84-9-1205>
- Tuller, S. E. (1977). The relationship between precipitable water vapor and surface humidity in New Zealand. *Archiv für Meteorologie, Geophysik und Bioklimatologie, Serie A*, 26, 197–212. <https://doi.org/10.1007/BF02247163>
- U.S. Weather Bureau (1941). Maximum possible precipitation over the Ohio River Basin above Pittsburgh, Pennsylvania, Hydrometeorological Report 2, Natl. Weather Serv., Silver Spring, Md.
- U.S. Weather Bureau (1947). Generalized estimates maximum possible precipitation over the United States east of the 105th meridian areas of 10, 200, and 500 square miles, Hydrometeorological Report 23, Natl. Weather Serv., Silver Spring, Md.
- U.S. Weather Bureau (1954). Probable maximum precipitation on Sierra slopes of the Central Valley of California, Cooperative Studies Report 12, Natl. Weather Serv., Silver Spring, Md.
- U.S. Weather Bureau (1960). Generalized estimates of probable maximum precipitation west of the 105th meridian, Technical Paper 38, Natl. Weather Serv., Silver Spring, Md.
- U.S. Weather Bureau (1963). Probable maximum precipitation in the Hawaiian Islands, Hydrometeorological Report 39, Natl. Weather Serv., Silver Spring, Md.
- Viswanadham, Y. (1981). The relationship between total precipitable water and surface dew point. *Journal of Applied Meteorology*, 20 (1), 3–8. [https://doi.org/10.1175/1520-0450\(1981\)020<0003:TRBTPW>2.0.CO;2](https://doi.org/10.1175/1520-0450(1981)020<0003:TRBTPW>2.0.CO;2)
- Walland, D., Meighen, J. Xuereb, K., Beesely, C., & Hoang, T. (2003). Revision of the Generalised Tropical Storm Method for Estimating Probable Maximum Precipitation,

Hydrology Unit, Bur. of Meteorol, Austria.

World Meteorological Organization (1986). Manual for estimation of probable maximum precipitation, WMO-No. 332, Geneva, Switzerland.

World Meteorological Organization (2009). Manual on estimation of probable maximum precipitation, WMO-No. 1045, Geneva, Switzerland. Retrieved from <http://www.wmo.int/pages/prog/hwrp/publications/PMP/WMO%201045%20en.pdf>

Yajima, H., Tsuji, M., Ikebuchi, S., & Nakakita E. (1996). Estimation method of probable maximum precipitation for short duration using convective simulation model. *Journal of Japan Society of Hydrology and Water Resources*, 9(2), 143-152. <https://doi.org/10.3178/jjshwr.9.143>

Yang, J.A., Kim, S.Y., Mori, N., & Mase, H. (2018). Assessment of long-term impact of storm surges around the Korean Peninsula based on a large ensemble of climate projections. *Coastal Engineering* 142, 1–8, <https://doi.org/10.1016/j.coastaleng.2018.09.008>

Yigzaw, W., Hossain, F., & Kalyanapu, A. (2013). Impact of Artificial Reservoir Size and Land Use/Land Cover Patterns on Probable Maximum Precipitation and Flood: Case of Folsom Dam on the American River. *Journal of Hydrologic Engineering*, 18(9), 1180-1190, [https://doi.org/10.1061/\(ASCE\)HE.1943-5584.0000722](https://doi.org/10.1061/(ASCE)HE.1943-5584.0000722)

Yu, Z., Miller, S., Montalto, F. & Lall, U. (2018). The bridge between precipitation and temperature – pressure change events: modeling future non-stationary precipitation, *Journal of Hydrology*, 562, 346-357, <https://doi.org/10.1016/j.jhydrol.2018.05.014>

